Università degli Studi di Ferrara

DOTTORATO DI RICERCA IN
"Farmacologia e Oncologia Molecolare"

CICLO XXIII

COORDINATORE Prof. Antonio Cuneo

OSTEOPROTEGERIN: A PANCREATIC ISLETS DYSFUNCTION AND VASCULAR INJURY MODULATOR

Settore Scientifico Disciplinare BIO/16

Dottoranda
Dott.ssa Toffoli Barbara

Tutore
Prof.ssa Secchiero Paola

Anni 2008/2010

TABLE OF CONTENTS

INTRODUCTION

1.1 TNF-Superfamily

The Tumor Necrosis Factor (TNF) superfamily of cytokines and their receptors regulates many areas of metazoan biology, and specifically plays foundamental roles in regulating myriad aspects of immune development and functions (Chan, 2007). The biological functions of this system encompass beneficial effects for the host in inflammation and protective immune responses in infectious diseases as well as crucial roles in organogenesis of secondary lymphoid organs and the maintenance of lymphoid structures throughout the body. At the same time, some members of this superfamily are responsible for host damaging effects in sepsis, fever syndromes, cachexia, and autoimmune diseases (e.g., psoriasis, inflammatory bowel disease, rheumatoid arthritis) (Hehlgans and Pfeffer, 2005; Aggarwal, 2003; Ware, 2003; Kwon et al., 2003).

In 1984, two forms of TNF, TNFα and LTα (lymphotoxin, TNFβ), were isolated from activated macrophages and T cells, respectively. Since their identification, these proteins have become representative of a unique superfamily of ligands, which currently includes at least 18 different human homologues (Baker and Reddy, 1998; MacEwan, 2008). The TNF-related ligands are type II transmembrane proteins (intracellular N-terminus) with a short cytoplasmic tail (15 to 25 residues in length) and a larger extracellular region (approximately 150 amino acids) containing the signature 'TNF homology domain' (THD) where the receptor-binding sites are located (Figure 1). The THD, that shares approximately 20-25% of sequence identity between family members, folds into an antiparallel β-sandwich that assembles into trimers, the functional unit of the ligand (Paul, 2008).

Some of these ligands, e.g. TNF, are active both as a membrane integrated and as a soluble form released after proteolytic cleavage, mainly by metalloproteinases induced by various stimuli. Certain ligands are expressed only as soluble molecules, e.g. LTα; but may also be recruited to the cell membrane to form heterotrimeric membrane anchored complexes and thereby enhancing regulatory specificity and complexity (Hehlgans and Pfeffer, 2005).

Thus far, 29 TNF receptor family members have been identified in humans (Figure 1). These are primarily type I transmembrane proteins characterized by cysteine-rich domains (CRD) that are the hallmark of the TNF superfamily receptors (TNFR). These 40 amino acid pseudorepeats are typically defined by 3 intrachain disulphides generated by 6 highly conserved cysteine residues within the receptor chains (Locksley et al., 2001). Most receptors

also exist in a soluble form, and the solubility is achieved by proteolitic cleavage or by alternative splicing of the exon encoding the transmembrane domain (Baker and Reddy, 1998).

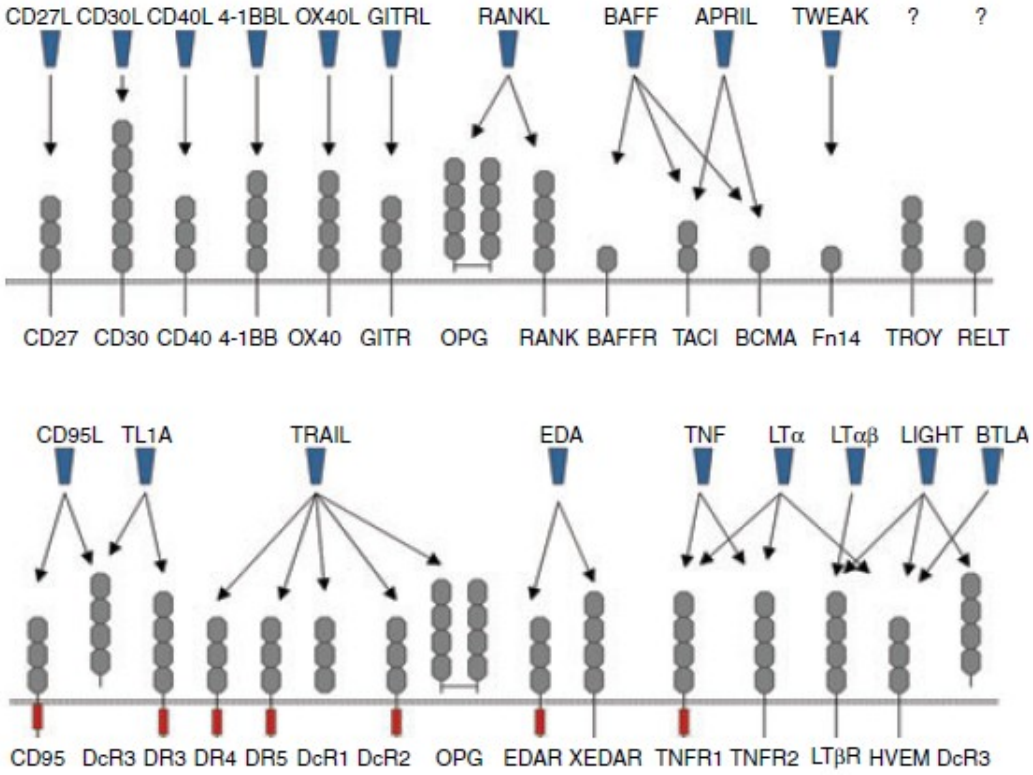

Figure 1. The TNF/TNFR superfamily. The TNF-related ligands are shown in blue and arrows indicate interactions with their receptors (Hehlgans and Pfeffer, 2005).

Although most members of the TNF superfamily of ligands interact with more than one receptor of the corresponding superfamily of cognate receptors, genetic based approaches, mainly conducted in gene targeted mouse strains, have clearly demonstrated that almost each receptor-ligand system have a unique and non-redundant function.

Receptor activation by the TNF family ligands causes recruitment of several intracellular adaptor proteins which activate multiple signal transduction pathways. Based on their intracellular sequences the members of the TNFR superfamily can be classified into three major groups. The first group, including molecules such as FAS and TNFRI, contains the so called death domains (DD) in their cytoplasmic domains. Activation of these receptors leads to recruitment of intracellular death domain containing adaptors such as FAS-associated death domain (FADD) and TNFR-associated death domain (TRADD), which subsequently promote the activation of the caspase cascade and induction of apoptosis. The second group of

receptors, that includes members like CD30, CD40 and receptor activator of NF-kB (RANK), contains one or more TNF-receptor associated factor (TRAF)- interacting motif (TIMs) in their cytoplasmic domain. Activation of TIM containing TNFR family members leads to the recruitment of TRAF family members and the subsequent activation of signal transduction pathways like nuclear factor kB (NF-kB), Jun N-terminal kinase (JNK), p38, extracellular signal-related kinase (ERK) and phosphoinositide 3-kinase (PI3K), which regulate cellular processes ranging from proliferation and differentiation to cell death. Finally, the third group of receptors, including TRAIL-R3 (DcR1), DcR3 and Osteoprotegerin, doesn't contain functional intracellular signaling domains or motifs, but instead compete with the other two groups of receptors for their corresponding ligands (Hehlgans and Pfeffer, 2005, Dempsey et al., 2003).

1.2 OPG structure and expression

Osteoprotegerin (OPG) is a secreted glycoprotein belonging to the TNFR superfamily and was initially identified by two separate groups in 1997. Both groups observed OPG to be central in the regulation of bone turnover through the inhibition of osteoclastogenesis. However, it was not until 1998 that the newly discovered proteins were found to be identical, hence OPG was alternatively termed osteoclast inhibitory factor (OCIF) (Reid and Holen, 2009). Its international name according to the TNF nomenclature is TNFRSF11B (Baud'huin et al., 2007).

The mouse and the human OPG genes have been cloned and characterized, and the human OPG gene is a single-copy gene that consists of five exons and spans 29 kb of the human genome located on chromosome 8 q23-24 (Morinaga et al, 1998; Mizuno et al.,a 1998).

Murine and human OPG proteins comprise 401 amino acids of which 21 form a signal peptide that is cleaved to generate a mature form of 380 amino acids (Figure 2). At the N terminus, there are four domains (D1-D4), which have cysteine-rich TNFR homologous motifs and are necessary and sufficient for inhibiting osteoclastic differentiation and activity both *in vitro* and *in vivo*. The carboxy-terminal portion of the protein with domains 5 and 6 (D5 and D6) contains two death domain homologous regions, motifs that are found in the cytoplasmic region of mediators of apoptosis such as TNFR 1, DR3 or CD95/Fas. In fact, D5 and D6 of OPG have been demonstrated to transduce an apoptotic signal when expressed as an OPG/Fas fusion protein in which the transmembrane region of Fas is inserted between domains 4 and 5 of OPG. Finally, domain 7 (D7) harbors a heparin-binding region, a common feature of peptide growth factors and signal molecules, as well as an unpaired cysteine residue

at position 400 required for homodimerization of the molecule (Zauli et al., 2009; Schoppet et al., 2002). OPG represents an atypical member of the TNFR family since it is a secreted protein with no transmembrane domain. OPG is produced as a monomer (55-62 kDa), undergoes homodimerization, and is secreted as a disulfide linked homodimeric glycoprotein with four or five potential glycosylation sites, generating a mature form of OPG of 110-120 kDa. The monomeric and the homodimeric forms are indistinguishable in stability, but the homodimeric exerts more potent biological activity and is stronger in heparin binding ability (Zauli et al., 2009; Tomoyasu et al., 1998).

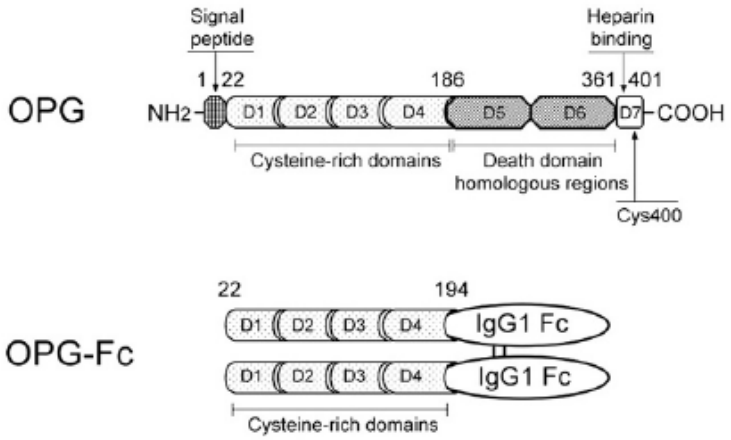

Figure 2. **Schematic representation of the protein structure of OPG and OPG-Fc.** Main domains and their biochemical and/or functional properties are indicated. Numbers in figure represent amino acids. NH_2 indicates N terminus, COOH, C terminus, Cys400, dimer formation site. Human OPG-Fc is a recombinant fusion protein, in which the Fc fragment of human IgG1 is fused to the C terminus of the 22-194 fragment of native OPG to maintain a dimeric molecule with a sustained circulating half-life (Zauli et al., 2009).

To enhance the pharmacological activity of native OPG, numerous constructs have been created wherein the signal peptide, heparin binding domain, and death domains were removed and the remaining peptide was fused to the Fc domain of human IgG1 (Figure 2). The Fc fusion partner maintains the potent dimeric nature of OPG while significantly increasing its circulating half-life (Kearns et al., 2008).

OPG is produced by a variety of tissues including the cardiovascular system (hearth, arteries, veins), lung, kidney, intestine, and bone, as well as hematopoietic and immune cells. The expression and production of the protein is modulated by various cytokines, peptides, hormones, and drugs. Cytokines, including TNFα, interleukin (IL)-1α, IL-18, transforming growth factor (TGFβ), bone morphogenetic proteins, and steroid hormones are known to up-regulate OPG mRNA levels. In contrast, glucocorticoids (known to promote bone resorption) and the immunosuppressant cyclosporine A (which has the propensity to cause osteoporosis

and vascular disease) or basic fibroblast growth factor, all suppress the expression of OPG (Schoppet et al., 2002).

1.3 OPG as a 'decoy receptor'

OPG acts as a decoy receptor for RANKL, preventing the stimulation and maturation of osteoclast precursors instigated by normal binding of RANKL to its constitutive receptor and as a soluble receptor for TRAIL (Emery et al, 1998).

1.3.1 OPG/RANKL and bone system

The important role of OPG in bone metabolism has been clearly demonstrated by the development of transgenic and knock-out mice. OPG knock-out mice are viable and fertile, but exhibit an osteoporotic phenotype due to enhance osteoclastogenesis. They are characterized by marked bone loss accompanied by destruction of growth plate and lack of trabecular bone in their femurs, and the strength of their bones dramatically decrease (Mizuno et al.,b 1998). In contrast, systemic delivery of OPG via the expression of rat or murine *opg* transgenes results in severe yet nonlethal osteopetrosis. The ostopetrotic phenotype caused by OPG overexpression differs significantly from those observed in other ostopetrotic models. *opg* transgenic mice are of normal size, have no apparent defects in tooth eruption, and have normally shaped bones. Histologically, they have a marked reduction in trabecular osteoclast but no deficiency of osteoclast precursors, suggesting a defect in the later stages of osteoclast differentiation (Simonet et al., 1997). These evidences, supported by confirmations in the *in vitro* experiments, demonstrate that the presence of OPG is absolutely required to maintain bone mass in physiological situations. Subsequently, molecular binding experiments have shown that OPG associates with the ligand of the receptor activator of NF-kB (RANKL), a member of TNF superfamily ligand, functioning as a decoy receptor. RANKL genes gives rise to splice variants that encode two forms of type II transmembrane proteins and one form of a secreted protein. Although high RANKL expression can be found in lymph nodes, thymus and lung, only low levels of RANKL can be detected in spleen, bone marrow, peripheral blood, leukocytes, hearth, placenta, skeletal muscle, stomach or the thyroid. In addition, RANKL expression is induced in mammary gland epithelial cells in pregnancy, activated T cells, and malignant tumor cells (Wong et al., 1999; Wada et al., 2006).

The receptor that mediates all known activities for RANKL is called receptor activator of NF-kB (RANK). The binding and activation of RANK, that is a homotrimeric TNFR family member, involve direct interactions between the extracellular receptor binding domain of

trimeric RANKL and the extracellular cysteine-rich domains of trimeric RANK. This interaction is thought to cause oligomerization of RANK and the subsequent activation of several signal transduction cascades, as the NF-kB, MAPK, and phosphatidylinositol pathways (Kearns et al., 2008; Wada et al., 2006).

One of the best characterized role of RANKL/RANK system is in the osteoclastogenesis. The key regulators of bone turnover are osteoblasts, which are involved in bone formation, and osteoclasts, which are responsible for bone resorption. RANKL expressed by osteoblasts as a transmembrane protein binds to RANK on the surface of osteoclasts and osteoclasts precursor. This leads to osteoclast formation, differentiation, activation and consequently bone resorption (Figure 3). To regulate the balance between bone formation and bone resorption, the RANKL-RANK interaction is inhibited by OPG. OPG produced by osteoblastic cells binds as a homodimer to the homotrimeric RANKL, thus inhibiting the terminal stage of osteoclastic differentiation (Reid and Holen, 2009; Baud'huin et al., 2007).

Although there are contradictory data, in general upregulation of RANKL is associated with downregulation of OPG, or at least lower induction of OPG, such that the ratio of RANKL to OPG changes in favour of osteoclastogenesis. Many reports have supported the assertion that the RANKL/OPG ratio is a major determinant of bone mass. Moreover, consistent with the osteoprotective role, mutation in the human OPG gene have been associated with idiopathic hyperphosphatasia, also known as Juvenile Paget's disease, an autosomal-recessive disorder characterized by increased bone remodeling, osteopenia, and fractures (Boyce and Xing, 2007).

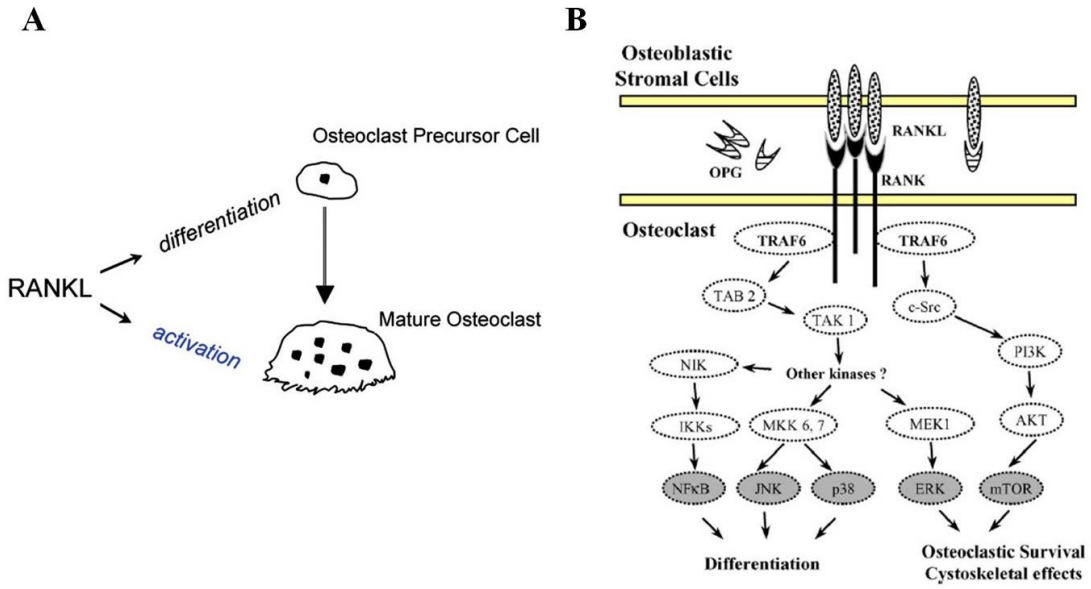

Figure 3. **In (A) Schematic representation of RANKL in osteoclastogenesis** (Zauli et al., 2009)**. In (B) RANK signaling pathways** (Theoleyre et al., b 2004).

1.3.2 OPG/TRAIL and tumorigenesis

In 1995 TNF-related apoptosis-inducing ligand (TRAIL) was identified and characterized as a member of the TNF family of death-inducing ligands. TRAIL is a type II transmembrane protein of about 33-35 kD, which can be cleaved from the cell surface to form a soluble ligand that retains biological activity. The extra-cellular domain of TRAIL forms a bell shaped homo-trimer, much like other ligands of the TNF family, but unlike the other members, it carries a zinc ion at the trimer interface, coordinated by the single unpaired cysteine residue of each monomer. This zinc ion is essential for structural integrity of TRAIL and to maintain its capacity to induce apoptosis (Degli-Esposti, 1999; Corallini et al., 2008). TRAIL is constitutively present in many tissues at the level of mRNA, but it is expressed mainly by activated cells of the immune system, especially natural killer (NK) cells, B cells, T cells, monocytes, and dendritic cells. TRAIL plays a crucial role in maintaining T cell homeostasis, as well as in killing of tumor and virally transformed cells by NK cells. Over the years, TRAIL has generated considerable interest among clinicians for its preferential toxicity toward transformed cells and tumor xenografts, with generally little or no toxicity to normal tissues, which makes it an ideal candidate for cancer therapy. As a result, recombinant TRAIL, as well as agonistic antibodies against TRAIL receptors, are currently in Phase I/II clinical trials for treatment of solid tumors and hematological malignancies (Griffith et al., 2009; Guicciardi and Gores, 2009; Ashkenazi and Herbst, 2008; Finnberg and El-Deiry, 2008).

With respect to other members of the TNF ligand superfamily, TRAIL shows the most complex ligand-receptor interaction, since it is able to bind to five different receptors found on a variety of cell types: four membrane-bound (TRAIL-R1/death receptor 4, TRAIL-R2/death receptor 5, TRAIL-R3/decoy receptor 1, TRAIL-R4/decoy receptor 2) and one soluble receptor (OPG). OPG acting as a decoy receptor, binds TRAIL and prevents its interaction with the functional death receptors, thus allowing cells to escape cell death (Figure 4). In this context, many different *in vitro* data demonstrated the ability of native OPG, produced by tumor cells or by bone marrow stromal cells, to efficiently counteract the pro-apoptotic activity of TRAIL in a variety of cell lines derived from prostate and breast cancers, ameloblastomas and multiple myeloma (Zauli et al., 2009; Reid and Holen, 2009).

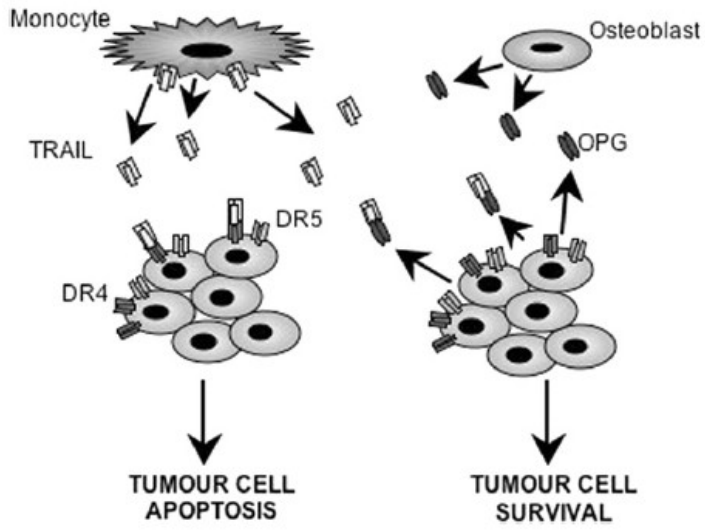

Figure 4. Role of OPG in cell survival. TRAIL is produced by immune cells that can infiltrate the tumor microenvironment. TRAIL can then bind to the death receptors 4 and 5 (DR4 and DR5) present on the surface of tumor cells, resulting in tumor cell apoptosis. OPG, secreted by tumor cells, acts as a decoy receptor for TRAIL. As a result, tumor cells escape from death (Reid and Holen, 2009).

Of note, in the light of recent *in vitro* studies that demonstated that the affinity of OPG for RANKL and TRAIL under physiological conditions is of a similar order of magnitude and that TRAIL is able to inhibit OPG-mediated inhibition of osteoclastogenesis, OPG acquires a key position in the regulation of the functions of these two important signaling pathways (Figure 5) (Vitovski et al., 2007).

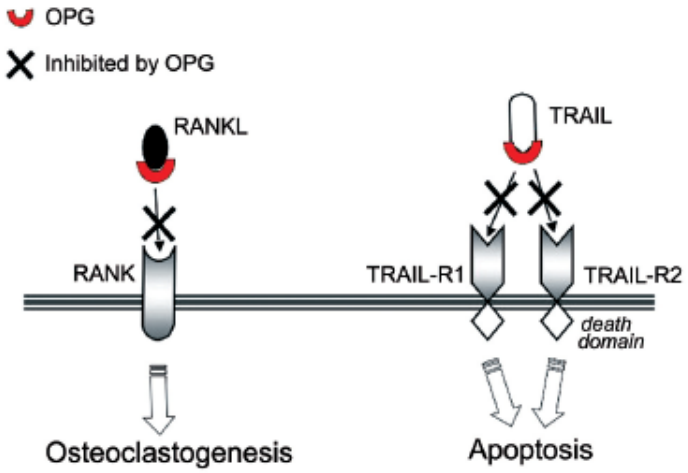

Figure 5. Mechanism of action of OPG on RANKL- and TRAIL- biological activities. The pro-apoptotic activity of TRAIL is mediated by two (TRAIL-R1 and TRAIL-R2) of its four membrane receptors. OPG by efficiently binding RANKL and TRAIL, counteracts both the RANKL-mediated osteoclastogenesis as well as the pro-apoptotic activity of TRAIL (Zauli et al., 2009).

Recently, many studies have demonstrated that OPG can exert direct biological activities independently of its neutralizing effects towards RANKL or TRAIL. In fact OPG has a highly basic heparin-binding domain (D7) that besides being responsible for the homodimerization of the molecule (Yamaguchi et al., 1998), makes interactions with heparin and heparan sulfates possible. Heparan sulfate proteoglycans are important participants in cell-surface

signaling and critical in controlling cell behavior. They are involved in actin cytoskeleton regulation, cell adhesion and migration, and modulation of specific receptor interactions. At the cell surface, proteoglycans of the syndecan family are the major source of heparan sulfate (Wright et al., 2009). In this context, different reports indicate that the heparin binding domain is involved in OPG-induced chemotaxis of human peripheral blood monocytes (Mosheimer et al., 2005), in controlling OPG release by vascular cells (Nybo and Rasmussen, 2008) and in the OPG-mediated osteopontin-increasing in human periodontal ligament cells (Yongchaitrakul et al., 2009). Of note, in multiple myeloma (Standal et al., 2002) and osteosarcoma (Lamoureux et al., 2009) it has been shown that also the decreased of the biological activity of the full-length OPG might be due to its bounding, internalization and degradation, syndecan-1 mediated.

1.4 OPG and the vascular system

While OPG, RANK and RANKL are produced by numerous cell types and a variety of tissues, their expression pattern targets three main biological systems where the molecular triad could be more specifically involved: the osteoarticular, immune, and vascular systems (Figure 6). Transgenic and knockout mice models as well as many *in vitro* experiments clearly revealed the potential involvement of these effectors in the three biological systems (Theoleyre et al., b 2004; Feige, 2001; Grĉević et al., 2001; Hofbauer et al., 2001; Josien et al., 2000; Schoppet et al., 2002).

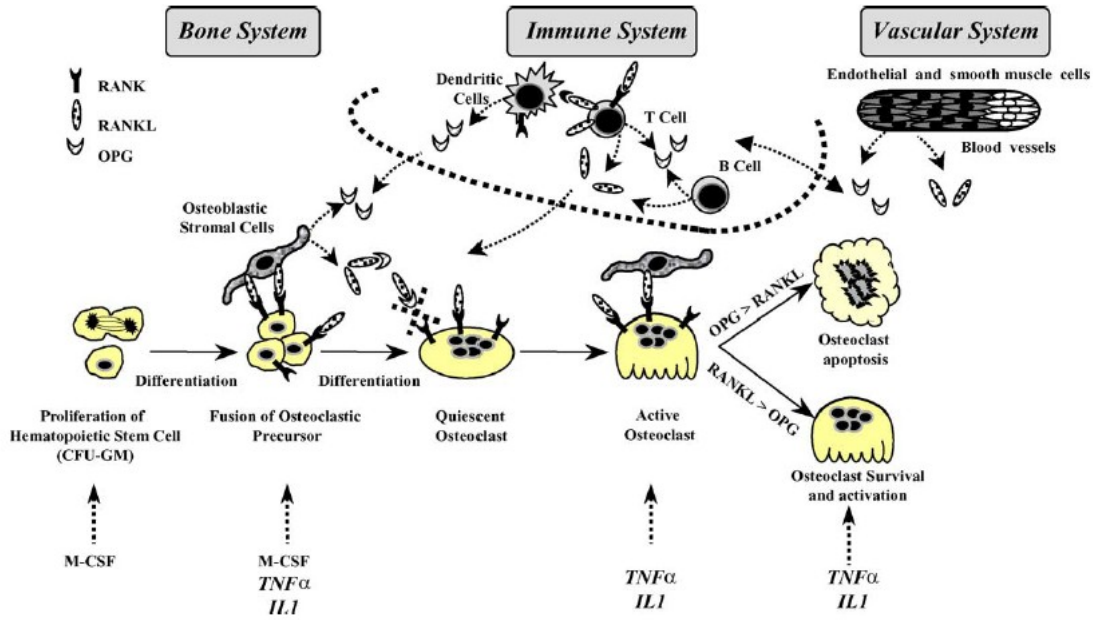

Figure 6. OPG/RANK/RANKL as common effectors of bone, immune and vascular system (Theoleyre et al., b 2004).

In fact, the first evidence for a role of OPG in the vasculature was given by a study of OPG knockout mice generated on a mixed genetic background. The selective deletion of OPG in mice resulted in early-onset severe osteoporosis as well as significant medial calcification of the aorta and renal arteries. The onset of arterial calcification could be completed prevented by transgenic OPG delivery from mid gestation through adulthood; in contrast, post-natal intravenous injection of recombinant OPG had no effect on the incidence of vascular calcification, suggesting that OPG cannot reverse the calcification process once it had occurred. Interestingly, both treatments effectively reversed osteoporotic bone loss phenotype. A vascular-protective role for OPG was also indicated by rat studies, in which OPG administration prevented calcification induced by warfarin (a vitamin K antagonist) or high vitamin D doses (Van Campenhout and Golledge, 2009; Venuraju et al., 2010; Collin-Osdoby, 2004). Furthermore, Morony et al. (2008), demonstrated that subcutaneous injection of pharmacological concentrations of human recombinant OPG (OPG-Fc) decreased the degree of atherosclerotic calcified lesions in atherogenic diet-fed ldlr knockout mice, without affecting the total burden of atherosclerotic lesions. To determine whether OPG plays a role in the calcification and chondrocyte metaplasia that has been reported in advanced atherosclerotic lesions in mice, Bennet et al. (2006) generated mice deficient in both OPG and apoE gene. They observed that the loss of OPG in this animal model led to larger atherosclerotic lesions in the innominate arteries of 40 and 60 weeks of age mice, coupled with more rapid and extensive calcification of both the media and the intima.

Although most animal studies supported a protective role for OPG in cardiovascular system, many clinical investigations revealed a positive association between high serum OPG levels and cardiovascular outcome. The first paper to report a relation between plasma OPG and vascular disease was published in 2001 (Browner et al.). An association was discovered between high plasma OPG levels and increased cardiovascular mortality in a cohort of elderly women primarily gathered to study osteoporosis risk factors. Subsequently, the connection between plasma OPG and cardiovascular disease was confirmed in populations of men with coronary artery disease (Schoppet et al., 2003), patients with myocardial infarction and heart insufficiency (Ueland et al., 2004), and in seemingly healthy individuals (Kiechl et al., 2004) where a high level of serum OPG was an independent risk factor for incident CVD and vascular mortality, but not for mortality due to non-vascular causes. Moreover, plasma OPG has also been found to be associated with intima-media thickness of the carotid artery as determined by ultrasound (Erdogan et al., 2004). Remarkably, two OPG genetic polymorphisms have been associated with an increase risk of coronary artery disease in

Caucasian men, and serum OPG levels correlated with one of these polymorphisms (Soufi et al., 2004). Thus, these studies strongly indicate that serum OPG levels frequently rise in clinical conditions that favor vascular dysfunction or atherosclerosis. Morena et al. (2006) demonstrated in hemodialysis patients as elevated plasma OPG predicted all-cause and CV mortality when adjusted for age, gender, dialysis vintage, diabetes, hypertension, and smoking. More recently OPG was described as an independent predictor factor both for early vascular adverse changes in osteoporotic postmenopausal women (Shargorodsky et al., 2009) and for cardiovascular mortality in patients with stable coronary artery disease (Jono et al., 2010). Mesquita et al. (2009) showed that OPG predicted mortality in chronic kidney disease patients and could be a valuable biomarker in early detection of coronary artery calcification in these patients.

Moreover, many different *in vitro* studies have clearly demonstrated that inflammatory cytokines promote the expression and release of OPG by endothelial cells (Secchiero et al., a 2006; Ben-Tal Cohen et al., 2007; Collin-Osdoby et al., 2001) and by vascular smooth muscle cells (Zhang et al., 2002; Moran et al., 2005). Because of the enormous surface area of the endothelium throughout the body as well as the relatively substantial levels of constitutive and regulated OPG produced by endothelial cells and vascular smooth muscle cells, vascular cells play a fundamental role in the contribution in circulating OPG in human serum. On the other side, if we consider that recent studies have shown that recombinant full-length OPG is able to promote leukocytes adhesion to endothelial cells (Zauli et al., 2007; Mangan et al., 2007), OPG seems to have an active role in disease progression more than serving as a compensatory/protective response to minimize disease progression. Anyway, considerable controversy still exist regarding the role of OPG/RANKL/RANK/TRAIL pathways in cardiovascular setting.

1.5 OPG and diabetes

Plasma osteoprotegerin concentration correlates to both diabetes and cardiovascular disease in cross-sectional studies. This was first shown by Browner et al. (2001), who reported that although no associations were seen between the bone parameters and plasma osteoprotegerin levels, individual with diabetes as well as persons with cardiovascular disease had increased values. In another investigation on 522 men that described a positive relationship between coronary arteriosclerosis (determined by CAG) and plasma OPG, diabetic patients were also observed to have elevated OPG plasma levels and the increase was more than could be expected when the degree of coronary sclerosis was considered (Schoppet et al., 2003). Since

then, these findings have been confirmed in both type 1 (Xiang et al., 2007; Galluzzi et al., 2005) and type 2 diabetes (Knudsen et al., 2003; Xiang et al., 2006) and it has been found that the increased OPG production characterizes an early event in the natural history of diabetes mellitus (Secchiero et al., a 2006).

In more recent studies performed in diabetic subjects a strong association between plasma levels of OPG and micro- and macroangiopathy was observed (Avignon et al., 2005; Grauslund et al., 2010; Knudsen et al., 2003; Xiang et al., 2009).

Osteoprotegerin has also been found to be accumulated in aorta from patients with type 1 and type 2 diabetes (Olesen et al., 2005). This accumulation is seen in the tunica media from areas of the tissue with and without atherosclerotic plaque. The accumulation of osteoprotegerin throughout the deeper layers of the vessels wall may reflect generalized changes in the arterial system in diabetes, as part of diffuse arterial changes such as alterations in glycoproteins (Takemoto et al., 2000), collagens (Rasmussen and Ledet, 1993) and glycosaminoglycans (Heickendorff et al., 1994). In addition, osteoprotegerin may be related to the development of medial calcification, which is frequently present in patients with diabetes (Niskanen et al., 1994; Lehto et al., 1996). Two recent experimental studies have confirmed the finding of increased levels of OPG in animals with experimental diabetes (Heinonen et al., 2007; Vaccarezza et al., 2007).

The mechanisms behind the increased circulating OPG levels in diabetes are unknown. Diabetic vasculopathy has an underlying low-grade inflammatory component, manifesting itself in the up-regulation of genes responsive to inflammatory processes (Secchiero et al., 2005; Joussen et al., 2002; Bulotta et al., 2001; Fujiwara et al., 2004; Sjöholm and Nyström, 2005). In this respect, it should be emphasized that OPG is an NF-kB-inducible gene (Collin-Osdoby et al., 2001), whose release in endothelial cell culture is significantly increased by inflammatory cytokines.

Considering the elevated levels of OPG detected also in patients affected by type 1 diabetes, hyperinsulinemia and insulin resistance are unlikely to play a key role in OPG induction. Accordingly Jørgensen et al. (2009) have recently demonstrated as acute hyperinsulinemia decreases plasma OPG in type 2 diabetes and obesity. In line with the hypothesis that insulin is not involved in the induction of OPG expression and secretion, Secchiero et al. (a 2006) have also demonstrated that OPG release is significantly up-regulated in the sera of diabetic apoE-knockout mice early after the induction of diabetes mellitus by streptozotocin (STZ) treatment. Of note, OPG serum levels in diabetic apoE-knockout mice positively correlated with the glycemic levels whereas they were inversely correlated to the levels of free RANKL.

Elevated levels of OPG were also observed in C57Bl littermates concomitantly with the induction of diabetes mellitus, suggesting that hypercholesterolemia, characterizing apoE-knockout mice, did not play a major role in the upregulation of serum OPG associated to diabetes mellitus.

Despite the *in vivo* data obtained in the mouse models of STZ-induced diabetes, in which it has been demonstrated the existence of a positive correlation between OPG and glycemic serum levels, high glucose levels per se were insufficient to modulate OPG release in endothelial cells, PBMCs, and macrophages. On the other hand, the proinflammatory cytokine TNF-α, which is known to be elevated in the sera of patients with diabetes mellitus (Joussen et al., 2002; Bulotta et al., 2001; Fujiwara et al., 2004), dose dependently up-regulated OPG secretion by endothelial cells. Importantly, the concentrations of TNF-α (10 pg/ml) required to induce a significant (approximately two-fold) increase in OPG, a situation mimicking the OPG rise observed in the serum of diabetic patients, were in the range of plasma concentrations reported in diabetic patients (Joussen et al. 2002; Bulotta et al., 2001; Fujiwara et al., 2004). These *in vitro* findings, coupled to the data obtained in the diabetic mouse models, clearly suggest that the inflammation-driven hyperglycemia, rather than the high glucose levels per se, is involved in the increase of OPG observed in both diabetic patients and diabetic mice. It is possible that the imbalance of OPG versus RANKL serum levels in both diabetic patients and diabetic apoE-knockout mice might contribute to endothelial cell dysfunction by blocking RANKL signaling, which is able to activate protective intracellular pathways in endothelial cells, such as the eNOS pathway. In this respect, it should be emphasized that diabetic vascular dysfunction is a major clinical problem that predisposes patients to a variety of cardiovascular diseases. In fact, diabetic patients frequently suffer from macroscopic and microscopic vasculopathy and accelerated atherosclerosis. The early impairment of nitric oxide release is a key feature of endothelial dysfunction, which invariably precedes permanent vascular alterations (Landmesser et al., 2004).

At present it is unclear whether OPG plays a pathogenetic or compensatory role in the vascular dysfunction and atherosclerosis associated to diabetes. Moreover the physiopathological role of elevated levels of OPG in pancreatic islet function is not known.

1.6 Atherosclerosis and animal models

Atherosclerosis is a high-cost disease and its complications still represent the first cause of death in most industrialized countries. Efficacious prevention includes treatment of the most

important cardiovascular risk factors, such as cigarette smoking, hypertension, hypercholesterolemia, diabetes and obesity. However, the absence of such 'traditional' risk factors does not completely protect from the disease and new 'emerging factors' have been identified, including markers of inflammation (Corrado et al., 2010; Libby, 2002). Although the clinical manifestations of cardiovascular disease, such as myocardial infarction, stroke, and peripheral vascular disease, appear from middle age, the process of atherosclerosis can begin early in childhood as an accumulation of fatty streaks-lipid engorged macrophages (foam cells) and T lymphocytes in the intima of the arteries. Fatty streaks may or may not progress, and may regress (Hong, 2010).

Under normal conditions, the endothelial cells of the arterial wall resist adhesion and aggregation of leukocytes and promote fibrinolysis. When activated by stimuli, like hypertension, an unhealthy diet, insulin resistance or inflammation, the endothelial cells express a series of adhesion molecules that selectively recruit various classes of leukocytes. Once the monocytes adhere to the activated endothelium, proinflammatory proteins provide a chemotactic stimulus that induces them to enter the intima. Within the intima, the monocytes mature into macrophages and start to express scavenger receptors, that allow them to engulf modified lipoprotein particles (especially highly oxidized LDL). Subsequently, the cytoplasm becomes engorged with lipid particles, giving the macrophages the typical microscopic frothy appearance of the foam cells found in atherosclerotic lesions (Libby et al., 2010).

The transition from the relatively simple fatty streak to the more complex lesion is characterized by the immigration of smooth muscle cells from the medial layer of the artery wall trough the internal elastic lamina into the intimal, or subendothelial, space. Intimal smooth muscle cells may proliferate and take up modified lipoproteins, contributing to foam cells formation, and synthesize extracellular matrix proteins that lead to the development of the fibrous cap. This phase of lesion development is influenced by interactions between monocytes/macrophages and T cells that result in a broad range of cellular and humoral responses and the acquisition of many features of a chronic inflammatory state.

Although advanced atherosclerotic lesions can lead to ischemic symptoms as a result of progressive narrowing of the vessel lumen, acute cardiovascular events that result in myocardial infarction and stroke are generally thought to result from plaque rupture and thrombosis. Plaque ruptures generally occur at the shoulder regions of the plaque and are more likely to occur in lesions with thin fibrous caps, a relatively high concentration of lipid-filled macrophages within the shoulder region, and a large necrotic core (Glass and Witztum, 2001; Lusis, 2000) (Figure 7).

Numerous animal species, especially transgenic mouse models, have been used to study the pathogenesis and the potential treatment of atherosclerotic lesions (Woollard and Geissmann, 2010). Until 1992, the majority of atherosclerotic research focused on mechanisms in rabbits, with a lesser number of studies in pigs and nonhuman primates. Despite the fact that rabbits do not develop spontaneous atherosclerosis, they have been useful for their high responsiveness to cholesterol manipulation and the capacity of developing lesions in a fairly short time.

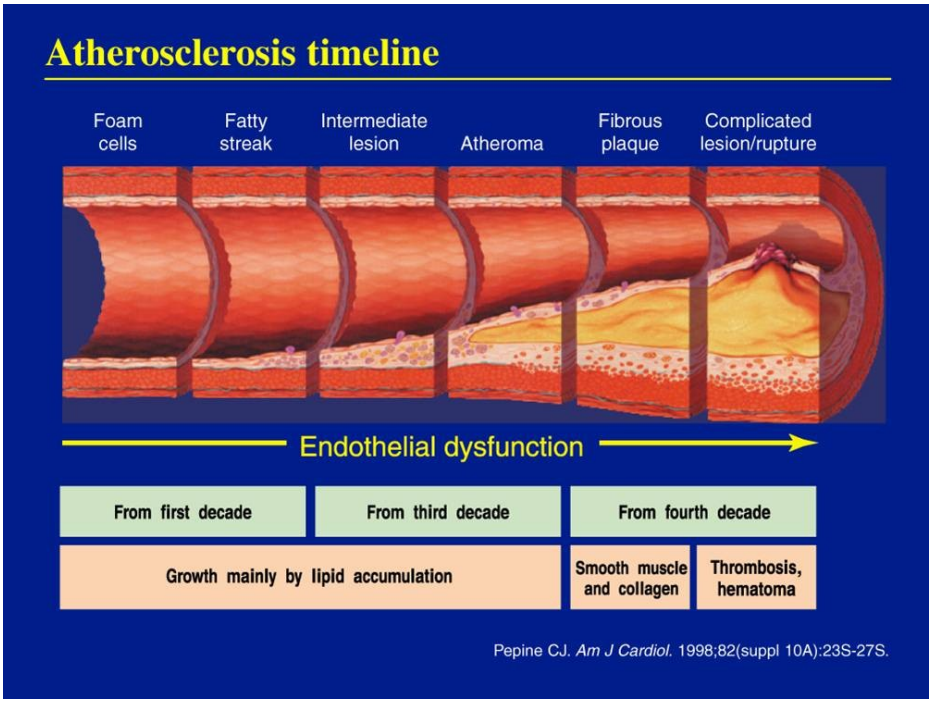

Figure 7. Atherosclerosis progression.

Unfortunately, rabbit lesions are much more fatty and macrophage-rich than those in humans and plasma cholesterol are extraordinary high. Pigs and monkeys are better suited to model human atherosclerotic lesions, but, obviously, they present many problems related to costs and maintaining/handling of the colonies. In recent years, there has been an explosion in the number of *in vivo* studies that is largely attributable to the use of small mouse models to study atherogenic mechanisms (Jawień et al., 2004). Among available models, the apolipoprotein E-deficient (ApoE-knockout) mice is particularly popular, because of its propensity to spontaneously develop a full range of atherosclerotic lesions from fatty streaks to fibrous plaques, that are distributed throughout the arterial tree (Figure 8) and that present many features characteristic in appearance and distribution of those observed in human lesions (Nakashima et al., 1994).

ApoE, a glycoprotein synthesized mainly in the liver and brain in both human and mice, is a constituent of all lipoproteins except low- density lipoproteins (LDL). It functions as a ligand for receptors that clear chilomicrons and very low-density lipoprotein (VLDL) remnants. ApoE is also synthesized by monocytes and macrophages in vessel, and is thought to have local effects on cholesterol homeostasis and on inflammatory reactions in atherosclerotic vessel. It may also function in dietary absorption and biliary excretion of cholesterol.

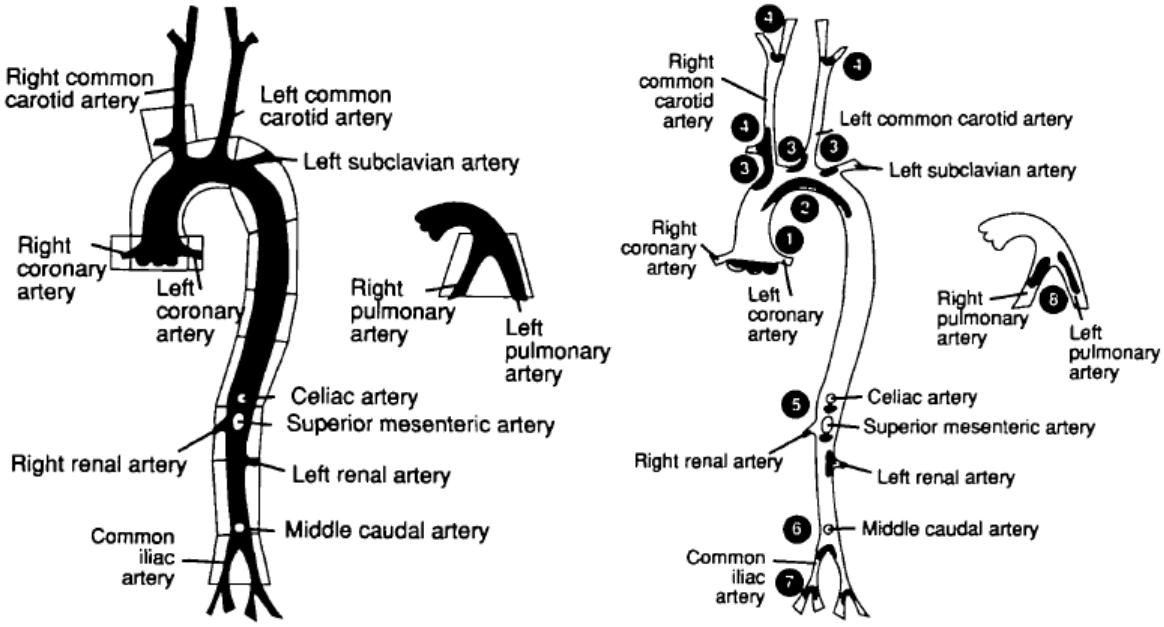

Figure 8. Line graphs showing the arteries from apoE-knockout mice. Left, Arteries that were observed under the dissecting microscope and dissected for further microscopic analysis. Right, Sites of predilection for lesions development are indicated in black: (1) aortic root, at the base of the valves; (2) lesser curvature of the aortic arch; (3) principal branches of the aortic arch; (4) carotid artery; (5) principal branches of the abdominal aorta; (6) aortic bifurcation; (7) iliac artery; and (8) pulmonary arteries (Nakashima et al., 1994).

The apoE-knockout mouse was created practically simultaneously in two separate laboratories, through gene inactivation by targeting. On a standard chow diet (0.02% cholesterol), the mice demonstrate a total cholesterol level >500mg/dl (5 times normal), mostly in the VLDL and chylomicron remnant fractions. These levels are unaffected by the age or sex of the animals. A Western- type diet (0.15% by weight cholesterol) quadruple these fractions. Interestingly, mice homozygous or heterozygous for the disrupted *ApoE* gene appear healthy and no difference in their body weights compared to normal mice is observed (Jawień et al., 2004; Meir and Leitersdorf, 2004).

Unlike normal mice, which don't develop atherosclerotic lesions (except for some strains on high fat/high cholesterol diets) (Vischer, 1999), a chronological analysis of atherosclerosis in

the apoE-knockout mouse has shown that the sequential events involved in lesion formation are strikingly similar to those in well-established larger animal models of atherosclerosis and in humans. Lesions in the apoE-knockout mice, as in humans, tend to develop at vascular branch points and progress from foam cell stage to the fibroproliferative stage with well-defined fibrous caps and necrotic lipid cores, although plaque rupture has not been observed in this or in any other mouse models. Progression of lesions appears to occur at a faster rate than in humans atherosclerosis, but the rapidity of the progression can be advantageous in many experimental situations. In particular, fatty streaks are first observed in the proximal aortas of a chow-fed, 3 months old mouse. On this diet, as early as 10 weeks of age, foam cells lesions are observed by light microscopy. Intermediate lesions containing foam cells and smooth muscle cells emerge around 15 weeks, and fibrous plaques appear at 20 weeks of age (Jawień et al., 2004; Meir and Leitersdorf, 2004).

These spontaneous lesions progress and cause severe occlusion of the coronary artery ostium by 8 months (Zhang et al., 1992). A western diet accelerates all the process (Figure 9).

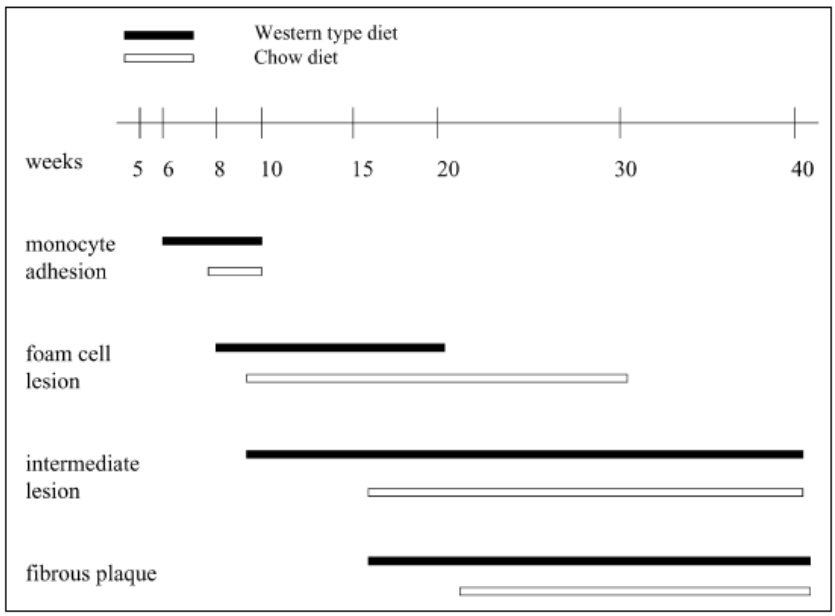

Figure 9. Diagram showing how lesion formation in chow-fed mice is delayed in comparison with mice fed the Western-type diet (Jawień et al., 2004).

Of note, the genetic background has a major effect on atherosclerosis susceptibility in strains of apoE-knockout mice. For example, lesions from 16-week chow diet C57BL/6 apoE-knockout are relatively larger than from FVB apoE-knockout mice and, in contrast to FVB mice, there is evidence of early development of fibrous caps (Jawień et al., 2004).

The development of murine models of atherosclerosis has revolutionized the approach to evaluating potential roles of specific proteins in lesion development. The crossing of these animals with mice that have been engineered to over-express or lack genes of interest, generating double knockout mice (e.g. iNOS$^{-/-}$ apoE$^{-/-}$; CCR2$^{-/-}$ apoE$^{-/-}$), has led to a growing list of proteins that accelerate or retard the rate at which lesions develop, and/or alter lesion composition (Glass and Witztum, 2001).

1.7 Renin-angiotensin system and diabetes development

1.7.1 Systemic versus local pancreatic RAS

The renin-angiotensin system (RAS) plays a key role in the regulation of fluid, electrolyte balance and arterial pressure (Reid et al., 1978). In the classical RAS, the glycoprotein Angiotensinogen is secreted into the circulation by the liver, where it is cleaved by renin, an aspartyl protease produced by the juxtaglomerular cells of the renal afferent arterioles, to release the decapeptide Angiotensin I. This decapeptide is further hydrolized by angiotensin converting enzyme (ACE), a metalloprotease produced by and anchored to the surface of endothelial cells, into the eight-amino acid peptide Angiotensin II (Ang II), which is able to bind to high affinity AT1 and AT2 cell-surface receptors (Lavoie and Sigmund; 2003). Ang II can also be formed via non-ACE and non-renin enzymes, including chymase, cathepsin G, cathepsin A, chymostatin-sensitive AII-generated enzyme (CAGE), tissue plasminogen activator (t-PA), and tonin (Urata et al., 1995; Urata et al., 1996). On the other side, ACE also breaks down bradykinin, a potent vasodilator and natriuretic hormone.

It has gradually become evident that in addition to the circulating RAS there is a local tissue RAS in most organs and tissues (Johnston et al., 1992; Paul et al., 2006). This makes RAS not only an endocrine, but also a paracrine and an intracrine system. Moreover the important discoveries of the renin/pro-renin receptor (Nguyen et al., 2002), the ACE2 enzyme (Donoghue et al., 2000; Tipnis et al., 2000), Angiotensin 1-7 as a biologic active metabolite of RAS (Santos and Ferreira, 2007), the Ang IV receptor as an insulin regulated aminopeptidase (IRAP) (Albiston et al., 2001), and the Mas as a receptor for Angiotensin 1-7 (Santos et al., 2003), have contributed to extend our view of the RAS from classical linear cascade to a more complex cascade with multiple mediators, receptors and functional enzymes (Figure 10).

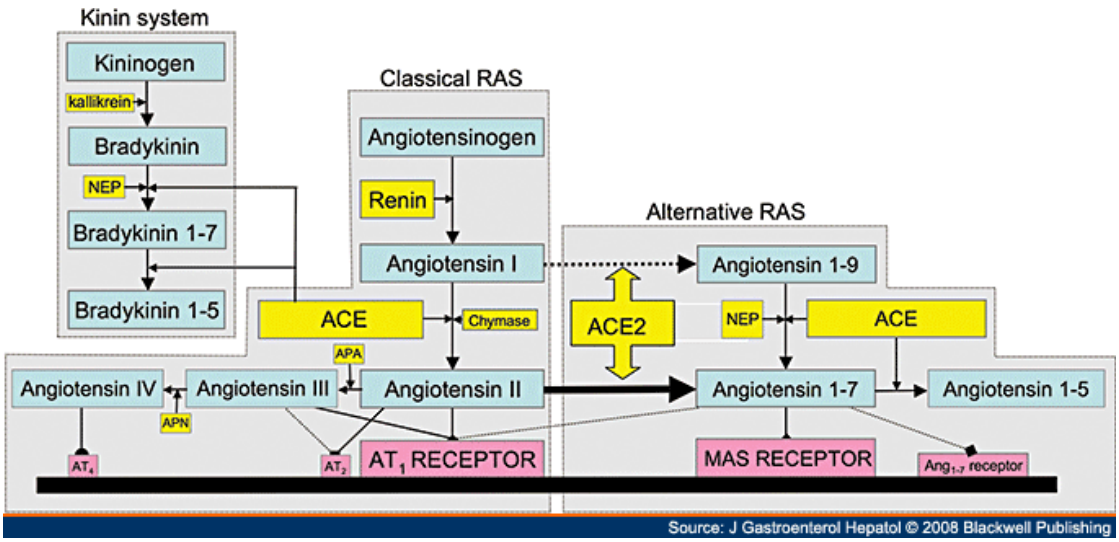

Figure 10. Enzymatic cascade of the renin-angiotensin system: classic and alternative pathways.

There is growing evidence supporting the existence of all the components of a functioning intrinsic RAS in the endocrine pancreas. (Pro)- renin is expressed in the islets of Langerhans, chiefly in the connective tissue surrounding the blood vessels and in reticular fibers within the islets (Leung and Chappell, 2003).

Both ACE and ACE2 mRNA has been found within islet with the former predominating in the microvasculature and the latter identifying within the centre of the islets (Tikellis et al., 2004).

Although initial studies, limited by low sensitivity of mRNA assays, found Angiotensinogen undetectable in normal rat pancreas (Campbell and Habener, 1986), more recent studies confirm that Angiotensinogen is expressed in glucagon-secreting α-cells located at the periphery of the islets of Langerhans (Regoli et al., 2003).

AT1 receptors have been detected in cells at the centre of the islet with its expression co-localized with that of insulin secreting beta cells. In contrast AT2 receptor has been localized to the outer region of islets and co-localizes with somatostatin-secreting cells (Tahmasebi et al., 1999).

Ang II is immunohistochemically localized predominantly in the endothelial cells of pancreatic blood vessels and the epithelial cells of pancreatic duct (Leung et al., 1998). Moreover, more recent studies have demonstrated that local genesis of Ang II occurs within pancreatic islets (Lau et al., 2004).

1.7.2 Physiological role of the RAS in the endocrine pancreas

There is converging evidence suggesting that in the endocrine pancreas, islet RAS has a role in regulating pancreatic islet secretion. In fact, Ang II has been shown to induce a dose-dependent reduction in both whole pancreatic and islet blood flow in the endocrine pancreas (Carlsson et al., 1998), and this effect, reversed by RAS antagonists, has suggested that locally released Ang II may consequently affect insulin release from pancreatic islets (Carlsson et al., 1998).

However, the precise mechanism by which Ang II is involved in islet dysfunction has yet to be elucidated. The regulation of insulin secretion by beta cells is different according to acute or chronic exposure of the pancreas to Ang II. Acute studies have demonstrated that Ang II inhibits insulin release in a dose-dependent manner from isolated mouse islets in response to a high glucose concentration (Lau et al., 2004). Similar results have been found in humans, where intravenous infusion of Ang II in pressor doses suppressed both basal and glucose-stimulated insulin secretion and increased insulin sensitivity in healthy volunteers (Townsend and DiPette, 1993). In chronic studies in mice, infusion of Ang II for 4 weeks cleared a glucose bolus faster than in mice treated with saline despite similar basal serum concentrations (Gletsu et al., 2005). Moreover, the increase in serum insulin was greater in Ang II treated mice, suggesting that Ang II-induced hyperinsulinemia may play a role in the development of insulin resistance in patients with hypertension (Gletsu et al., 2005).

Angiotensin II acting through AT2 receptor may stimulate somatostatin in a dose-dependent manner (Wong et al., 2004).

Taked together, these data suggest that both the local and systemic RAS have a functional role in regulating pancreatic islet insulin and somatostatin secretion although the relevance of these actions for normal activity in the healthy state remains to be established.

1.7.3 RAS and beta cell dysfunction

At a local level, the activity of the RAS in the endocrine pancreas is significantly upregulated in response to chronic hyperglycemia (Tikellis et al., 2004). Moreover it is now apparent that blockade of the RAS has important and direct effects in the prevention of islet cell dysfunction associated with type 2 diabetes (Tikellis et al., 2006; Lastra and Manrique, 2007). Beta cell damage in type 2 diabetes is likely due to a combination of genetic and acquired factors, still to be fully clarifed (Kahn et al., 2006). Among acquired factors, glucose toxicity, free fatty acids, amylin, islet fibrosis and oxidative stress may contribute to beta cell

dysfunction. RAS may potentiate the action of each of these pathways thus contributing to beta cell dysfunction.

Glucotoxicity: It is well established that chronic hyperglycemia leads to beta cell dysfunction and impaired-induced insulin gene expression and secretion (Poitout and Robertson, 2002). Moreover it has also been reported that hyperglycemia yields an increased apoptosis in cultured human pancreatic islets (Federici et al., 2001). Mechanisms implicated in glucotoxicity include: enhanced activity of protein kinase C (Oliveira et al., 2003), overactivation of the hexosamine pathway (Andreozzi et al., 2004) and generation of advanced glycation end products (AGEs) which in turn are associated with the reduced transcription of genes involved in insulin production (Tajiri et al., 1997). Notably, all these pathways lead to augmented production of reactive oxygen species (ROS) and the secondary oxidative stress could explain most of the observed beta cells defects (Robertson, 2004). Chronic hyperglycaemia per se can activate RAS in the endocrine pancreas (Lupi et al., 2006), and, under high glucose concentrations, ACE inhibition exerted beneficial effects on beta cells regarding insulin production and oxidative stress (Lupi et al., 2006). The RAS also significantly interacts with the generation and accumulation of AGEs in diabetes. It has been recently shown that blockade of the RAS attenuates the formation and tissue accumulation of AGEs in experimental diabetes (Forbes et al., 2002; Davis et al., 2004).

Lipotoxicity: Chronically elevated levels of fatty acid (FA) in plasma and in pancreatic islets have a negative impact on beta cell function resulting in decrease of glucose-stimulated insulin secretion (Jacqueminet et al., 2000). Importantly *in vitro* and *in vivo* studies have provided evidence that lipotoxicity only occurs in the presence of concomitantly elevated glucose levels (Harmon et al., 2001). Among the possibly mechanisms involved, inhibition of insulin gene expression, increased beta cell apoptosis and increased ceramide production are likely to play the major roles (Poitout and Robertson, 2008; Lupi et al., 2002). Notably, different FA have different effects on beta cells, with palmitate showing much more marked deleterious action than oleate (Poitout and Robertson, 2008; Marchetti et al., 2008). An increase of trigycerides accumulation in islets (Lee et al., 1994; Dubois et al., 2004) as well as an alteration in cholesterol metabolism may also play a relevant role in beta cell dysfunction. Experimental studies suggest that low density lipoprotein (LDL) and very low density lipoprotein (VLDL) exert proapoptotic actions on beta cells, an action that appears to be prevented by high density lipoprotein (HDL) (Roehrich et al., 2003).

Activation of the local RAS may interfere with some of the mechanisms of lipotoxicity. Independent from its hypotensive actions, the AT1 receptor blocker, olmesartan, is able to reduce the overproduction of trigycerides in fructose-fed (Okada et al., 2004) and Zucker fatty rats (Ran et al., 2004).
Ang II also inhibits proliferation of adipocytes (Janke et al., 2002) whereas blockade of the AT1 receptor stimulates adipogenesis (Schling and Löffler, 2001).

Fibrosis: The maintenance of the specialized architecture of the pancreatic islets is relevant for normal function (Charollais et al., 2000). Type 2 diabetes is associated with fibrosis within the islet interstitium causing disruption of islet architecture and loss of cell-to cell comunication (Tikellis et al., 2004). The RAS has been linked to increased fibrosis in a variety of tissues including the heart (Seccia et al., 2003), kidney (Satoh et al., 2001) and liver (Yoshiji et al., 2001). Locally increased production of Ang II results in AT1 mediated up regulation of the fibrogenic cytokines and growth factors including TGFβ and CTGF (Sun et al., 2000). In experimental diabetes blockade of the RAS is associated with attenuation of islet fibrosis and reduction of beta cell apoptosis (Tikellis et al., 2004).

Amyloid: Islet amyloid polipeptide (IAPP) or amylin is consistently found within the pancreatic islet in >90% of the type 2 diabetic patients and may contribute to beta cell dysfunction and death (Höppener et al., 2000). Amyloid-induced cytotoxicity appears to be mediated, at least in part, by increased oxidative stress in addition to increased apoptosis (Lastra and Manrique, 2007). IAPP gene is expressed almost exclusively in beta cells and the protein is co-secreted with insulin (Marchetti et al., 2008).
Recently it has been shown that it is the process of amyloid fibril formation or the formation of toxic IAPP oligomers, rather than the deposit of mature fibrils, to be cytotoxic (Meier et al., 2006).
The interaction between amylin and RAS has long been established. Amylin has been shown to increase plasma renin and aldosterone concentrations (Cooper et al., 1995), and, recently, it has been reported that treatment with either ACE inhibitors or AT1 receptor blockers is associated with a reduction in pancreatic amylin content (Satoh et al., 2001).

Oxidative stress: The beta cells are quite vulnerable to oxidative stress because of their low endogenous antioxidant activity (Hayden and Sowers, 2007). In experimental models of type 2 diabetes, increased level of oxidative stress are observed in the pancreas (Bindokas et al., 2003). Recent studies demonstrated that beta cells express p22 phox and gp91phox, the

membranous components of NADPH oxidase (Oliveira et al., 2003) and in beta cells glucose promotes the production of ROS at least in part by protein kinase C-dependent activation of NADPH oxidase (Oliveira et al., 2003). Ligand engagement of RAGE by ACE also results in the production of cellular ROS by activation of NADPH oxidase (Thallas-Bonke et al., 2008). It has been shown that the induction of oxidative stress results in decreased insulin expression and increased rate of apoptosis of beta cells both *in vivo* and *in vitro* with reduced expression and reduced nuclear translocation of PDX-1 (Kawamori et al., 2003).

Ang II increases NADPH oxidase activity in islets via AT1 receptors (Griendling et al., 1994). It has been shown that ACE inhibitors and AT1 receptor blockers inhibit NADPH oxidase in both *in vitro* (Griendling et al., 1994; Cai et al., 2002) and *ex vivo* (Onozato et al., 2002; Shao et al., 2006) studies.

Furthermore blockade of the RAS with perindopril or irbesartan significantly decreases oxidative stress within the endocrine pancreas as measured by percentage of nitrotyrosine in ZDP rats (Tikellis et al., 2004).

1.7.4 RAS inhibition and prevention of type 2 diabetes

A large body of evidence suggests that RAS blockade with either an ACE inhibitor or an AT1 receptor blocker may protect against the development of type 2 diabetes in patients with or without hypertension and at high risk for developing diabetes.

The first study was the Captopril Prevention Project (CAPPP), which evaluated the effects of captopril in comparison with conventional antihypertensive therapy (beta blockers or thiazide diuretic) in nearly 11000 hypertensive patients. Among the study participants, the incidence of new onset diabetes was reduced by 11% in the captopril treated group compared with conventional treatment after a mean follow up period of 6,1 years (Hansson et al., 1999). However there has been some debate over whether this finding might be attributable to adverse metabolic effects of the non-ACE inhibitor medications.

A post hoc analysis of the Heart Outcomes Prevention Evaluation (HOPE) trial showed a reduced incidence of new-onset diabetes in patients treated with ramipril also as compared with placebo, thus suggesting a true antidiabetic effect of ACE inhibitors (Yusuf et al., 2000). In this context, relevant are the results of the Antihypertensive and Lipid-lowering Treatment to prevent Heart Attack Trial (ALLHAT) study which demonstrated that new onset diabetes was lowest in the lisinopril group when compared not only with the thiazide diuretic chlortalidone, but also with amlodipine, a metabolically neutral calcium channel blocker (ALLHAT Officers and Coordinators for the ALLHAT Collaborative Research Group ,

2002). Similar results have been reported in other 3 trials with ACE inhibitors. Like the ACE inhibitors, also AT1 receptor blockers are known to exert positive metabolic effects. As with ACE inhibitors, initial evidence of the effects of AT1 receptor blockers on new-onset of diabetes come from studies like Losartan Intervention For Endpoint reduction (LIFE) trial (Lindholm et al., 2002) and the Antihypertensive treatment and Lipid Profile In a North-Sweden Evaluation (ALPINE) trial (Lindholm et al., 2003) in which they were compared with conventional therapies. Nevertheless the favorable effect of AT1 receptor blockers on new onset diabetes was observed also when they were compared with placebo (Yusuf et al., 2005) or calcium channel blockers (Julius et al., 2004). Recently a meta-analysis of 13 major trials was performed in an attempt to evaluate the effect of inhibiting the RAS system on the incidence of diabetes mellitus. The meta-analysis found an overall decrease in the incidence of diabetes mellitus from 9% to 7,1% when ACE inhibitors or AT1 receptor blockers were used (Andraws and Brown, 2007).

Several mechanisms have been suggested to explain the reduction in diabetes with RAS inhibition: enhanced insulin sensitivity, prevention of potassium depletion, effects on adipose tissue and protective effects on pancreatic structure and function. These mechanisms are not mutually exclusive and it is possible that several may combine to provide beneficial effects on metabolic function.

RATIONALE AND OBJECTIVES

In the general population, OPG is an independent risk factor for the progression of atherosclerosis and onset of cardiovascular disease (Kiechl et al., 2004; Ueland et al., 2005). Moreover, in patients with coronary artery disease OPG is associated with the severity of coronary atherosclerosis and mortality (Jono et al., 2002; Lieb et al., 2010; Schoppet et al., 2003; Ueland et al., 2004). Interestingly, different groups of investigators have reported that serum OPG levels are significantly increased in both type 1 and type 2 diabetic patients (Browner et al., 2001; Galluzzi et al., 2005; Knudsen et al., 2003; Rasmussen et al., 2006; Secchiero et al., a 2006) and in more recent studies performed in diabetic subjects a strong association between plasma levels of OPG and micro- and macroangiopathy was observed (Avignon et al., 2005; Grauslund et al., 2010; Knudsen et al., 2003; Xiang et al., 2009). A possible pathogenetic link between elevated levels of OPG and inflammation has been suggested by recent *in vitro* studies by our group (Zauli et al., 2007) and that of Mangan et al. (2007) demonstrating that exposure to recombinant OPG promotes leukocyte adhesion to endothelial cells. These findings are particularly noteworthy since atherosclerosis, which constitutes the single most important contributor to the growing burden of cardiovascular disease, is regarded as a form of chronic low-grade inflammatory process, which can ultimately lead to the development of complex lesions, or plaques, that protrude into the arterial lumen (Libby, 2002). Moreover, it has been recently demonstrated that OPG might be involved in the pathogenesis of pulmonary hypertension by promoting the growth of human vascular smooth muscle cells (VSMC), obtained from pulmonary artery (Lawrie et al., 2008). OPG is produced by a wide range of tissues, but it is noteworthy that different studies *in vitro* have demonstrated that OPG can be up-regulated in both endothelial cells (Secchiero et al., a 2006; Ben-Tal Cohen et al., 2007) and vascular smooth muscle cells (Zhang et al., 2002).

On these bases, my studies aimed to:

1. investigate whether OPG is involved in pathogenetic aspects of atherosclerosis, by coupling *in vitro* studies, performed by using murine primary VSMC, with *in vivo* studies, conducted in the apoE-knockout mice, that represent an optimal model for studies on the pathogenesis/treatment of atherosclerosis, in particular after induction of diabetes mellitus;

2. investigate whether OPG is involved in pancreatic beta cell dysfunction, using an *in vivo* model represented by C57Bl/6J mice, that do not spontaneously develop atherosclerotic lesions with a normal chow diet. Moreover, taking in consideration some evidences for an interplay between OPG and the RAS pathways in human aortas, where OPG has been shown to modulate angiotensin II type 1 receptor gene expression (Moran et al., 2009) and, in turn, angiotensin II promotes OPG production (Zhang et al., 2002), investigate whether the long term co-treatment with the ACE inhibitor ramipril could eventually hinder the effect of exogenous OPG on beta cells remodelling and function.

MATERIALS AND METHODS

STUDY 1. A-B

3.1 Animals and experimental protocol

Animal care and treatments were conducted in conformity with institutional guidelines in compliance with national and international laws and policies (EEC Council Directive 86/609, OJL 358, December 12th 1987). 80 apoE-knockout ($apoE^{-/-}$) male mice were further randomized into 4 groups (n=20) and followed for 3 months. One group of non diabetic animals received every 3 weeks an intraperitoneal (i.p.) injection of vehicle (HEPES-buffered saline) and served as a control; another group of non-diabetic animals received every 3 weeks an i.p. injection of human recombinant OPG (OPG) (R&D Systems) (1µg/mouse in a total of 200µl HEPES-buffered saline). The other two groups, rendered diabetic by 5 daily i.p. injections of streptozotocin (STZ) (55mg/Kg body weight), received injections of OPG or an equivalent volume of vehicle. After 3 months, the animals were anesthetized by an i.p. injection of pentobarbital sodium (60 mg/Kg body weight) and sacrificed for blood tests and histological examination. In half of the animals in each group, aortas were collected and placed in 10% neutral buffered formalin for subsequent immunohistochemical analysis. In the other half, aortas were snap frozen in liquid nitrogen and stored at –80°C for subsequent RNA extraction. In each group of animals, serum glucose, glycosylated hemoglobin (HbA_{1c}), systolic blood pressure, triglycerides, total and HDL cholesterol were determined according to standard procedure (Candido et al.; 2004, Secchiero et al., b 2006).

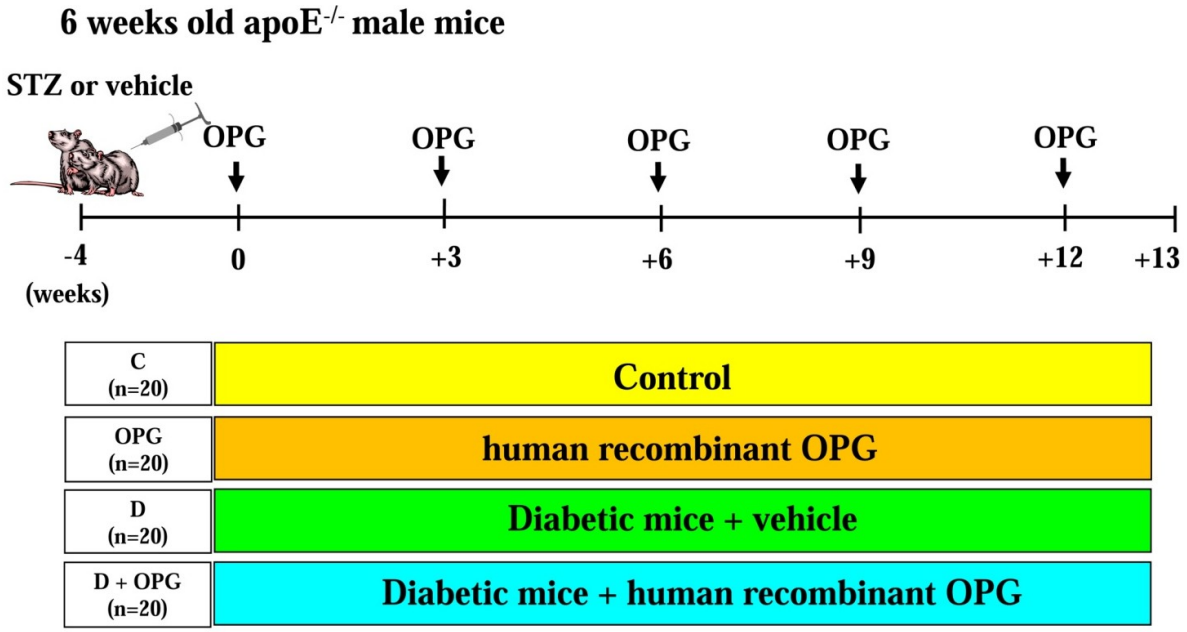

3.2 Evaluation of atherosclerotic plaques

To evaluate the atherosclerotic lesions, two complementary approaches were used: en face whole and histological section analyses. The en face approach was used to obtain information about distribution and extent of atherosclerosis in the aorta, whereas microscopic histological analysis was used to evaluate the lesion composition and complexity. In brief the entire aorta, stained with Sudan IV-Herxheimer's solution (Sigma), was opened longitudinally and lesion area measurements were performed by calculating the proportion of aortic intimal surface area occupied by the red stain in the arch, descending thoracic and abdominal aorta, with the use of a video-based image analysis program (MCID; Imaging Research). All aortic segments were next paraffin-embedded, and 4-μm thick cross-sectional serial sections were obtained. Hematoxylin-eosin staining of the aorta was used for featuring plaque morphology.

3.3 Masson's trichrome staining

Cross-sectional paraffin aortic serial sections four micron thick were prepared and stained with Masson's trichrome to evaluate the presence of collagen. Collagen was quantified by calculation of the proportion of area occupied by the Masson's trichrome staining within the aortic media or within the plaque by use of an image analysis system (Image Pro Plus® 6.3 Software, Media- Cybernetics) associated with a videocamera and a computer (Candido et al.; 2004).

3.4 Immunohistochemistry

For immunohistochemical analysis, four micron paraffin serial sections of aorta were de-waxed and hydrated, and the endogenous peroxidase was neutralized with 3% (v/v) hydrogen peroxide in phosphate-buffered saline (PBS, pH 7.4) for 20 minutes. Subsequently, aortic sections were incubated with the following primary antibodies: α-smooth muscle actin (α-SMA, smooth muscle cell marker) and proliferating cell nuclear antigen PCNA (both from DAKO; diluted 1:50). Biotinilated immunoglobulins (Vector Laboratories; diluted 1:200) were then applied as a secondary antibody, followed by horseradish peroxidase-conjugated streptavidin (DAKO; diluted 1:625). Macrophage detection was performed by using the primary antibody for F4/80 (Serotec; diluted 1:200), followed by secondary anti-rat immunoglobulins (Vector Laboratories; diluted 1:200) and the CSA mouse amplification kit (DAKO), following manufacturer's instructions. Syndecan-1 detection was performed using monoclonal rat anti-mouse CD138 (BD Pharmingen; diluted 1:500), followed by secondary biotinylated rabbit anti-rat antibody (Vector Laboratories; diluted 1:200) and the ABC kit

(Vector Laboratories), following the manufacturer's instructions. OPG localization was performed by using biotinylated primary antibody for OPG (R&D Systems; diluted 1:10) and the CSA mouse amplification kit.

3,3'-diaminobenzidine tetrahydrochloride (Sigma Chemical) was used as a chromogen, with subsequent nuclear counterstaining with hematoxylin. All the sections were then examined by light microscopy and digitized using an high-resolution camera. Atherosclerotic lesions were manually traced on the computer, taking care to exclude normal-appearing media and to include only the intimal/subintimal atherosclerotic lesion. Quantifications of collagen staining and of the specific immunostainings within the plaques or in the aortic media were assessed using Image Pro Plus® 6.3 analysis system.

3.5 Real-time quantitative PCR

Total RNA was isolated from cultured vascular smooth muscle cells (VSMC) and tissue samples by the TRIZOL method (Invitrogen, Milan, Italy) . A reverse transcriptase reaction was performed on three micrograms of RNA using random hexamers, dNTPs and M-MLV reverse transcriptase (Invitrogen). Angiopoietin 2, vascular cell adhesion molecule-1 (VCAM-1), osteoprotegerin (OPG), alpha-smooth muscle actin (αSMA), fibronectin (Fibr), vimentin (Vim), connective tissue growth factor (CTGF), collagen I (col I), collagen III (col III), collagen IV (col IV), nuclear factor kB (NF-kB), and transforming growth factor-beta (TGFβ) gene expressions were analyzed by real-time quantitative RT-PCR using the TaqMan system based on real-time detection of accumulated fluorescence (ABI Prism 7900HT, Applied Biosystems). To control for variation in the amount of cDNA available for PCR in the different samples, gene expression of the target sequence was normalised in relation to the expression of an endogenous control, 18S ribosomal RNA (rRNA) (18S rRNA TaqMan Control Reagent kit; Applied Biosystems). Specific primers and Taqman probes (Table 1) were constructed with the help of Primer Express (PE Applied Biosystems). Results were expressed relative to control which was arbitrarily assigned a value of 1. Values are shown as means ± SEM unless otherwise specified.

3.6 Cell cultures

Isolated primary rat aortic VSMC were purified and used between passages 3 and 6 (Pandolfi et al., 2003). Aortic mouse VSMC were kindly provided by Doctor Agrotis (Baker Institute, Melbourne, Australia) and generated as previously described by his group (Agrotis et al., 2004).

Subcultured mouse VSMC were maintained in high glucose (25mM) DMEM containing 10%FBS at 37°C, 5% CO_2. Experimental treatments were in serum reduced conditions (2% FBS) with recombinant human TGFβ1 (1-10ng/ml) or recombinant human OPG (1-40ng/ml) (both from R&D Systems) for 48h. To examine the effect of the block of the TGFβ- type 1 receptor, the inhibitor SB431542 (R&D Systems) was added 1 hour before the addition of TGFβ or OPG. The experiments were designed so that the cells, seeded in 6-well plates, reached 90-95% confluence the day of the harvesting. At the end of the incubation time, the media was collected, centrifuged to discard dead cells, and stored aliquoted at -80°C for the subsequent soluble murine OPG quantification. The cells monolayer was then washed two times with ice-cold PBS, and RNA was extracted for gene expression evaluation.

For cell cycle analysis, rat primary VSMC were seeded at subconfluence, made quiescent by using serum-reduced (0.1% FBS) medium and either left untreated or exposed to OPG (10-100pg/ml) for 36 hours before incubation with 5-bromodeoxyuridine (BrdU; Sigma Chemical) at 37°C for 1 hour. Anti-BrdU antibody was bound to BrdU incorporated into neosynthesized DNA, and the complex was detected by fluorescein isothiocyanate-conjugated secondary antibody. Cells were stained with propidium iodide (PI) and analyzed by flow cytometry. The percentage of cells in the S phase of the cell cycle was calculated from the flow cytograms and expressed as the percentage of the total population. As positive control, cells were treated with insulin. To avoid nonspecific fluorescence from dead cells, live cells were gated tightly using forward and side scatter, according to standard method (Borgatti et al., 1997).

3.7 Immunofluorescence

VSMC were grown on coverslips, washed twice with PBS, fixed in ice cold acetone for 10 minutes, permeabilized using 0.1% Triton X- 100, and incubated in a blocking buffer (10% normal rabbit serum in PBS) for 30 minutes. Primary antibody against αSMA (DAKO) was incubated with cells overnight, followed by a rabbit anti mouse 488. Coverslips were mounted using Prolong Gold antifade reagent with DAPI (Invitrogen) and cells viewed using an Olympus BX61 Fluorescence microscope.

3.8 Osteoprotegerin ELISA

Mouse OPG was measured in diluted growth media by using a sandwich-type enzyme-linked immunosorbent assay (DuoSet ELISA Development System, R&D Systems) . Microtitre wells were coated with 4.0μg/ml of a rat anti-mouse OPG capture antibody, and detection was

done with 200ng/ml of a biotinylated goat anti- mouse OPG antibody. Streptavidin conjugated to horseradish-peroxidase was used for detection of bound biotynilated immunoglobulin, and tetramethylbenzidine was added as substrate. The optical density was read at 450nm on a microplate reader and compared to a seven point standard curve made with recombinant mouse OPG. All standards and samples were loaded in duplicate.

3.9 Statistical analysis

The mean, median, minimum, and maximum values were calculated for each group of data. Box plots were used to show the median, minimum and maximum values and 25th to 75th percentiles. Data were analyzed by ANOVA and with the Mann-Whitney rank-sum test. Comparison of group means was performed by Bonferroni method. Correlation coefficients were calculated by the Spearman's method. Statistical significance was defined as $p<0.05$.

Table 1. TaqMan Primers and Probe Sequences used for real-time RT-PCR in mouse VSMC and aortas extracts

Name	Sequence
Angiopoietin 2 probe	FAM-5'- CAGCCAACCAGGAAG -MGB
Angiopoietin 2 primer F	5'- GTCCAACTACAGGATTCACCTTACAG -3'
Angiopoietin 2 primer R	5'- TTGTCCGAATCCTTTGTGCTAA -3'
Osteoprotegerin probe	FAM-5'- CGAACCTCACCACAGAG -3'-MGB
Osteoprotegerin primer F	5'- GCGTGCAGCGGCATCT -3'
Osteoprotegerin primer R	5'- TCAATCTCTTCTGGGCTGATCTT -3'
CTGF probe	FAM-5'-ACTGCCTGGTCCAGAC-MGB
CTGF primer F	5'-GCTGCCTACCGACTGGAAGA-3'
CTGF primer R	5'-CTTAGAACAGGCGCTCCACTCT-3'
VCAM-1 probe	FAM-5'-CGGCATCCTGCAGCTGTGCCT-3'-TAMRA
VCAM-1 primer F	5'-AAGTCTGTGGATGGCTCGTACA-3'
VCAM-1 primer R	5'-TCAGTCTTAGATTCACACTCGTATATGC-3'
αSMA probe	FAM-5'- TGCCAGATCTTTTCC -3'-MGB
αSMA primer F	5'- GACGCTGAAGTATCCGATAGAACA -3'
αSMA primer R	5'- GGCCACACGAAGCTCGTTAT -3'
Fibronectin probe	FAM-5'- CCCCGTCAGGCTTA -3'-MGB
Fibronectin primer F	5'- ACATGGCTTTAGGCGGACAA -3'
Fibronectin primer R	5'- ACATTCGGCAGGTATGGTCTTG -3'
Vimentin probe	FAM-5'- CCGCACCAACGAGA -3'-MGB
Vimentin primer F	5'- CGCCATCAACACTGAGTTCAA -3'
Vimentin primer R	5'- TGGCAAAGCGGTCATTCA -3'
collagen I probe	FAM-5'- ATCGACCCTAACCAAG -3'-MGB
collagen I primer F	5'- GACTGGAAGAGCGGAGAGTACTG -3'
collagen I primer R	5'- CCTTGATGGCGTCCAGGTT -3'
collagen III probe	FAM-5'- AATATCAAACACGCAAGGC -3'-MGB
collagen III primer F	5'- GGGAATGGAGCAAGACAGTCTT -3'
collagen III primer R	5'- TGCGATATCTATGATGGGTAGTCTCA -3'
collagen IV probe	FAM-5'- CAGTGCCCTAACGGT -3'-MGB
collagen IV primer F	5'- GGCGGTACACAGTCAGACCAT -3'
collagen IV primer R	5'- GGAATAGCCGATCCACAGTGA -3'

NF-kB probe	FAM-5’- AGCTCAAGATCTGCCG -3’-MGB
NF-kB primer F	5’- TCTCACATCCGATTTTTGATAACC -3’
NF-kB primer R	5’- CGAGGCAGCTCCCAGAGTT -3’
TGFβ probe	FAM-5’-AAAGCCCTGTATTCCGT-MGB
TGFβ primer F	5’-GCAGTGGCTGAACCAAGGA-3’
TGFβ primer R	5’-GCAGTGAGCGCTGAATCGA-3’

FAM=6-carboxyfluorescein, TAMRA (quencher)=6-carboxy-tetramethylrhodamine, MGB=minor groove binder

STUDY 2

4.1 Animals and experimental protocol

Animal care and treatments were conducted in conformity with institutional guidelines in compliance with national and international laws and policies for the care and use of laboratory animals. 40 male mice C57B1/6J, aged 10 weeks, were randomized into 4 groups and studied for 12 weeks. Group 1 received every 3 weeks an i.p. injection of vehicle and served as a control. Group 2 received every 3 weeks an i.p. injection of human recombinant OPG (R&D Systems), (1μg/mouse in a total of 200 μl HEPES-buffered saline). Group 3 received the ACE inhibitor ramipril (Sigma Aldrich) at the dose of 10 mg/Kg/die in drinking water in co-treatment with i.p. injections of vehicle. Group 4 received ramipril in co-treatment with i.p. injections of OPG. The animals were maintained on regular mouse chow. Ramipril was added to the drinking water, stored at 4°C and replaced twice a week. Previous studies had demonstrated that ramipril remains stable in water for more than four days at room temperature and that the dosage used in mice is well below the toxic range and equivalent to the maximum therapeutic dose of 10 mg per day in humans (Gross et al., 2003). Adjustment of drug concentration according to the fluid intake ensured that the daily dose was applied during the whole experiment. In addition, our group has previously shown the effectiveness of an oral chronic delivery of ACE inhibitor (Candido et al., 2002).

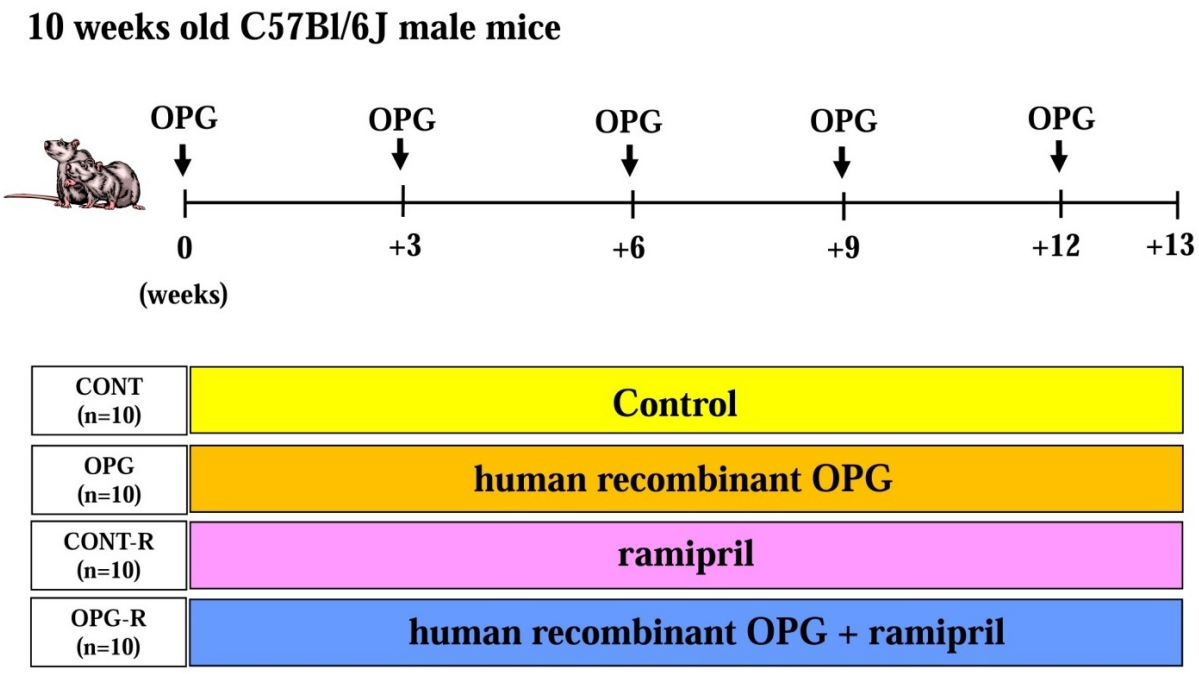

4.2 Measurement of physiological and biochemical parameters

At 4-week intervals, the following parameters were measured in all groups: body weight; systolic blood pressure measured by tail-cuff plethysmography in conscious, prewarmed mice; fasting glucose levels using a glucose oxidase method (Menarini); and fasting insulin serum levels. After 3 months, animals were anesthetized by an i.p. injection of pentobarbital sodium (60 mg/Kg body weight). Blood was collected from the left ventricle and centrifuged and serum was stored at -20° C for subsequent analysis. The mouse pancreas was rapidly dissected out and bisected longitudinally, with one half snap frozen in liquid nitrogen and stored at -80° C for subsequent quantitative RT-PCR measurements, and the other half fixed in 4% paraformaldehyde and embedded in paraffin for immunohistochemical studies.

4.3 Oral glucose tolerance test

An oral glucose tolerance test was performed at the end of the experimental study. For this purpose, conscious mice, overnight fasted, received an oral glucose bolus (1g/Kg body weight) by gavage and blood was collected from the tail vein at 0, 30, 90 and 120 minutes (Chu et al., 2006). Serum insulin levels were determined by using the Mouse Insulin ultrasensitive ELISA kit (DRG International).

4.4 Picrosirius red staining

Interstitial fibrosis was determined after picrosirius red staining. Four-micron paraffin sections were prepared from 4% paraformaldeyde-fixed, paraffin-embedded mice pancreas. Sections were stained with 0.1% Sirius red (Direct red 80; Fluka Chemika) in satured picric acid for 90 minutes and mounted; subsequently all the sections were examined by bright-field and polarization microscopy (Olympus BX50WI) and then digitized with a high resolution camera (Q-Imaging Fast 1394). Collagen deposition appears red in sections analyzed in bright-field microscopy, whereas exhibits strong birefringence in polarized light microscopy. The quantification of fibrosis was performed calculating the proportional area of each islet or of islet boundaries occupied by the positive red staining, using an image analysis system (Image Pro-Plus 6.3 Software).

4.5 Immunohistochemistry

The expression of the beta cell marker insulin, ACE and AT1 receptor were examined by immunohistochemistry on four-micron paraffin pancreas sections. The primary antibodies used were a polyclonal guinea pig anti-swine insulin antibody (DAKO; diluted 1:100), a

monoclonal mouse anti-human ACE antibody (Chemicon, diluted 1:100), and a polyclonal rabbit anti-human AT1 receptor antibody (Santa Cruz Biotechnology; diluted 1:200). After neutralization of endogenous peroxidase, the sections were incubated with the primary antibodies for 1 hour at room temperature for ACE and AT1 receptor or overnight at 4°C for insulin. After washing, biotinylated secondary antibodies (all from Vector Laboratories) were applied for 60 minutes for ACE and AT1 receptor or 30 minutes for insulin. Specific immunohistochemical staining was detected using the standard avidin-biotin complex (Vector Laboratories) method. After an extensive washing, the final detection step was carried out using 3,3'-diaminobenzidine tetrahydrochloride as the chromogen.

Detection of cells of the monocytic/macrophagic lineage was performed by using the primary antibody for F4/80 (AbD Serotec; diluted 1:200), followed by secondary anti-rat immunoglobulins (Vector Laboratories; diluted 1:200) and the CSA mouse amplification kit, following manufacturer's instructions.

After counterstaining with hematoxylin, all the sections were examined by light microscopy (Olympus BX50WI) and digitized with a high resolution camera (Q-Imaging Fast 1394). Semiquantitative assessment of islet proteins was performed by determining the percentage proportion of area or number of cells per islet section occupied by the brown (DAB) staining within each islet (20X objective) using an image analysis system (Image Pro Plus® 6.0 Software). A total of 40-50 islets per mouse pancreas (n=10 mice/group) were analyzed.

Pancreatic beta cell mass was estimated by multiplying the mean density of staining for insulin in the islet sections by the mean islet area per area of pancreas. This was expressed in arbitrary units adjusted for the pancreatic wet weight for individual animals (Tikellis et al., 2004).

4.6 In situ detection of apoptosis

The localization of beta cell apoptosis was identified using dual immunofluorescence for Terminal Deoxynucleotidyl Transferase-Mediated dUTP Nick End Labeling (TUNEL) and insulin staining. After digestion with Proteinase K (20 μg/ml; Sigma Chemical), four micron paraffin sections were labeled with polyclonal guinea pig anti swine insulin (DAKO; diluted 1:100), followed by a Texas Red dye-conjugated secondary antibody (Vector Laboratories; diluted 1:100). Slides were subsequently labeled for TUNEL-positive cells and visualized using fluorescein dye according to the manufacturer's instructions (Roche Diagnostic). TUNEL-positive beta cells were identified by the presence of green nuclei and red cytoplasm.

4.7 Real-Time quantitative PCR

Total RNA was isolated from snap-frozen pancreatic tissue after homogenisation in Trizol (Invitrogen), and processed as reported in paragraph *3.5* of the Material and Methods section. Briefly, angiotensin converting enzyme (ACE), angiotensin II type 1 (AT1) receptor, monocyte chemotactic protein (MCP-1), vascular adhesion molecule type 1 (VCAM-1), transforming growth factor-β (TGFβ) and connective tissue growth factor (CTGF) gene expressions were analyzed by real-time quantitative RT-PCR using the TaqMan system (ABI Prism 7900HT). To control for variation in the amount of cDNA available for PCR in the different samples, gene expression of the target sequence was normalized in relation to the expression of an endogenous control, 18S ribosomal RNA. Specific primers and Taqman probes for ACE, AT1 receptor, MCP-1, VCAM-1, TGFβ and CTGF (Table 2) were constructed with the help of Primer Express (PE Applied Biosystem). Each sample was tested in triplicate. Results were expressed relative to control pancreas values, which were arbitrarily assigned a value of 1.

4.8 Statistical analysis

Analysis of variance (ANOVA), calculated using Statview 512 software for Apple Macintosh computer (Brainpower), was used to determine the presence of significant difference between groups. Comparisons of group means were performed by Fisher's least significant difference (LSD) method unless otherwise specified. Results are expressed as mean ± SEM. A p value of less than 0.05 was considered statistically significant.

Table 2. TaqMan Primers and Probe Sequences used for real-time RT-PCR in pancreas extracts

Name	Sequence
ACE probe	FAM-5'-CAACAAGACTGCCACCTGCTGGTCC-3'-TAMRA
ACE primer F	5'-CAGAATCTACTCCACTGGCAAGGT-3'
ACE primer R	5'-TCGTGAGGAAGCCAGGATGT-3'
AT1 receptor probe	FAM-5'-TACCAGTGGCCCTTCGGCAATCA-3'-TAMRA
AT1 receptor primer F	5'-GGGCAGTTTATACCGCTATGGA-3'
AT1 receptor primer R	5'-TGGCCGAAGCGATCTTACAT-3'
CTGF probe	FAM-5'-ACTGCCTGGTCCAGAC-MGB
CTGF primer F	5'-GCTGCCTACCGACTGGAAGA-3'
CTGF primer R	5'-CTTAGAACAGGCGCTCCACTCT-3'
VCAM-1 probe	FAM-5'-CGGCATCCTGCAGCTGTGCCT-3'-TAMRA
VCAM-1 primer F	5'-AAGTCTGTGGATGGCTCGTACA-3'
VCAM-1 primer R	5'-TCAGTCTTAGATTCACACTCGTATATGC-3'
MCP-1 probe	FAM-5'-TCCCTGTCATGCTTCTGGGCCTGT-3'-TAMRA
MCP-1 primer F	5'-CTTCCTCCACCACCATGCA-3'
MCP-1 primer R	5'-CCAGCCGGCAACTGTGA-3'
TGFβ probe	FAM-5'-AAAGCCCTGTATTCCGT-MGB
TGFβ primer F	5'-GCAGTGGCTGAACCAAGGA-3'
TGFβ primer R	5'-GCAGTGAGCGCTGAATCGA-3'

FAM=6-carboxyfluorescein, TAMRA (quencher)=6-carboxy-tetramethylrhodamine, MGB=minor groove binder

RESULTS

STUDY 1.A

5.1 Increase of atherosclerotic plaque development in diabetic apoE$^{-/-}$ mice after in vivo administration of full-length recombinant human OPG

Since it has been previously demonstrated that the serum levels of OPG are elevated in diabetic and nondiabetic patients affected by cardiovascular disease (Jono et al., 2002; Schoppet et al., 2003; Kiechl et al., 2004; Moran et al., 2005; Secchiero et al., a 2006; Shin et al., 2006; Abedin et al., 2007), in the first group of experiments we investigated the possible role of OPG *in vivo* in the pathogenesis of atherosclerosis. For this purpose we utilized the apoE$^{-/-}$ mouse model, that spontaneously develop atherosclerotic lesions, which are increased after induction of diabetes and resemble in appearance and distribution those observed in humans (Calkin and Allen, 2006). Therefore, 3 weeks after STZ or vehicle (buffer citrate alone) multiple injections, the animals were randomized to be i.p. injected either with recombinant human OPG or with control vehicle (HEPES buffered saline). It should be noticed that repeated i.p. injections of human recombinant OPG (every 3 weeks for 3 months) were well tolerated by the apoE$^{-/-}$ mice. After 3 months, diabetic and control animals were analyzed for various parameters, as reported in Table 1, and then sacrificed to perform pathological examination. Diabetic animals gained less weight than did control mice. Blood glucose, HbA_{1c}, total cholesterol, triglycerides and HDL cholesterol were increased in diabetic apoE$^{-/-}$ mice compared with nondiabetic control mice. All of these parameters were not significantly different in diabetic animals injected or not with human recombinant OPG. The OPG injections in apoE$^{-/-}$ mice did not alter significantly the general parameters, however a slight increase in serum glucose levels was seen in respect to control animals. Systolic blood pressure levels did not differ significantly among all the groups studied. Moreover, no gross abnormalities at necroscopic examination were observed in OPG-treated animals with respect to vehicle-treated apoE$^{-/-}$ mice.

En face dissection of aorta segments revealed that diabetes was associated with a significant increase in percentage of plaque area in the entire aorta (means ± SEM: 1.64 ± 0.15 vs 0.51 ± 0.05, in diabetic vs control apoE$^{-/-}$ mice respectively; $p<0.0001$) as well as in each segment (means ± SEM in arch: 3.87 ± 0.51 vs 1.24 ± 0.34, $p<0.001$; means ± SEM in thoracic aorta: 1.0 ± 0.14 vs 0.13 ± 0.04, $p<001$; means ± SEM in abdominal aorta: 1.1 ± 0.22 vs 0.19 ± 0.13, $p<0.05$).

Moreover, in non-diabetic control mice most plaques were fatty streaks, whereas in the aorta

of diabetic mice there were predominantly advanced lesions, characterized by an asymmetrically thickened intima and an increase in the collagen content within the plaque, clearly detected by Masson's trichrome staining (Figure 1).

While non-diabetic apoE$^{-/-}$ mice injected with OPG did not show a significant change in the plaque area extent (means ± SEM: 0.74 ± 0.23), interestingly, OPG treatment in diabetic apoE$^{-/-}$ mice induced a significantly (means ± SEM: 2.25 ± 0.24, $p<0.05$) increase in the total plaque area with respect to diabetic mice injected with vehicle alone (Figure 2). Such increase could not be ascribed to an aspecific, allergic or toxic effect consequent to the injection of a human protein in the apoE$^{-/-}$ animals since the administration of recombinant human TRAIL promoted the opposite effect, decreasing the total plaque area extent (Secchiero et al., b 2006).

Parameters	**C (n = 20)**	**OPG (n = 20)**	**D (n = 20)**	**D + OPG (n = 20)**
Body weight (g)	34 ± 4	36 ± 3	25 ± 2*	24 ± 3*
Serum glucose (mg/dl)	157 ± 38	187 ± 73	549 ± 42*	532 ± 39*
HbA_{1c} (%)	3.9 ± 0.9	4.0 ± 0.7	14.0 ± 1.2*	13.3 ± 1.3*
SBP (mmHg)	86 ± 10	86 ± 9	87 ± 9	94 ± 8
Total cholesterol (mg/dl)	448 ± 100	538 ± 155	915 ± 105*	949 ± 119*
Triglycerides (mg/dl)	111 ± 33	120 ± 42	208 ± 44*	200 ± 16*
HDL cholesterol (mg/dl)	66 ± 14	68 ± 14	116 ± 27*	91 ± 12*

Table 1. Characteristics of the mice at the end of the study. Data are expressed as mean ± SD and statistically (ANOVA) compared. SBP, systolic blood pressure; C, control mice; OPG, mice injected with recombinant human OPG; D, diabetic mice injected with vehicle; D + OPG, diabetic mice injected with OPG. *$p<0.01$ vs C group

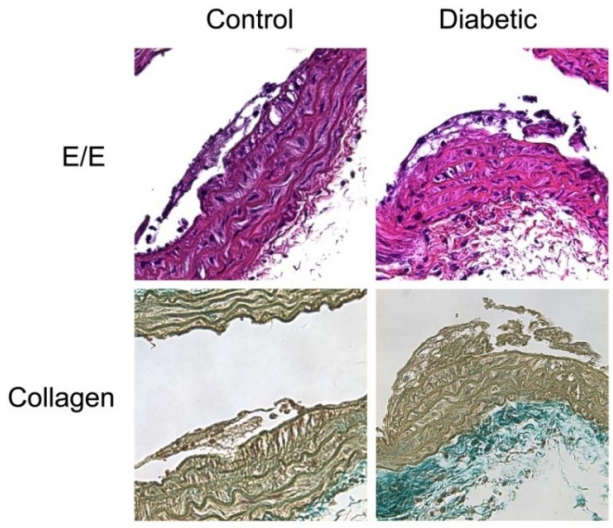

Figure 1. Increase in atherosclerotic lesions in the aorta of apoE$^{-/-}$ mice following induction of diabetes. Representative images of aorta of control and diabetic apoE$^{-/-}$ mice stained with hematoxylin and eosin (upper panel) and with Masson's trichrome for collagen detection (lower panel, light blue staining). Original magnification X20.

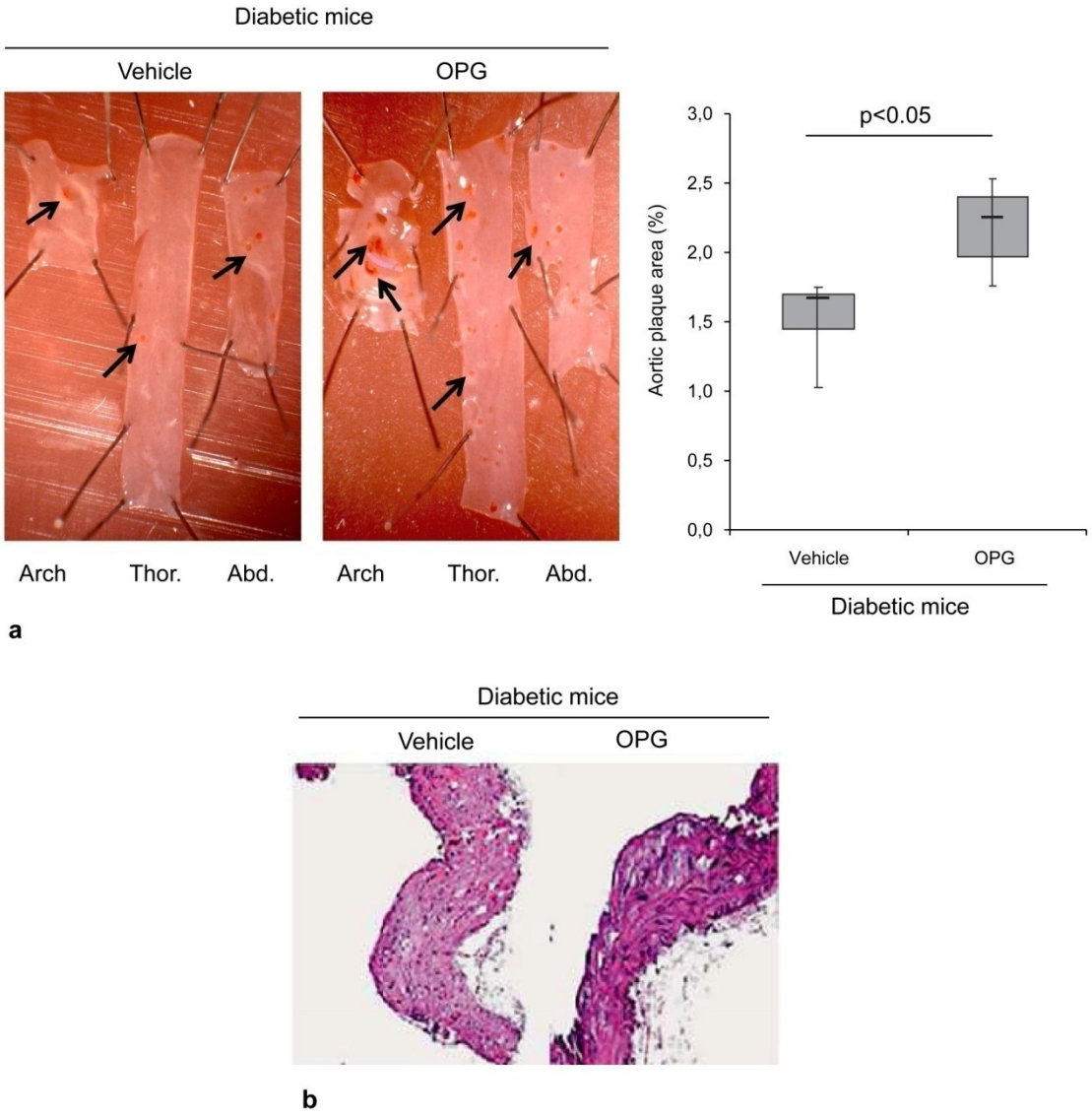

Figure 2. Increase in the total extent of atherosclerotic plaques in diabetic mice following the OPG injections. a. Representative images of en face dissection of aortic arch, thoracic and abdominal aorta, stained with Sudan IV, showing atherosclerotic lesions (red, with arrows) in diabetic apoE$^{-/-}$ mice treated with either vehicle (n=10) or recombinant human OPG (n=10). Atherosclerotic involvement for each mouse was quantitatively determined in en face sections by measuring the proportion of aortic intimal surface area stained red (Sudan IV-positive) in each of the 3 aortic segments. Horizontal bars are medians of the percentage of plaque area in the total aortas, upper and lower edges of the boxes are 75th and 25th percentiles and vertical lines are 10th and 90th percentiles. **b**. Representative hematoxylin-eosin-stained histological cross-sections are shown. Original magnification X20.

5.2 Recombinant human OPG injected in vivo in apoE$^{-/-}$ diabetic mice induces changes in the histological composition of the atherosclerotic plaques

Subsequently, we investigated whether, besides increasing the extension of atherosclerotic lesions in diabetic mice, OPG treatment also affected the histological characteristics of the plaques. For this purpose, cross-sectional serial paraffin sections of the aortic atherosclerotic lesions of apoE$^{-/-}$ diabetic mice were quantitatively analyzed for the presence of collagen and the cell composition of the plaques (Figure 3,4). Of note, no significant differences in the

percentage of infiltrating macrophages or in the collagen content were observed between OPG- and vehicle-injected mice (Figure 3a,b).

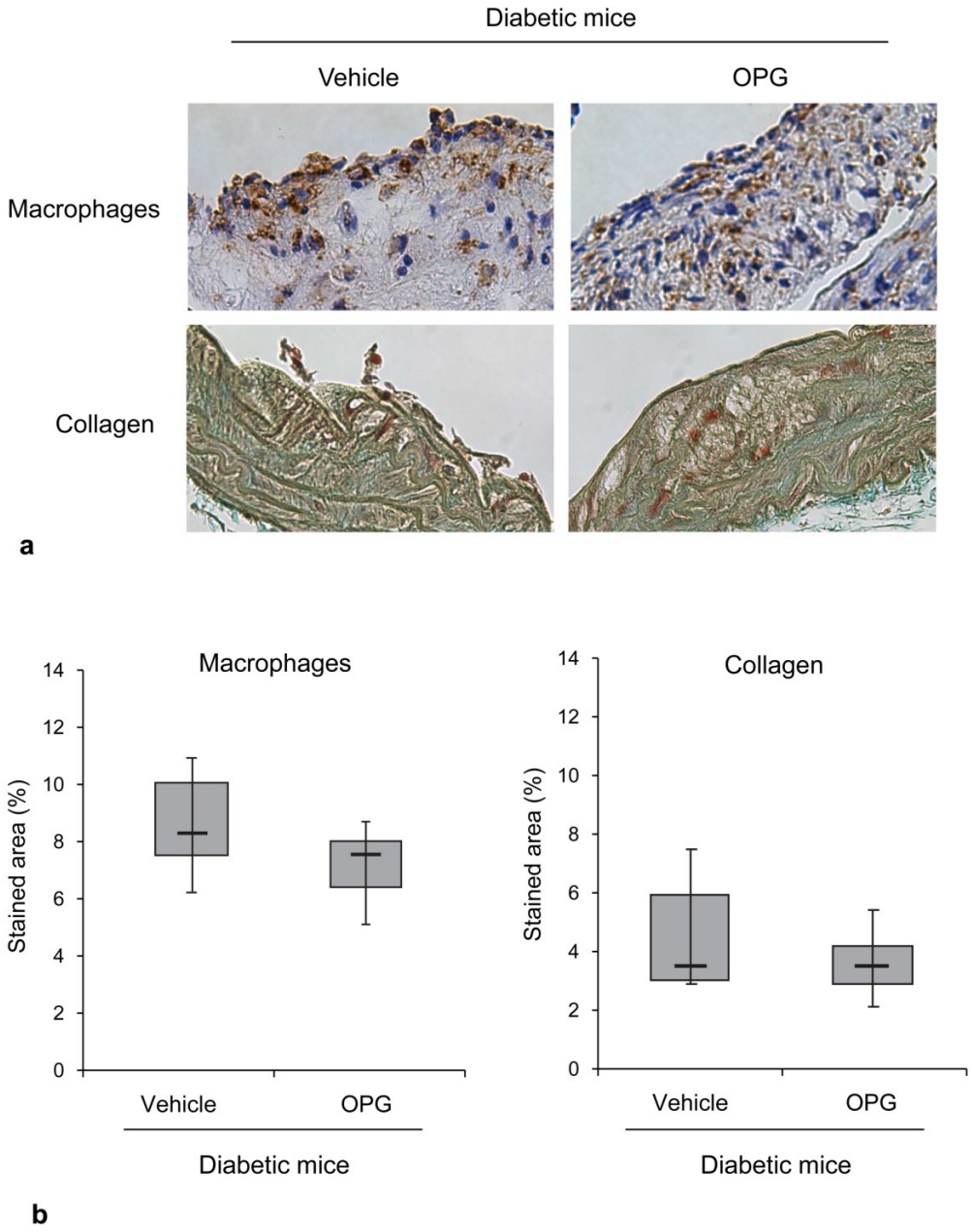

Figure 3. OPG treatment did not affect the macrophage infiltration or interstitial collagen content in the atherosclerotic plaques of apoE$^{-/-}$ diabetic mice. Serial sections from aortas of apoE$^{-/-}$ diabetic mice injected intraperitoneally with either vehicle (n=10) or recombinant OPG (n=10) were analyzed to quantitatively evaluate the presence/percentage of macrophages (using F4/80 marker), as well as the interstitial collagen content (trichrome staining) in the aortic intima. Staining results, representatively shown in **a** (original magnification X20), were quantitatively determined in each mouse with the Image Pro Plus® 6.3 analysis program and expressed as the percentage of stained area. In **b**, horizontal bars are medians, upper and lower edges of the boxes are 75th and 25th percentiles and vertical lines extending from the boxes are 10th and 90th percentiles.

In the same way, the expression of Syndecan-1, which has been proposed to act as a ligand for OPG in multiple myeloma (Standal et al., 2002), was not modified in the aortas of OPG-

injected mice compared to vehicle treated animals (means ± SEM (%): 6.6 ± 1.8 vs 5.8 ± 2.1, in OPG treated diabetic mice vs diabetic apoE$^{-/-}$ mice respectively).

Interestingly, on the other hand, the percentage of VSMC (αSMA-positive cells) was significantly ($p<0.05$) increased in the aortic lesions of OPG-injected apoE$^{-/-}$ diabetic animals with respect to diabetic animals injected with vehicle alone (Figure 4a,b).

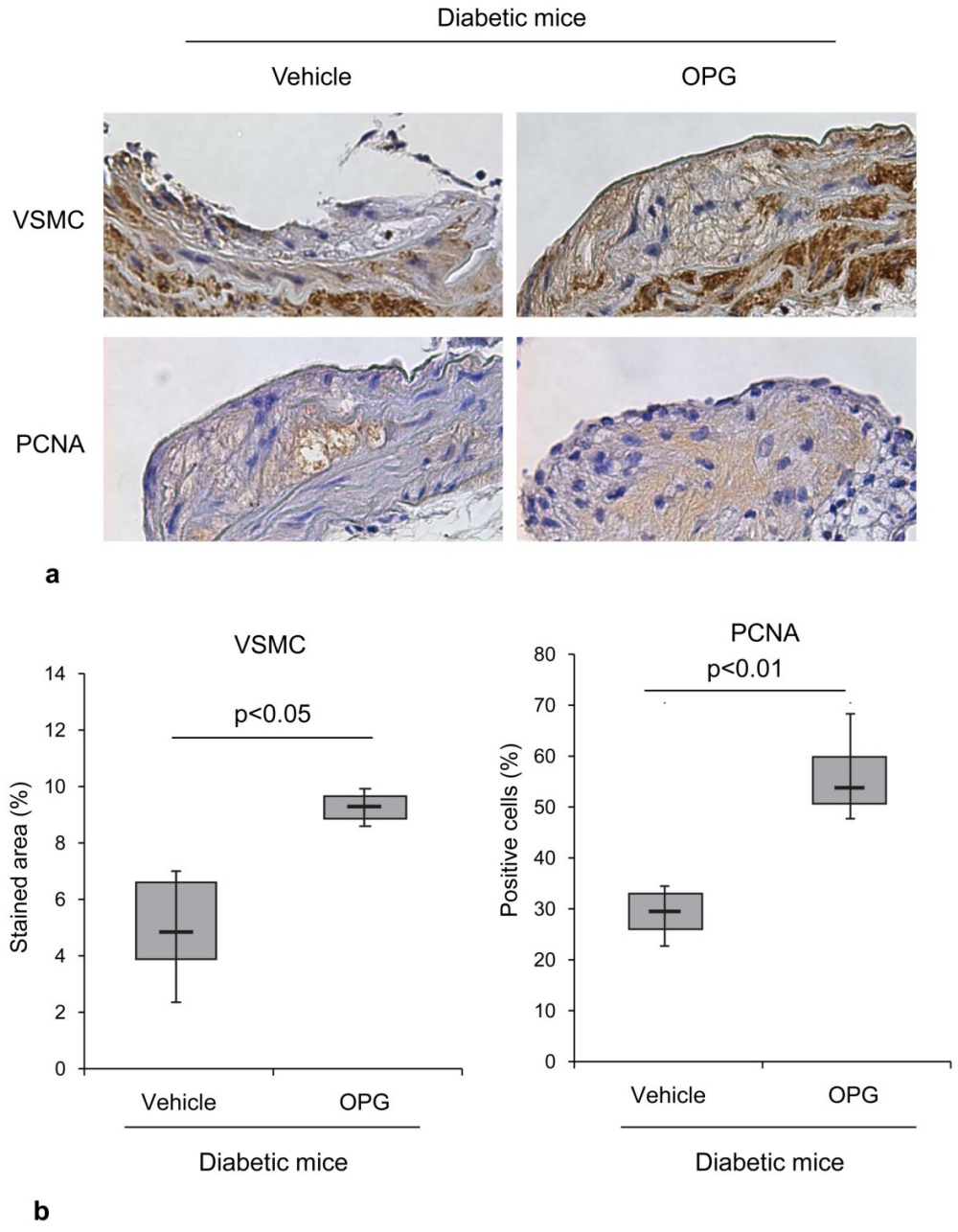

Figure 4. OPG treatment increased the content of VSMC and their proliferative activity in the atherosclerotic plaques of apoE$^{-/-}$ diabetic mice. Serial paraffin sections from aortas of apoE$^{-/-}$ diabetic mice injected intraperitoneally with either vehicle (n=10) or recombinant OPG (n=10) were analyzed to quantitatively evaluate the percentage of VSMC (using αSMA marker) and the content of PCNA-positive cells in the aortic intima. Staining results, representatively shown in **a** (original magnification X20), were quantitatively determined in each mouse with the Image Pro Plus® 6.3 analysis program and expressed as the percentage of stained area or of positive cells. In **b**, horizontal bars are medians, upper and lower edges of the boxes are 75th and 25th percentiles and vertical lines are 10th and 90th percentiles.

In order to evaluate whether the increased content of VSMC observed in the plaques of OPG-injected animals was accompanied by an increase in cell proliferation, we analyzed the percentage of PCNA-positive cells, which accurately reflects the degree of cell proliferation, within the plaques. As shown in Figure 4a and b, OPG administration promoted a significant ($p<0.01$) increase in PCNA-positive cells. Interestingly, the percentage of PCNA-positive cells evaluated in all animals showed a significant positive correlation with the percentage of the αSMA-positive area evaluated in the plaques of each mouse ($R=0.76$, $p<0.05$), suggesting that VSMC were the major cell type involved in cell proliferation within the plaques.

5.3 Increase of the mRNA expression of angiopoietin 2 in the aorta of apoE$^{-/-}$ diabetic animals after in vivo administration of recombinant human OPG

Taking into account that a recent *in vitro* study demonstrated that angiopoietin 2 plays a key role in promoting inflammation of the vessel wall (Fiedler et al., 2006), we next investigated whether the *in vivo* injection of human full-length OPG was able to modulate angiopoietin 2 expression in the aortic wall of apoE$^{-/-}$ diabetic mice. The constitutive steady-state mRNA levels of angiopoietin 2 were quantitatively evaluated by real time RT-PCR in RNA extracted from aortic samples of OPG- and vehicle-treated diabetic mice (Figure 5). The mRNA levels of angiopoietin 2 were significantly ($p<0.05$) higher in the aortas of OPG-treated diabetic animals than in the aortas obtained from vehicle-treated diabetic animals (Figure 5). On the other hand, the inflammatory cell adhesion molecule VCAM-1 (Wara et al., 2008) did not show significant modifications in OPG-treated versus vehicle-treated diabetic mice (Figure 5).

5.4 Induction of primary rodent VSMC proliferation by recombinant human OPG

In the light of the *in vivo* results, in which the plaques in OPG-treated diabetic mice showed a significant increase in the number of VSMC, we have investigated *in vitro* whether the exposure to recombinant full-length human OPG had any effect on cell cycle progression of murine VSMC, analyzed by BrdU incorporation assay (Figure 6). As shown in Figure 6, full-length recombinant human OPG at concentrations similar to those found in human serum significantly ($p<0.05$) promoted the proliferation of VSMC (Secchiero et al., a 2006).

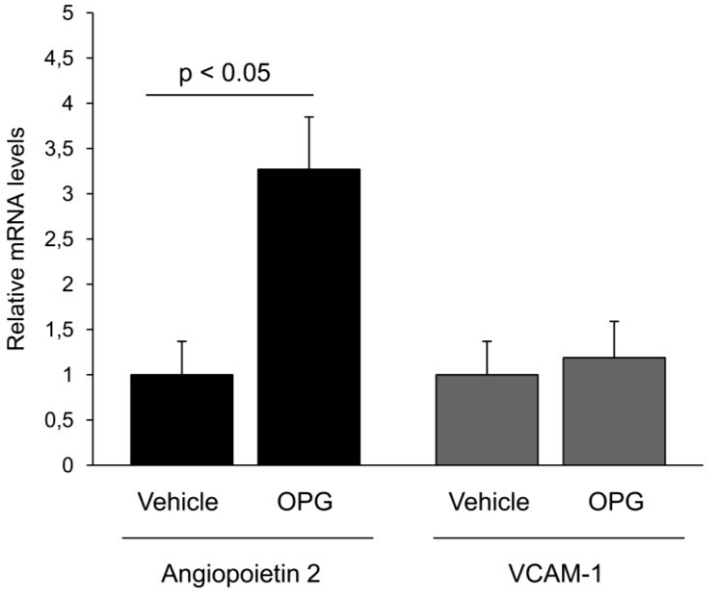

Figure 5. Effect of full-length OPG treatment on angiopoietin 2 and VCAM-1 mRNA levels in aortas from diabetic apoE$^{-/-}$ mice. mRNA levels of angiopoietin 2 and VCAM-1 in RNA extracted from aortic samples of OPG- and vehicle-treated apoE$^{-/-}$ diabetic mice were quantitatively analyzed by real-time RT-PCR. After normalization to the level of 18S, gene specific RNA levels in control aortas (from vehicle-treated mice) were set as 1. Bars indicate mean ± SEM.

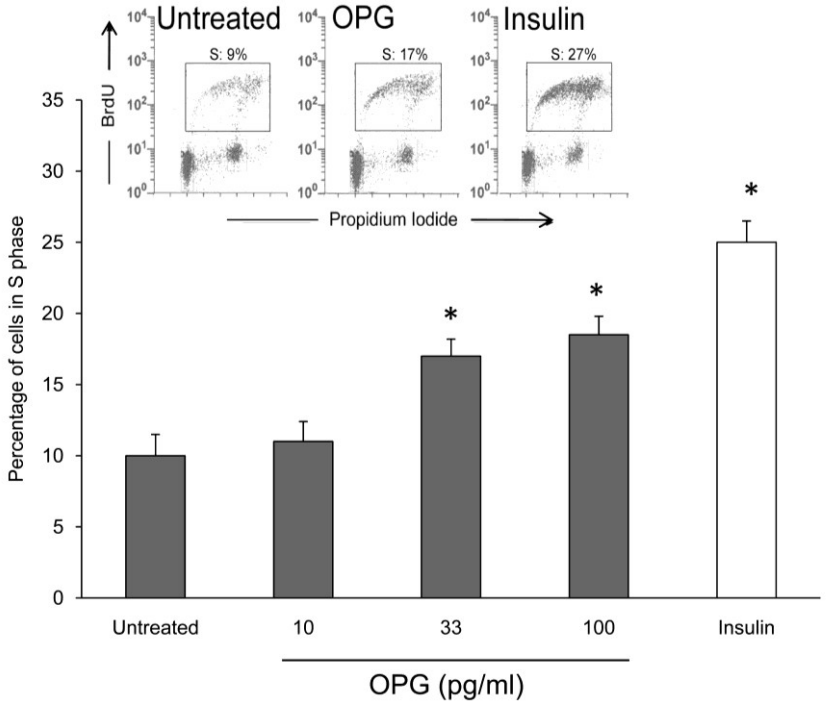

Figure 6. Recombinant human OPG promoted the proliferation of primary aortic VSMC. Aortic murine VSMC were seeded at subconfluence, serum-starved and either left untreated or exposed to the indicated concentrations of OPG for 36 hours. After BrdU/PI staining, percentage of cells in S phase of the cell cycle, which have incorporated BrdU, was calculated from the flow cytograms and expressed as the percentage of the total population. As positive control, cells were treated with Insulin and are shown for comparison. Values are expressed as means ± SD of results from four independent experiments. *p<0.05 compared to untreated cells.

STUDY 1.B

5.5 The in vivo injection of recombinant human OPG modulates the histological composition of aortic media in apoE$^{-/-}$ mice

Taking in consideration our results on the effect of OPG treatment in inducing an increase in the extension of atherosclerotic lesions and in promoting VSMC proliferation both *in vitro* and *in vivo* in diabetic animals, and considering that an increase in OPG levels characterizes the early onset of diabetes (Secchiero et al., a 2006), in the second part of our study, we focalized our attention on the effect of OPG treatment in the aortic media of apoE$^{-/-}$ mice without diabetes in respect to control and diabetic mice.

As expected, aortas of diabetic mice injected with vehicle showed an increase in TGFβ and fibronectin gene expression (by 7.5- and 11-fold, respectively; $p<0.05$), as well as an increase in both osteoprotegerin mRNA expression (by 4-fold; $p<0.05$) and protein content compared to nondiabetic control mice (Figure 7a,b). Furthermore, interstitial collagen content was markedly increased in the aortic media of diabetic mice with respect to control animals ($p<0.0001$) (Figure 8).

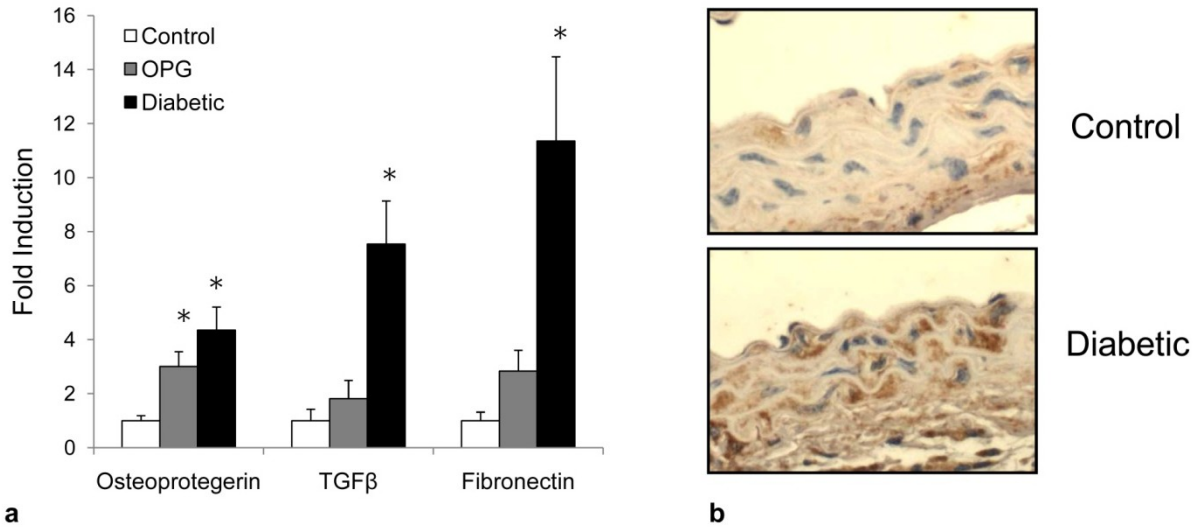

Figure 7. Changes in molecular and cellular parameters in OPG-treated and diabetic mice aortas. (a) Gene expression analysis was assessed by quantitative RT-PCR on whole aorta of control, apoE$^{-/-}$ mice injected intraperitoneally with human recombinant OPG (OPG) and diabetic apoE$^{-/-}$ mice. Significant increases were observed for osteoprotegerin, TGFβ and fibronectin in diabetic mice compared to controls (*$p < 0.05$). OPG treatment promoted an increase in osteoprotegerin mRNA levels, whereas induced no significant modifications on TGFβ and fibronectin mRNA levels. **(b)** Immunohistochemical analysis demonstrated increased staining for osteoprotegerin in the aortic media of diabetic apoE$^{-/-}$ mice compared to controls (microscope magnification X20). Positive staining is shown as brown in aortic medial layer. Sections are counterstained with hematoxylin.

The injections with recombinant human OPG promoted a significant increase in osteoprotegerin gene expression, whereas TGFβ and fibronectin did not show significant modifications in OPG-treated versus control mice (Figure 7a). Interestingly, the percentage of collagen content was significantly ($p<0.05$) increased in the aortic media of OPG-injected apoE$^{-/-}$ animals compared to untreated animals (Figure 8).

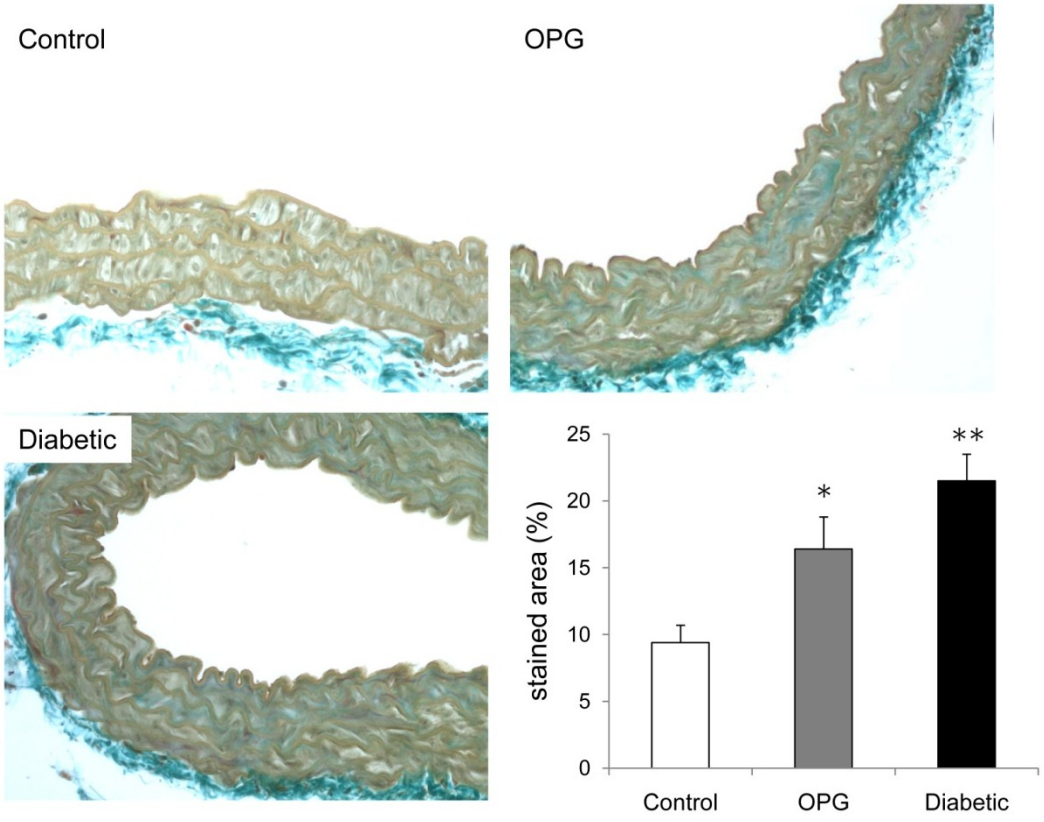

Figure 8. Recombinant human OPG increased the interstitial collagen content in the aortic media of apoE$^{-/-}$ mice. Representative histological sections (original magnification X20) of aortas from control, apoE$^{-/-}$ mice injected intraperitoneally with human recombinant OPG (OPG) and diabetic apoE$^{-/-}$ mice. Serial sections were analyzed to quantitatively evaluate the interstitial collagen content (trichrome staining) in the aortic media and the results were expressed as the percentage of stained area. *$p<0.05$ or **$p<0.0001$ vs control group). All bars represent mean ± SEM.

5.6 TGFβ stimulates OPG production in mouse primary VSMC

TGFβ is expressed by cells in the vessel wall and is capable of modulating vascular development and remodeling by altering cell differentiation, proliferation, migration and extracellular matrix production (Bobik, 2006). To assess the effect of TGFβ on VSMC, cells were treated with 10ng/ml of TGFβ for 48h in high glucose media and in serum reduced condition (2%). Cells incubated with TGFβ exhibited an elongated and broadened morphology, associated with an increased staining for αSMA (Figure 9a). Significant

increases were observed in the mRNA levels of αSMA, fibronectin (Fibr), vimentin (Vim), CTGF, collagen I (col I), collagen III (col III) and collagen IV (col IV) (Figure 9b).

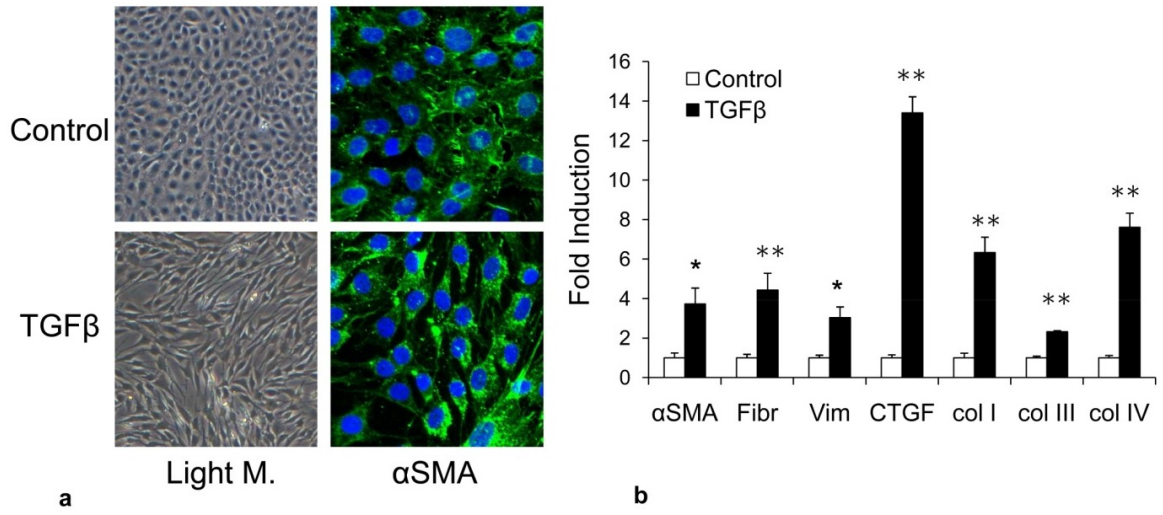

Figure 9. TGFβ induced changes in VSMC morphology, protein and gene expression. (a) Mouse aortic vascular smooth muscle cells (DMEM, 25mM glucose, 2% serum) were treated with TGFβ (10 ng/ml, 2 days). Changes in morphology are evident by light microscopy (original magnification X10) with cells adopting a more elongated appearance following TGFβ treatment. Immunostaining of VSMC revealed increased αSMA (green fluorescence) after TGFβ treatment (original magnification X20). Nuclei were stained with DAPI (blue fluorescence). **(b)** Gene expression analysis was assessed by quantitative RT-PCR and significant changes in response to TGFβ are indicated (*$p<0.05$ or **$p<0.0001$ vs control group). Bars indicate mean ± SEM.

To determine whether OPG expression is regulated by TGFβ in VSMC, cells were stimulated with increasing concentrations of TGFβ (1-10ng/ml) for 48h. The treatment increased the OPG mRNA expression in a dose-dependent manner, whereas OPG protein expression reached a plateau since from the lowest concentration used (Figure 10a). To further confirm that the OPG release was mediated specifically by TGFβ, VSMC were pre-incubated with SB431542, the selective TGFβ-type 1 receptor inhibitor, at the concentration of 2μM for 1 hour and then treated with TGFβ 1ng/ml for 48h. SB431542 completely blocked the OPG expression both at mRNA and protein level (Figure 10b).

5.7 Recombinant full-length OPG increases the mRNA expression of NF-kB, TGFβ and pro-fibrotic markers in mouse primary VSMC

According to the fact that OPG levels were increased in the aortic media of diabetic mice, the effect of increasing concentrations of OPG on VSMC was investigated *in vitro*. Treatment with 1-40ng/ml of OPG for 48h increased the mRNA expression of fibronectin, collagen I, collagen III and collagen IV in a dose dependent manner, which peaks at 10ng/ml.

Interestingly, with the same pattern, an increased level of TGFβ and NF-kB was also observed (Figure 11).

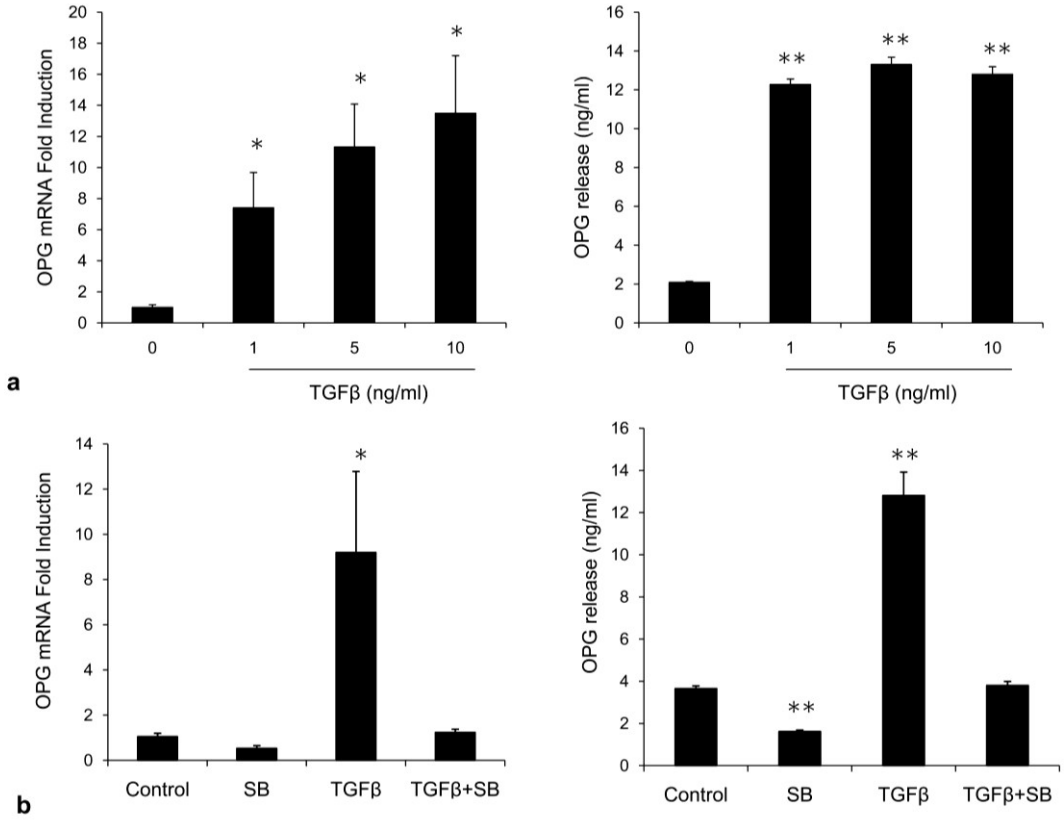

Figure 10. TGFβ induced OPG mRNA and protein expression in VSMC. (a) Gene expression analysis by quantitative real-time PCR revealed a dose dependent induction of OPG mRNA expression in VSMC by TGFβ over 48h. Gene expression is expressed relative to not-treated group, which was arbitrarily designated as 1 (*$p<0.05$ compared to control group) (left panel). Evaluations of OPG production in VSMC supernates following TGFβ (1-10ng/ml) treatment over 48h, determined by an ELISA kit (**$p<0.0001$ compared to control group) (right panel). (**b**) VSMC were treated with TGFβ (1ng/ml) for 48h after pre-incubation with SB431542 (2μM) inhibitor for 1h. SB431542 completely blocked the OPG expression at mRNA and protein level. *$p<0.05$ or **$p<0.0001$ vs control group. Bars represent mean ± SEM.

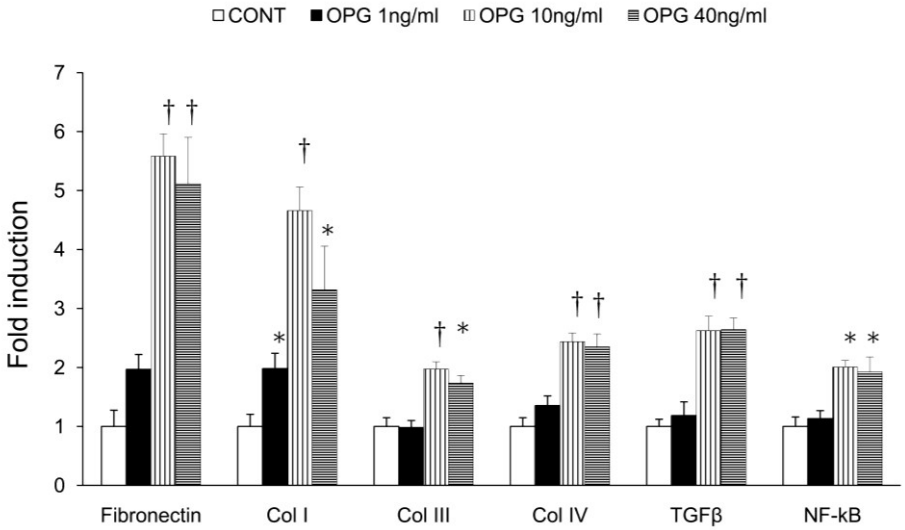

Figure 11. Dose response effect of OPG treatment on VSMC gene expression. VSMC (DMEM, 25mM glucose, 2% serum) were treated with increasing concentrations of OPG (1-40ng/ml) for 48h. The expression of several genes was assessed by quantitative real-time PCR and the significant changes caused by OPG treatment are indicated (*p<0.05 or †p<0.0001 vs control group). Bars indicate mean ± SEM.

5.8 Recombinant full-length OPG increases both OPG protein and mRNA expression in mouse primary VSMC

In the light of the *in vivo* results, in which OPG-treated apoE$^{-/-}$ mice showed an increase in OPG mRNA expression in the whole aorta, we have investigated *in vitro* whether the exposure to recombinant full-length human OPG had any effect on OPG release from aortic VSMC. As shown in Figure 12, the 48 hours treatment with full-length OPG promoted an increase in the OPG expression both at mRNA and protein level in murine aortic VSMC.

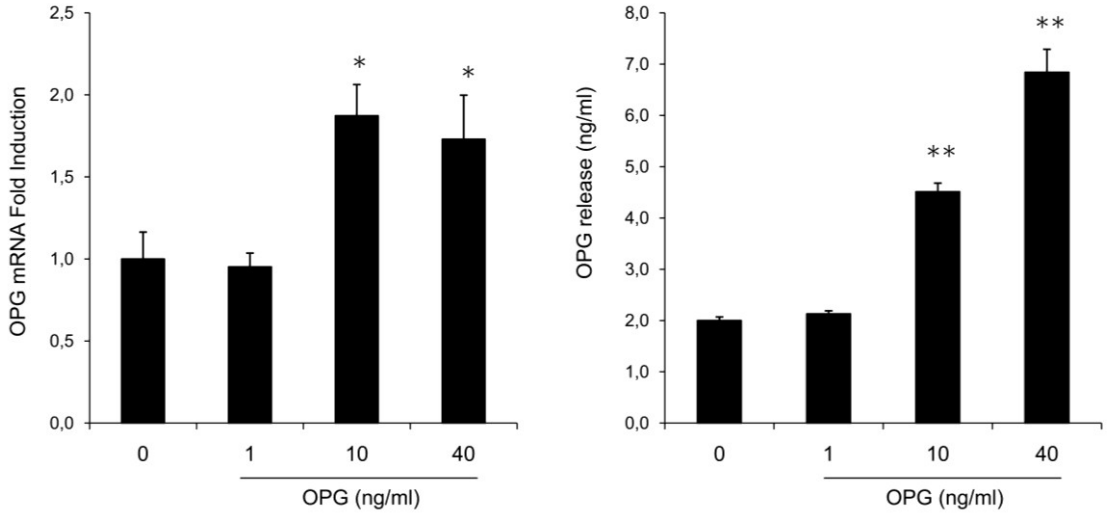

Figure 12. Full-length recombinant human OPG induced OPG mRNA and protein expression in murine VSMC. Gene expression analysis by quantitative real-time PCR revealed a dose dependent induction of OPG mRNA expression in VSMC by full-length human OPG over 48h. Gene expression is expressed relative to not-treated group, which was arbitrarily designated as 1 (*p<0.05 compared to control group) (left panel). Evaluations of OPG production in VSMC supernates following full-length human OPG (1-40ng/ml) treatment over 48h, determined by an ELISA kit (**p<0.0001 compared to control group) (right panel).

STUDY 2

6.1 In vivo injection of low concentrations of full-length recombinant human OPG induces a glycemic increase and an insulin levels reduction in C57Bl/6J mice

Although serum osteoprotegerin is significantly increased in diabetic subjects (Browner et al., 2001; Galluzzi et al., 2005; Knudsen et al., 2003; Rasmussen et al., 2006; Secchiero et al., a 2006), its potential role in beta cell dysfunction has not been investigated. For this purpose 40 male mice C57Bl/6J, aged 10 weeks, were further randomized to be i.p. injected either with recombinant human OPG or with control vehicle. In addition, in order to explore the possible interplay of OPG with the renin-angiotensin system (RAS), 20 mice received the ACE inhibitor ramipril in co-treatment with i.p. injections of OPG or vehicle alone. It should be noticed that repeated i.p. injections of human recombinant OPG (every 3 weeks for 3 months) were well tolerated by the C57Bl/6J mice. After 3 months, animals were analyzed for various parameters, as reported in Table 2, and then sacrificed to perform pathological examination. No difference between body weight and baseline systolic blood pressure was determined in animals prior to randomization. The body weight and systolic blood pressure were not significantly different in animals injected or not with human recombinant OPG. Treatment with ramipril did not influence body weight, but, however, induced a significant reduction in systolic blood pressure. Moreover no gross abnormalities at necroscopic examination were observed in OPG-treated animals with respect to vehicle- or ramipril-treated C57B1/6J mice.

Parameters	**CONT (n=10)**	**OPG (n=10)**	**CONT-R (n=10)**	**OPG-R (n=10)**
Body weight (g)	29.5 ± 1.5	31.2 ± 1.3	30.1 ± 1.6	28.5 ± 2.0
SBP (mmHg)	95 ± 2	98 ± 3	80 ± 2*	83 ± 2*
AUC (μg/L/min)	150 ± 20	90 ± 15**	145 ± 18	143 ± 17

Table 2. Characteristics of the mice at the end of the study. SBP, systolic blood pressure; AUC, area under insulin curve; CONT, control mice; OPG, mice injected with recombinant human OPG; CONT-R, mice injected with vehicle and treated with ramipril; OPG-R, mice injected with OPG and treated with ramipril. *$p<0.05$ vs CONT and OPG groups; **$p<0.01$ vs other groups. Data are expressed as mean ± SEM.

Fasting blood glucose levels were measured every 4 weeks for 3 months using a glucose oxidase method. Mice injected with recombinant human OPG had significantly higher blood glucose levels after 2 and 3 months of treatment compared to control mice ($p<0.05$). Treatment with ramipril completely prevented the glycemic increase induced by OPG

administration ($p<0.05$) (Figure 13a). Consistently with the situation of fasting hyperglycemia, OPG-treated mice exhibited a reduction in serum insulin with respect to the control animals, that was statistically significant after 3 months of treatment ($p<0.05$). In the same way, co-treatment with the ACE inhibitor significantly improved insulin secretion in OPG injected mice ($p<0.05$) (Figure 13b).

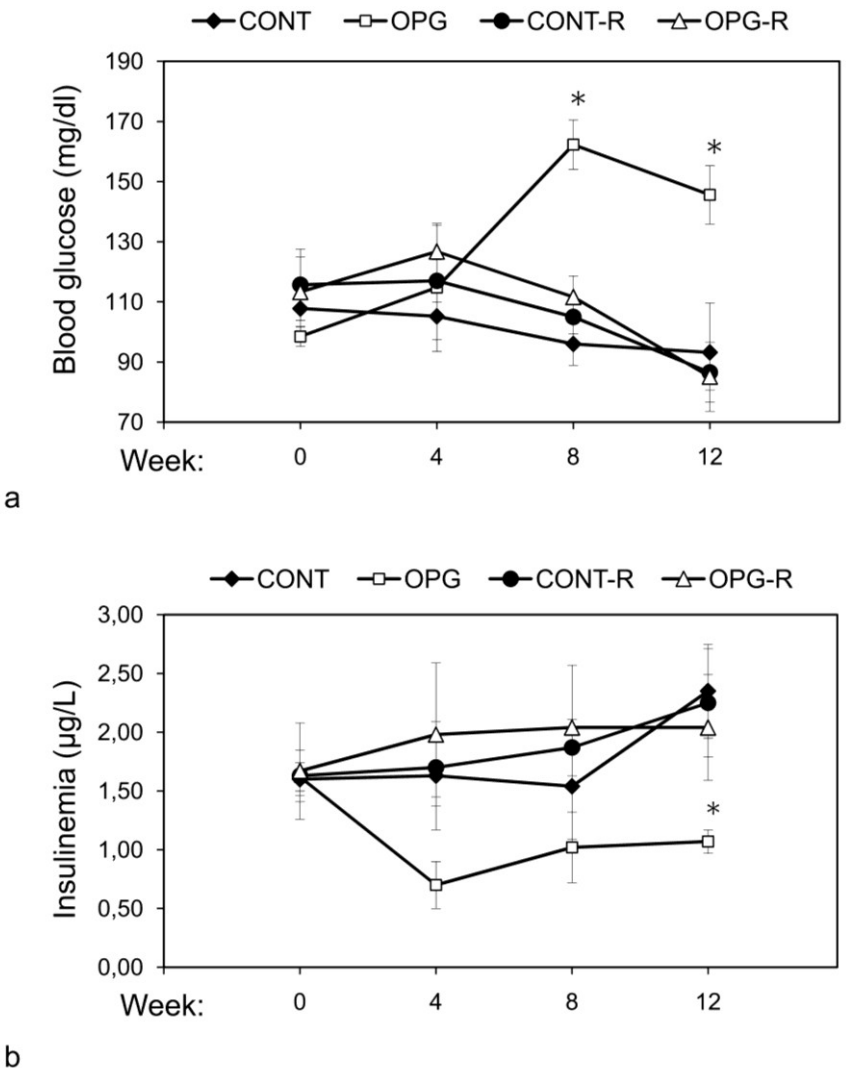

Figure 13. Effect of *in vivo* injections of recombinant OPG on fasting blood glucose and insulin serum levels. Kinetics of blood glucose levels, measured using a glucose oxidase method (**a**) and insulin serum levels, determined by an ELISA kit (**b**). Results are reported as mean ± SEM. *$p<0.05$ vs other groups.

Similarly the area under the insulin curve (AUC), evaluated between 0 and 120 minutes after the glucose challenge, was significantly reduced in OPG-treated mice compared to control animals ($p<0.01$). The co-treatment with ramipril induced a statistically significant improve in

the AUC of the OPG injected mice ($p<0.01$). Treatment with ramipril alone didn't alter the AUC with respect to untreated mice (Table 2).

6.2 In vivo injection of recombinant human OPG promotes a reduction in insulin staining density and in beta cell mass in C57Bl/6J mice

Immunohistochemical staining for the beta cell marker insulin was strong and intense in control mice islets. In contrast, mice injected with recombinant human OPG presented islets that showed an attenuated and variable pattern of staining suggestive of progressive beta cell loss (Figure 14). Consistent with these evidences, the mean percentage of proportional area staining positively for insulin in the OPG treated mice was significantly reduced with respect to control mice (means ± SEM (%): CONT 47.1 ± 1.3; OPG 39.6 ± 1.4; $p<0.0001$). Treatment with ramipril significantly increased the staining density for insulin (mean ± SEM (%): OPG-R 50.7 ± 1.5; vs OPG $p<0.0001$). No difference in insulin pattern was observed in mice treated with ramipril alone compared to control mice islets (mean ± SEM (%): CONT-R 49.6 ± 1.3).

Pancreatic beta cell mass was estimated by multiplying the mean islet density of staining for insulin by the mean islet area per area of pancreas. This was expressed in arbitrary units adjusted for the pancreatic wet weight for individual animals. OPG treated mice had a marked reduction in beta cell mass with respect to the mice injected with vehicle (means ± SEM: CONT 14.8 ± 1.6; OPG 9.56 ± 0.9; $p<0.05$). Blockade of the RAS further increased total pancreas insulin content (mean ± SEM: OPG-R 14.2 ± 1.6 vs OPG $p<0.05$). Treatment with ramipril alone had no effect on the total beta cell mass (mean ± SEM: CONT-R 13.9 ± 1.5).

6.3 In vivo administration of recombinant human OPG induces alterations in the histological composition of the pancreatic islets in C57Bl/6J mice

Islets in OPG treated animals were significantly enlarged with disarray of islet architecture, and irregular islet boundaries. Treatment with ramipril largely attenuated these changes (Figure 14). The *in vivo* administration of human OPG increased significantly Picrosirius staining both within and at the boundary of the islets ($p<0.05$) and this increase was completely prevented by ramipril treatment. Ramipril alone didn't alter the total collagen content of the islets compared to the control animals (Table 3).

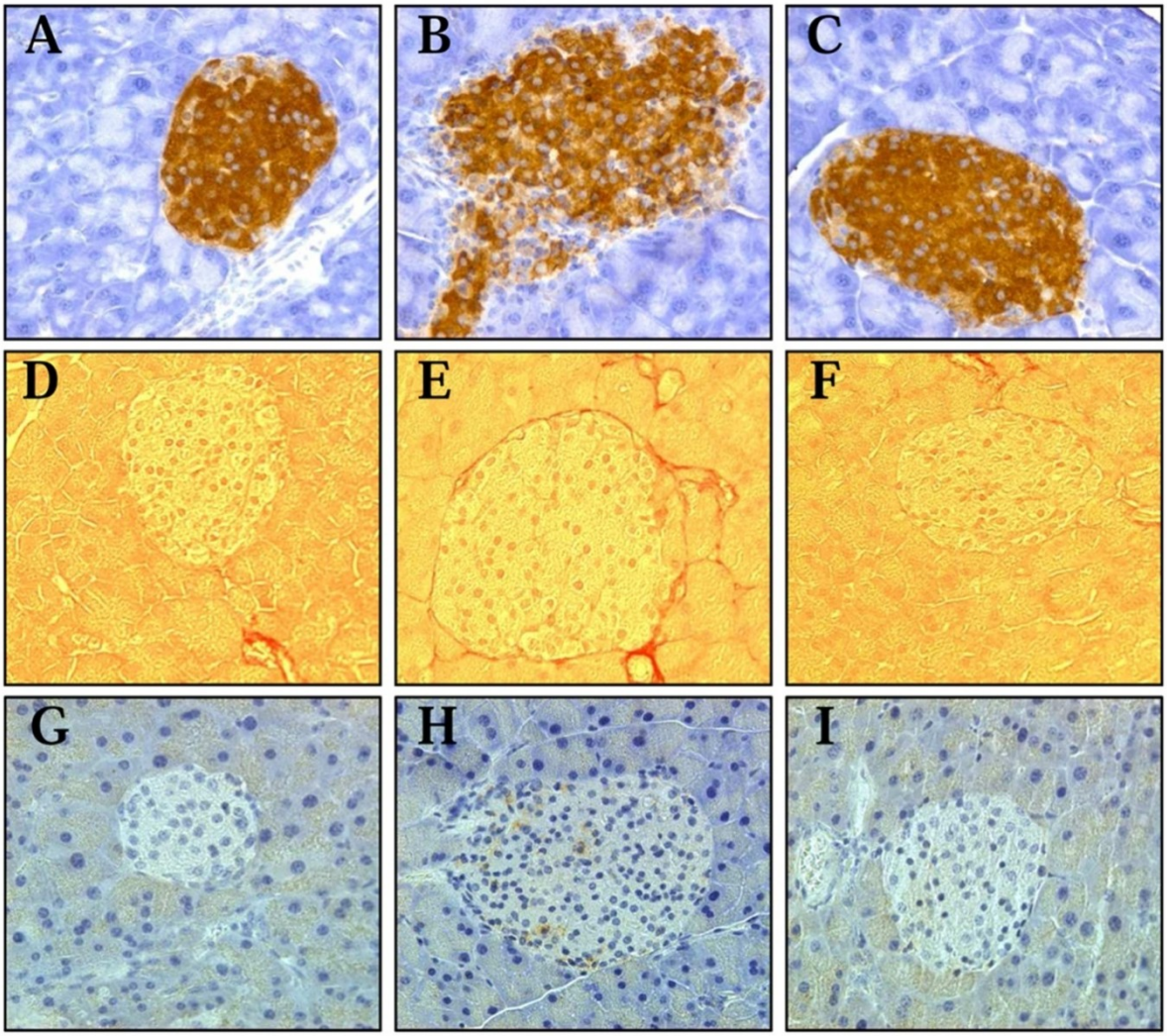

Figure 14. Effect of human recombinant OPG injections on pancreas islet morphology. Representative histological sections of pancreas (microscope magnification X20); specimens from control (CONT), OPG injected (OPG) and OPG injected treated with ramipril (OPG-R) mice. Dense immunostaining for insulin (upper panel) in CONT islets (**A**) and diffuse staining in OPG islets (**B**). Increased staining density after blockade of the RAS with ramipril (**C**). Staining for picrosirius red (middle panel) and for F4/80 (lower panel, brown staining) in islets from CONT (**D, G**), OPG (**E, H**) and OPG-R (**F, I**) mice.

	Picrosirius		**F4/80**	
	Intra-islet	**Peri-islet**	**Intra-islet**	**Peri-islet**
CONT	3.7 ± 0.3	12.4 ± 0.9	0.019 ± 0.005	0.163 ± 0.036
OPG	6.3 ± 0.7*	16.6 ± 1.2*	0.098 ± 0.01*	0.406 ± 0.079*
CONT-R	3.0 ± 0.4	11.3 ± 0.3	0.013 ± 0.009	0.197 ± 0.086
OPG-R	3.9 ± 0.1	13.5 ± 0.8	0.017 ± 0.007	0.132 ± 0.038

Table 3. Intra- and peri-islet fibrosis and macrophages infiltration. Data for picrosirius are expressed as proportional area (%) of each islet (intra-) or of islet boundaries (peri-) occupied by positive red staining, shown as mean ± SEM. Data for F4/80 are expressed as average of the number of cells staining positive (brown staining) in insular- or peri-insular level ± SEM. *$p<0.05$ vs all groups.

In order to evaluate whether the reduction in beta cell mass observed in OPG-treated animals might involve the induction of apoptosis by OPG, a double immunofluorescence staining performed by combining TUNEL plus a specific beta cell marker (insulin) was applied to identify apoptotic cells within islet boundaries in C57Bl/6J mice treated or not with OPG. As shown in Figure 15, intraislet cell death was significantly greater in OPG injected mice (7-fold) compared with infrequent apoptotic cells seen in control islets ($p<0.01$). Blockade of the RAS with ramipril reduced TUNEL staining within islet cells to control levels.

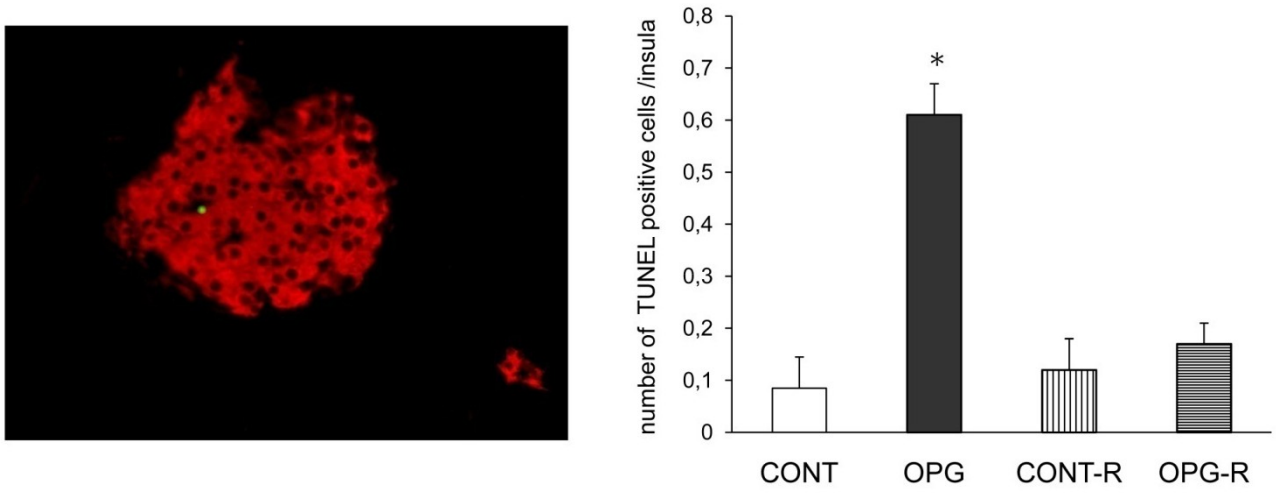

Figure 15. Effect of *in vivo* injections of recombinant full-length OPG on beta cell apoptosis. Representative image of a pancreatic insula from OPG treated mice, double-stained for TUNEL (green) plus insulin antibody, followed by a Texas Red-dye conjugated secondary antibody (red) to visualize the beta cells. Beta cell apoptosis is expressed as the average number of TUNEL positive cells per insula in control (CONT), OPG injected (OPG), control treated with ramipril (CONT-R) and OPG injected treated with ramipril (OPG-R) C57B1/6J mice. Bars indicate mean ± SEM (n=6 animals per group). *$p<0.01$ vs other groups.

To investigate whether OPG treatment affected the degree of infiltration of cells of the monocytic/macrophagic lineage, serial sections of paraffin-embedded pancreas were stained for F4/80 antigen (Figure 14). Peri-insular and intra-insular infiltrations were significantly ($p<0.05$) increased in OPG-injected mice (2- and 3.7 fold, respectively) when compared with control animals injected with vehicle. Co-treatment with lifelong ramipril significantly reduced the expression of F4/80 protein in islets (Table 3).

6.4 Treatment with recombinant human OPG increases pancreatic mRNA expression of MCP-1, VCAM-1, TGFβ and CTGF in C57Bl/6J mice

To quantify mRNA levels of the inflammatory and pro-fibrotic cytokines, reverse transcription polymerase chain reaction was performed in whole pancreas extracts. The injections with recombinant human OPG promoted a significant increase in MCP-1, VCAM-1, TGFβ and CTGF gene expression (Figure 16). These increases were completely prevented by the treatment with the ACE inhibitor ramipril (Figure 16).

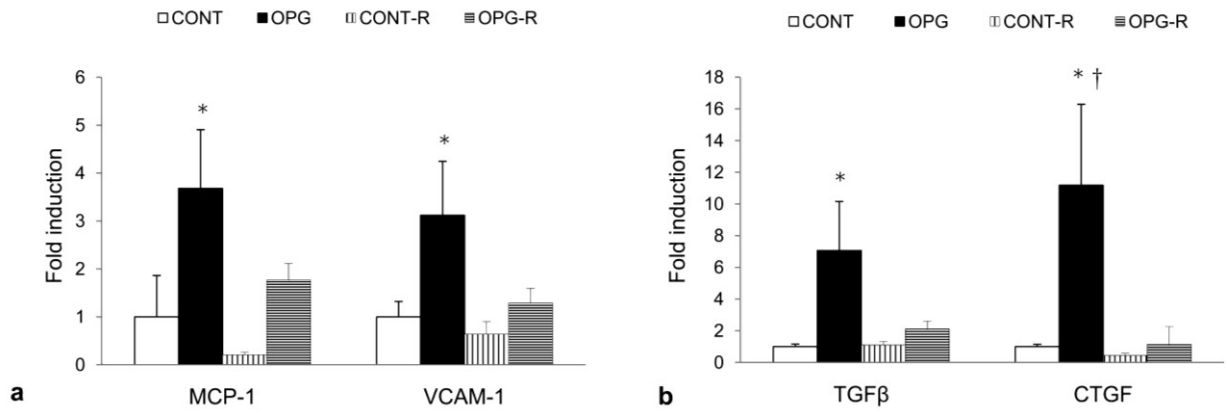

Figure 16. Effect of full-length OPG treatment on MCP-1, VCAM-1, TGFβ and CTGF RNA levels in pancreas. Gene expression analysis was assessed by quantitative RT-PCR on whole pancreas extracts of control (CONT), OPG injected (OPG), control treated with ramipril (CONT-R) and OPG injected treated with ramipril (OPG-R) C57B1/6J mice. Gene expression is expressed relative to the CONT group, which was arbitrarily designated as 1. In panel **a**, mRNA expression of monocyte chemotactic protein-1 (MCP-1) (*p<0.05 vs other groups), and vascular adhesion molecule-1 (VCAM-1) (*p<0.05 vs other groups). In panel **b**, mRNA expression of transforming growth factor-β (TGFβ) (*p<0.05 vs other groups), and connective tissue growth factor (CTGF) (*p<0.05 vs CONT and OPG groups; †p<0.0001 vs CONT-R group). Bars indicate mean ± SEM (n=6 animals per group).

6.5 In vivo injection of human recombinant OPG induces an activation of the local pancreatic RAS in C57Bl/6J mice

OPG-treated mice showed an activation of the local RAS as assessed by a significant increase in ACE and AT1 receptor gene expression (by 8.7- and 2.2 fold, respectively) in the pancreas when compared with control animals (Table 4). Densitometric analysis of pancreatic ACE and AT1 receptor demonstrated the same pattern as seen with respect to ACE and AT1 gene expression. Ramipril treatment prevented the up-regulation of ACE and AT1 receptor compared to treated OPG animals with mRNA and proteins levels similar to that observed in control animals (Table 4).

	ACE	AT1 receptor
Immunohistochemistry		
CONT	8.0 ± 1.7	2.7 ± 1.0
OPG	16.1 ± 3.2*	5.5 ± 0.6*
CONT-R	6.3 ± 2.2	2.9 ± 0.8
OPG-R	8.7 ± 1.1	3.1 ± 0.5
Real-time RT-PCR		
CONT	1.0 ± 0.6	1.0 ± 0.2
OPG	8.7 ± 2.8†	2.2 ± 0.4*
CONT-R	0.6 ± 0.1	1.0 ± 0.2
OPG-R	0.7 ± 0.3	1.1 ± 0.3

Table 4. Expression of components of the RAS as quantified by immunohistochemistry and real-time RT-PCR.
Data are proportional area (%) of each islet occupied by positive staining for specific islet proteins, shown as mean ± SEM (for immunohistochemistry); and data are results from gene expression study presented as a ratio compared with CONT, shown as mean ± SEM (for real-time RT-PCR). *$p<0.05$ vs other groups; †$p<0.0001$ vs other groups.

DISCUSSION

Many different studies have shown that increased amounts of serum OPG correlate with increased cardiovascular risk in both diabetic and non-diabetic patients (Jono et al., 2002; Schoppet et al., 2003; Kiechl et al., 2004; Moran et al., 2005; Secchiero et al., a 2006; Shin et al., 2006; Abedin et al., 2007). Possible interpretations of this positive relationship include OPG playing an active role in disease progression or OPG serving as a compensatory response to reduce disease progression, or OPG representing a noncompensatory (neutral) response to disease. The interpretation that OPG serum elevation represents a compensatory mechanism mainly relies on studies conducted on OPG knockout mice showing a protective role of OPG against vascular calcifications (Bucay et al., 1998; Price et al., a 2001; Bennet et al., 2006). However, in each of these models the prevention of vascular calcification by OPG was associated with strong suppression of bone turnover. Furthermore, both recombinant OPG (Price et al., a 2001) and bisphosphonate (Price et al., b 2001) treatments of rats suppressed vascular calcification in a warfarin model of vascular calcification, in association with suppression of bone turnover. Taken these data together, seems that the ability of OPG to inhibit vascular calcification is an indirect effect of its anti-osteoclastic activity. In contrast, *in vitro* studies have clearly shown that the expression and release of OPG by vascular cells is markedly induced in response to inflammatory cytokines, such as TNF-α and platelet-derived growth factor (PDGF) (Olesen et al., 2005; Zhang et al., 2002), and that OPG promotes leukocytes adhesion to endothelial cells (Zauli et al., 2007; Mangan et al., 2007), suggesting an active role of OPG in disease progression. On these bases, the aims of our studies were elucidate the potential roles of OPG in the pathogenesis of atherosclerosis and in pancreatic beta cell dysfunction. To investigate whether OPG is involved in pathogenetic aspects of atherosclerosis, apoE$^{-/-}$ mice, with or without diabetes, were injected every 3 weeks with recombinant full-length OPG and studied for 3 months. Subsequently, the animals were analyzed for the total plaque area and for the plaque cellular content, as well as for the media histology. Moreover, in parallel to *in vivo* studies, the effect of increasing concentrations of OPG were analyzed *in vitro*, using murine primary VSMC [see 7.1-section].

On the other side, to investigate whether OPG is involved in pathogenetic aspects of diabetes mellitus, C57Bl/6J mice, that do not spontaneously develop atherosclerotic lesions with a normal chow diet, were injected every 3 weeks with recombinant full length OPG and, after 3 months, sacrificed to perform the analysis of the pancreatic beta cells structure and function.

In addition, starting from some evidences for an interplay between OPG and the RAS pathways in human aortas, the long term co-treatment with the ACE inhibitor ramipril was investigated in order to evaluate if it could hinder the effect of exogenous OPG on beta cells remodelling and function [see 7.2-section].

7.1 OPG and diabetes associated atherosclerosis

The first part of our study showed that repeated injections of relatively low concentrations of human OPG resulted in a significant increase in the total aortic plaque area in apoE$^{-/-}$ diabetic mice, a well characterized animal model of diabetes-accelerated atherosclerosis, which have been shown to develop aortic lesions characteristic in appearance and distribution to those observed in humans (Nakashima et al., 1994; Wu and Huan, 2007). Taking into account that a series of *in vitro* and *in vivo* experiments, conducted previously by our group, have demonstrated that soluble recombinant TRAIL shows anti-inflammatory (Secchiero et al., 2003; Zauli et al., 2003; Secchiero et al., 2005) and anti-atherosclerotic (Secchiero et al., b 2006) activity, a mechanism by which OPG might accelerate the development of atherosclerotic lesions is through the inhibition of soluble circulating TRAIL. Moreover, the demonstration that OPG significantly increases the mRNA expression of angiopoietin 2 at the aortic level is in line with a recent *in vitro* study (Mangan et al., 2007). Since angiopoietin 2 has been shown to play a key role in the early steps of atherosclerosis (Fiedler et al., 2006), the ability of OPG to increase the expression of angiopoietin 2 might represent an important additional pathogenetic mechanism to explain the ability of OPG to promote atherosclerosis. On the other side, we also noticed a slight trend for an increase in systolic blood pressure in the OPG-treated diabetic mice, which might account for the changes observed in atherosclerotic plaques.

It is also noteworthy that the aortic plaques in OPG-treated diabetic apoE$^{-/-}$ mice presented a significant increase in the percentage of VSMC. Furthermore, in line with the *in vivo* results, *in vitro* data demonstrated that recombinant full-length OPG promoted also the proliferation of primary rodent cultured VSMC. In this context, is important to underline that the full-length recombinant OPG, that we used for our experiments, possess an heparin binding domain, that is essential to mediate important pro-inflammatory effects of OPG (Vitovski et al., 2007; Zauli et al., 2007; Mangan et al., 2007), in an independent manner to its role of decoy receptor for TRAIL and RANKL. According to this, we should consider that the

VSMC migration and proliferation, could be mediated by the interactions between the heparin binding domain of OPG and cell surface proteoglycans (Rauch et al., 2005).

Besides contributing to vessel wall inflammation and lipoprotein retention, VSMC play a foundamental role in the formation of the fibrous cap that provides stability to the plaques, preserving them from rupture, and therefore the benefit/risk of therapeutic inhibition of VSMC proliferation in atherosclerosis is unclear (Libby, 2002). In this context, the effect of OPG on plaque formation seems to be twofold: on one side, it increases the extent of the total plaque area, but on the other side it may contribute to plaque stabilization by promoting the proliferation of VSMC.

Subsequently, in the second part of our study, we analyzed whether *in vivo* administration of human recombinant OPG could induce some modifications in VSMC of the aortic media too, in the absence of a diabetes associated atherosclerosis. Basically, the strategy adopted of delivering human OPG intraperitoneally was chosen in order to try to mimic the effect of a small elevation of OPG serum levels, by allowing a prolonged release of the molecule into the general circulation.

The possible existence of a link between the high levels of OPG and TGFβ observed in diabetes was suggested by our preliminary results, showing that OPG and TGFβ were augmented in aortas of diabetic animals.

Interestingly, apoE$^{-/-}$ mice injected with OPG presented a trend for an increase in TGFβ, fibronectin and OPG gene expression and, more importantly, a significant increase in the interstitial medial aortic collagen content, resembling an intermediate situation between diabetic and control animals injected with vehicle.

TGFβ is generally accepted to be the main pro-fibrotic factor in diabetic complications, and several evidences support its important role in development of glomerulosclerosis and interstitial fibrosis (Ban and Twigg, 2008), and in regulating cardiac extracellular matrix deposition (ECM) (Westermann et al., 2007). Several different investigations supported the hypothesis that an increased expression of TGFβ, which is the main responsible for ECM accumulation, is involved in many cardiovascular complications by participating in the fibrotic process (Yokoyama and Deckert, 1996; Piao and Tokunaga, 2006; Pham et al., 2010; Ruiz-Ortega et al., 2007).

On the other side, many studies demonstrated that OPG secretion is regulated in smooth muscle cells by different stimuli, such as insulin (Olesen et al, 2005), angiotensin II (Moran et al., 2009) or proinflammatory cytokines, like tumor necrosis α (Moran et al., 2005). Clearly, many other factors could also play a role in high serum OPG levels that characterized both

type 1 and type 2 diabetes (Secchiero et al., a 2006; Galluzzi et al., 2005; Rasmussen et al., 2006; Browner et al., 2001; Knudsen et al., 2003; Avignon et al., 2005; Anand et al., 2006).

To further explore this potential link between TGFβ and OPG, we carried out a series of *in vitro* experiments using mouse primary aortic VSMC. Interestingly, VSMC treated with TGFβ, as well as having an elongated and broadened morphology and an increased expression of ECM components and profibrotic markers, showed an increased expression of OPG both at protein and mRNA level since from the lowest concentration used. This finding suggests that TGFβ could actively participate in the increased amounts of OPG seen in the aortic vessel of the diabetic animals.

Subsequently, in order to analyze the possible phisiopathological role of high concentrations of OPG observed in diabetes, we investigated the effect of this molecule in the same *in vitro* model, represented by the mouse primary aortic VSMC. OF note, VSMC treated with OPG presented an increased expression of fibronectin and profibrotic markers that resembled what TGFβ, in the same experimental conditions, did. Furthermore, in this system, a significant increase in TGFβ expression, as well as an auto-induction of OPG release were also observed, suggesting that probably a vicious cycle exists between TGFβ and OPG.

As a major transcription factor in inflammatory responses, nuclear factor kB is involved in the regulation of inflammatory and immune genes, apoptosis, and cell proliferation. Taking in consideration that inflammatory events characterize all stages of the atherosclerotic process , NF-kB has been considered a crucial element in the initiation of atherogenesis (Monaco and Paleolog, 2004; de Winther et al., 2005) . According to this, it is noteworthy that the NF-kB increase, induced by OPG treatment, supports the potential proinflammatory role of OPG, which is consistent to what we and other groups have previously shown (Zauli et al., 2007; Mangan et al., 2007).

In summary, taking in consideration that collagen synthesis occurs very early in lesion development (Rekhter, 1999) and an increase in OPG levels characterizes the early onset of diabetes (Secchiero et al., a 2006), our data, from *in vitro* and *in vivo* models, suggest that OPG is involved in diabetes-induced vascular ECM accumulation, probably via TGFβ induction, and that the up-regulation of TGFβ actively participates in the increased amount of OPG seen in diabetes, suggesting a positive feedback regulatory mechanism.

In conclusion, overall these data together, suggest that high OPG levels could definitely play an important role in the development and progression of diabetic atherosclerosis.

7.2 OPG and pancreatic beta cells dysfunction

Results obtained from *in vivo* studies performed in C57Bl/6J mice have demonstrated that the systemic administration of recombinant human OPG promotes significant histopathological changes in pancreatic islets including selective loss of beta cells by apoptosis, increased infiltration of monocytes/macrophages, increased expression of inflammatory molecules and fibrosis. In addition, exogenous administration of OPG also induced a significant increase of gene and protein expression of ACE and AT1 receptor and we have also observed the attenuation of these changes after chronic blockade of the RAS, in keeping with previous strong evidence that most of the components of functioning RAS are present locally in the endocrine pancreas and that islet RAS has a role in regulating pancreatic islet function (Leung and Carlsson, 2001; Tikellis et al., 2006). These findings are particularly relevant since it has been shown that angiotensin II plays an important role in regulating insulin islet secretion (Carlsson et al., 1998; Lau et al., 2004) and the process that leads to beta cell loss and dysfunction in type 1 and type 2 diabetes are significantly influenced by local activation of the RAS (Tikellis et al., 2006).

The molecular mechanism by which OPG controls ACE and AT1 gene expression is not known. The expression of ACE and AT1 receptor have been shown to be associated with activation of the mitogen-activated protein kinase (MAPK) and nuclear factor-kB transduction pathways (Cowling et al., 2002; Koka et al., 2008; Martin et al., 2007). In this respect, it should be emphasized that OPG is able to stimulate MAPK signaling (Theoleyre et al., a 2004). Taking these data together with the present study it prompts us to hypothesize that OPG might control transcription mechanism governing ACE and AT1 gene expression. In this context, it should also be taken into account that pancreatic inflammation may also result in the upregulation of local RAS as demonstrated in animal models of pancreatitis (Kuno et al., 2003). In our experimental setting, an islet accumulation of cells of the monocytic/macrophagic lineage was noted after OPG administration, and this was associated with an increased expression of MCP-1, a proinflammatory chemoattractant whose expression correlates with the progression of insulitis and beta cell destruction in different murine models (Chen et al., 2001; Ehses et al., 2009). In addition, the endothelial adhesion molecule VCAM-1, which is important for the adhesion of macrophages to the vascular wall, as demonstrated in experimental diabetes (Candido et al., 2004), was also significantly increased in OPG-treated animals. Previous studies have demonstrated that the pro-inflammatory effect of OPG is mediated by a direct interactivity with cell surface heparan solfate (Mosheimer et al., 2005)

or alternatively by preventing the antiinflammatory activity of TRAIL (Zauli et al., 2009). In this respect, it is particularly noteworthy that the TRAIL death pathway is present in islet beta cells (Ou et al., 2002) and we have recently demonstrated that recombinant TRAIL ameliorates the severity of streptozotocin-induced type 1 diabetes (Zauli et al., 2010). Therefore, a possible mechanism by which OPG might contribute to beta cell dysfunction is by inhibiting the antiinflammatory activity of circulating TRAIL. Notwithstanding these multiple potential pathways mediating the inflammatory response to OPG, all the inflammatory effects observed in our study after administration of OPG may be explained by the local RAS upregulation and its downstream sequelae. In accordance with this hypothesis, ACE inhibitor treatment prevented all the OPG-induced inflammatory changes.

In native tissues, the interaction between pancreatic beta cells and elements of their local micro-environment including extracellular matrix is essential to activate intracellular signaling pathways that regulate cell proliferation, survival and function. Loss of cell-to-cell communications associated with increased intraislet fibrosis may reduce the secretory efficiency of the islet and promote islet cell apoptosis (Tikellis et al., 2004). We report here that chronic OPG treatment increases peri- and intrainsula fibrosis and promotes the expression of TGFβ mRNA and its downstream effector CTGF in the pancreas. Both TGFβ and CTGF have been associated with fibrosis in diabetic nephropathy (Murphy et al., 1999) and pancreatitis (di Mola et al., 1999; Kuno et al., 2003). Also the RAS has been linked to increased fibrosis in a variety of tissues including the heart (Seccia et al., 2003), kidney (Satoh et al., 2001) and liver (Yoshiji et al., 2001). In fact, locally produced angiotensin II is thought to upregulate, via AT1 receptor, the expression of fibrogenic cytokines and growth factors including TGFβ and CTGF (Ruperez et al., 2003). Moreover, the use of an ACE inhibitor or AT1 receptor antagonist have been shown to result in reduced fibrosis from inhibtion of TGFβ and CTGF in animal models of diabetes mellitus (Tikellis et al., 2004) and pancreatitis (Kuno et al., 2003). It is conceivable that the reduction in islet fibrosis observed in this study after treatment with ramipril may be mediated through a similar pathway.

Pancreatic beta cell death by apoptosis is believed to be the primary mechanism for the reduction of beta cell mass and volume in both type 1 and type 2 diabetes (Thomas et al., 2009). Apoptosis in beta cell is a highly complex process and angiotensin II has been shown to play a relevant role in the control of beta cell life and death (Yuan et al., 2010). In the present study the OPG induction of islet apoptosis is closely related to upregulation of pancreatic RAS and these changes were prevented after treatment with ramipril. The

maintenance of beta cell area/density is important for maintaining a correct insulin secretion. Consistently with a protective role of ramipril the levels of insulinemia were significantly higher in mice treated with OPG + ramipril, and OPG + ramipril treated animals showed reduced level of hyperglycemia throughout the whole period of the study with respect to OPG-injected animals. Moreover ramipril co-treatment significantly ameliorated insulin response after the glucose challenge, suggesting an improvement in beta cell function. Because disruption of contacts between beta cells and beta cell loss reduces the secretory efficiency of islets, the results illustrated in our study suggest a potential mechanism to explain why pathologically elevated serum OPG levels, frequently occurring in both type 1 and type 2 diabetes (Browner et al., 2001; Galluzzi et al., 2005; Knudsen et al., 2003; Rasmussen et al., 2006; Secchiero et al., a 2006), are linked to the development and/or maitenance of diabetes mellitus.

In conclusion the present study indicates in the overactivity of the local RAS one of the possible mechanisms responsible for the OPG-induced islet beta cell dysfunction, suggesting that elevated level of OPG may have an active role in pancreatic islet pathophysiology.

7.3 Perspective

In vitro and *in vivo* data indicate that OPG might have an important role in promoting pro-atherogenic and pro-fibrotic effects in vascular physiopathology, as well as in inducing pancreatic beta cell dysfunction. Furthermore, full-length OPG seems to have a clear inflammatory activity, that is in line with many recent *in vitro* studies reported by our and other groups (Zauli et al., 2007; Mangan et al., 2007).

Considerable controversy still exists regarding the role of OPG/RANKL/RANK/TRAIL in cardiovascular disease and there is as yet no hypothesis unifying the apparent dichotomy in the nature of this system noted in animal and human studies (Venuraju et al., 2010). As already reported, serum OPG levels are elevated in both type 1 and type 2 diabetic patients and progressively increase with the duration of diabetes. Unfortunately at the moment there are no clear evidences of a relationship between an increase in OPG serum levels and any prediabetic condition. Consequently, OPG serum levels that could be potentially responsible for beta cell dysfunction are already unknown, also considering that once diabetes has been established, serum OPG levels are influenced by several factors such as arterial accumulation of the molecule and increased production from vascular smooth muscle cells induced by many different cytokines like TNF-α and TGFβ. Although it cannot be ruled out that high plasma OPG levels are an epiphenomenon of inflammatory processes harbored in vascular

lesions, our data suggest rather that elevated level of OPG in diabetes may have an active role in the development and progression of atherosclerosis as well as in pancreatic islet pathophysiology. Moreover our results indicate in the overactivity of the local RAS one of the possible mechanisms responsible for the OPG-induced islet beta cell dysfunction, and this may explain why the use of an ACE inhibitor, currently and safely used in clinical setting, may be suitable to target OPG pancreatic effect.

Of note, the triad RANKL/RANK/OPG plays a central role in coupling bone formation and resorption during normal bone turnover and in a wide spectrum of diseases characterized by disturbed bone remodeling, increased bone resorption and bone destruction (osteoporosis, Paget's disease of bone, rheumatoid arthritis, metastatic bone disease). While little doubts exist on the ability of pharmacological concentrations of recombinant chimeric OPG-Fc, in which the signal peptide, the heparin-binding domain and the death domain homologous regions are removed, to efficiently counteract bone turnover associated to different pathological conditions (Zauli et al., 2009), the overall effects of full-length OPG are much less clear. Anyhow, an important implication of our data is that denosumab, a fully human monoclonal antibody which blocks osteoclastogenesis by inhibiting RANKL (Kearns et al., 2008; Geusens, 2009), might be preferable to recombinant OPG for the treatment of pathologies associated with high bone turnover, such as osteoporosis.

LIST OF PUBLICATIONS 2008-2010

1) Cocchietto M, Zorzin L, **Toffoli B**, Candido R, Fabris B, Stebel M, Sava G. Orally administered microencapsulated lysozyme downregulates serum AGE and reduces the severity of early-stage diabetic nephropathy. *Diabetes Metab* 2008; 34:587-94.
2) Candido R, **Toffoli B**, Corallini F, Bernardi S, Zella D, Voltan R, Grill V, Celeghini C, Fabris B. Human full-length osteoprotegerin induces the proliferation of rodent vascular smooth muscle cells both *in vitro* and *in vivo*. *J Vasc Res* 2010; 47:252-61.
3) Zauli G, **Toffoli B**, di Iasio MG, Celeghini C, Fabris B, Secchiero P. Treatment with recombinant tumor necrosis factor-related apoptosis-inducing ligand alleviates the severity of streptozotocin-induced diabetes. *Diabetes* 2010; 59:1261-5.
4) Thomas MC, Pickering RJ, Tsorotes D, Koitka A, Sheehy K, Bernardi S, **Toffoli B**, Nguyen-Huu TP, Head G, Fu Y, Chin-Dusting J, Cooper ME, Tikellis C. Genetic Ace2 Deficiency Accentuates Vascular Inflammation and Atherosclerosis in the ApoE Knockout Mouse. *Circ Res* 2010; 107:888-97.
5) Bernardi S, Candido R, **Toffoli B**, Carretta R, Fabris B. Prevention of accelerated atherosclerosis by AT1 receptor blockade in experimental renal failure. *Nephrol Dial Transplant* 2010. [Epub ahead of print].
6) **Toffoli B**, Bernardi S, Candido R, Sabato N, Carretta R, Corallini F, Secchiero P, Zauli G, Fabris B. Osteoprotegerin induces morphological and functional alterations in mouse pancreatic islets. *Mol Cell Endocrinol* 2011; 331:136-42.
7) Fabris B, Candido R, Bortoletto M, **Toffoli B**, Bernardi S, Stebel M, Bardelli M, Zentilin L, Giacca M, Carretta R. Stimulation of cardiac apoptosis in ovariectomized hypertensive rats: potential role of the renin-angiotensin system. *J Hypertens* 2011; 29: 273-81.
8) **Toffoli B**, Bernardi S, Candido R, Zacchigna S, Fabris B, Secchiero P. TRAIL shows potential cardioprotective activity. *Invest New Drugs* 2011 Jan 4. [Epub ahead of print]
9) Fischetti F, Candido R, **Toffoli B**, Durigutto P, Bernardi S, Carretta R, Tedesco F, Fabris B. Innate immunity, through late complement components activation, contributes to the development of early vascular inflammation and morphologic alterations in experimental diabetes. *Atherosclerosis*. IN PRESS

REFERENCES

Abedin M, Omland T, Ueland T, Khera A, Aukrust P, Murphy SA, Jain T, Gruntmanis U, McGuire DK, de Lemos JA. Relation of osteoprotegerin to coronary calcium and aortic plaque (from the Dallas Heart Study). *Am J Cardiol* 2007; 99:513-8.

Aggarwal BB. Signalling pathways of the TNF superfamily: a double-edged sword. *Nat Rev Immunol* 2003; 3:745-56.

Agrotis A, Kanellakis P, Kostolias G, Di Vitto G, Wei C, Hannan R, Jennings G, Bobik A. Proliferation of neointimal smooth muscle cells after arterial injury. Dependence on interactions between fibroblast growth factor receptor-2 and fibroblast growth factor-9. *J Biol Chem* 2004; 279:42221-9.

Albiston AL, McDowall SG, Matsacos D, Sim P, Clune E, Mustafa T, Lee J, Mendelsohn FA, Simpson RJ, Connolly LM, Chai SY. Evidence that the angiotensin IV (AT(4)) receptor is the enzyme insulin-regulated aminopeptidase. *J Biol Chem* 2001; 276:48623-6.

ALLHAT Officers and Coordinators for the ALLHAT Collaborative Research Group. The Antihypertensive and Lipid-Lowering Treatment to Prevent Heart Attack Trial. Major outcomes in high-risk hypertensive patients randomized to angiotensin-converting enzyme inhibitor or calcium channel blocker vs diuretic: The Antihypertensive and Lipid-Lowering Treatment to Prevent Heart Attack Trial (ALLHAT). *JAMA* 2002; 288:2981-97.

Anand DV, Lahiri A, Lim E, Hopkins D, Corder R. The relationship between plasma osteoprotegerin levels and coronary artery calcification in uncomplicated type 2 diabetic subjects. *J Am Coll Cardiol* 2006; 47:1850-7.

Andraws R, Brown DL. Effect of inhibition of the renin-angiotensin system on development of type 2 diabetes mellitus (meta-analysis of randomized trials). *Am J Cardiol* 2007; 99:1006-12.

Andreozzi F, D'Alessandris C, Federici M, Laratta E, Del Guerra S, Del Prato S, Marchetti P, Lauro R, Perticone F, Sesti G. Activation of the hexosamine pathway leads to phosphorylation of insulin receptor substrate-1 on Ser307 and Ser612 and impairs the phosphatidylinositol 3-kinase/Akt/mammalian target of rapamycin insulin biosynthetic pathway in RIN pancreatic beta-cells. *Endocrinology* 2004; 145:2845-57.

Ashkenazi A, Herbst RS. To kill a tumor cell: the potential of proapoptotic receptor agonists. *J Clin Invest* 2008; 118:1979-90.

Avignon A, Sultan A, Piot C, Elaerts S, Cristol JP, Dupuy AM. Osteoprotegerin is associated with silent coronary artery disease in high-risk but asymptomatic type 2 diabetic patients. *Diabetes Care* 2005; 28:2176-80.

Baker SJ, Reddy EP. Modulation of life and death by the TNF receptor superfamily. *Oncogene* 1998; 17:3261-70.

Ban CR, Twigg SM. Fibrosis in diabetes complications: pathogenic mechanisms and circulating and urinary markers. *Vasc Health Risk Manag* 2008; 4:575-96.

Baud'huin M, Lamoureux F, Duplomb L, Rédini F, Heymann D. RANKL, RANK, osteoprotegerin: key partners of osteoimmunology and vascular diseases. *Cell Mol Life Sci* 2007; 64:2334-50.

Bennett BJ, Scatena M, Kirk EA, Rattazzi M, Varon RM, Averill M, Schwartz SM, Giachelli CM, Rosenfeld ME. Osteoprotegerin inactivation accelerates advanced atherosclerotic lesion progression and calcification in older ApoE-/- mice. *Arterioscler Thromb Vasc Biol* 2006; 26:2117-24.

Ben-Tal Cohen E, Hohensinner PJ, Kaun C, Maurer G, Huber K, Wojta J. Statins decrease TNF-alpha-induced osteoprotegerin production by endothelial cells and smooth muscle cells in vitro. *Biochem Pharmacol* 2007; 73:77-83.

Bindokas VP, Kuznetsov A, Sreenan S, Polonsky KS, Roe MW, Philipson LH. Visualizing superoxide production in normal and diabetic rat islets of Langerhans. *J Biol Chem* 2003; 278:9796-801.

Bobik A. Transforming growth factor-betas and vascular disorders. *Arterioscler Thromb Vasc Biol* 2006; 26:1712-20.

Borgatti P, Zauli G, Colamussi ML, Gibellini D, Previati M, Cantley LL, Capitani S. Extracellular HIV-1 Tat protein activates phosphatidylinositol 3- and Akt/PKB kinases in CD4+ T lymphoblastoid Jurkat cells. *Eur J Immunol* 1997; 27:2805-11.

Boyce BF, Xing L. Biology of RANK, RANKL, and osteoprotegerin. *Arthritis Res Ther* 2007; 9 Suppl 1:S1.

Browner WS, Lui LY, Cummings SR. Associations of serum osteoprotegerin levels with diabetes, stroke, bone density, fractures, and mortality in elderly women. *J Clin Endocrinol Metab* 2001; 86:631-7.

Bucay N, Sarosi I, Dunstan CR, Morony S, Tarpley J, Capparelli C, Scully S, Tan HL, Xu W, Lacey DL, Boyle WJ, Simonet WS. Osteoprotegerin-deficient mice develop early onset osteoporosis and arterial calcification. *Genes Dev* 1998; 12:1260-8.

Bulotta S, Barsacchi R, Rotiroti D, Borgese N, Clementi E. Activation of the endothelial nitric-oxide synthase by tumor necrosis factor-alpha. A novel feedback mechanism regulating cell death. *J Biol Chem* 2001; 276:6529-36.

Cai H, Li Z, Dikalov S, Holland SM, Hwang J, Jo H, Dudley SC Jr, Harrison DG. NAD(P)H oxidase-derived hydrogen peroxide mediates endothelial nitric oxide production in response to angiotensin II. *J Biol Chem* 2002; 277:48311-7.

Calkin AC, Allen TJ. Diabetes mellitus-associated atherosclerosis: mechanisms involved and potential for pharmacological invention. *Am J Cardiovasc Drugs* 2006; 6:15-40.

Campbell DJ, Habener JF. Angiotensinogen gene is expressed and differentially regulated in multiple tissues of the rat. *J Clin Invest* 1986; 78:31-9.

Candido R, Jandeleit-Dahm KA, Cao Z, Nesteroff SP, Burns WC, Twigg SM, Dilley RJ, Cooper ME, Allen TJ. Prevention of accelerated atherosclerosis by angiotensin-converting enzyme inhibition in diabetic apolipoprotein E-deficient mice. *Circulation* 2002; 106:246-53.

Candido R, Allen TJ, Lassila M, Cao Z, Thallas V, Cooper ME, Jandeleit-Dahm KA. Irbesartan but not amlodipine suppresses diabetes-associated atherosclerosis. *Circulation* 2004; 109:1536-42.

Carlsson PO, Berne C, Jansson L. Angiotensin II and the endocrine pancreas: effects on islet blood flow and insulin secretion in rats. *Diabetologia* 1998; 41:127-33.

Chan FK. Three is better than one: pre-ligand receptor assembly in the regulation of TNF receptor signaling. *Cytokine* 2007; 37:101-7.

Charollais A, Gjinovci A, Huarte J, Bauquis J, Nadal A, Martín F, Andreu E, Sánchez-Andrés JV, Calabrese A, Bosco D, Soria B, Wollheim CB, Herrera PL, Meda P. Junctional communication of pancreatic beta cells contributes to the control of insulin secretion and glucose tolerance. *J Clin Invest* 2000; 106:235-43.

Chen MC, Proost P, Gysemans C, Mathieu C, Eizirik DL. Monocyte chemoattractant protein-1 is expressed in pancreatic islets from prediabetic NOD mice and in interleukin-1 beta-exposed human and rat islet cells. *Diabetologia* 2001; 44:325-32.

Chu KY, Lau T, Carlsson PO, Leung PS. Angiotensin II type 1 receptor blockade improves beta-cell function and glucose tolerance in a mouse model of type 2 diabetes. *Diabetes* 2006; 55:367-74.

Collin-Osdoby P, Rothe L, Anderson F, Nelson M, Maloney W, Osdoby P. Receptor activator of NF-kappa B and osteoprotegerin expression by human microvascular endothelial cells,

regulation by inflammatory cytokines, and role in human osteoclastogenesis. *J Biol Chem* 2001; 276:20659-72.

Collin-Osdoby P. Regulation of vascular calcification by osteoclast regulatory factors RANKL and osteoprotegerin. *Circ Res* 2004; 95:1046-57.

Cooper ME, McNally PG, Phillips PA, Johnston CI. Amylin stimulates plasma renin concentration in humans. *Hypertension* 1995; 26:460-4.

Corallini F, Rimondi E, Secchiero P. TRAIL and osteoprotegerin: a role in endothelial physiopathology? *Front Biosci* 2008; 13:135-47.

Corrado E, Rizzo M, Coppola G, Fattouch K, Novo G, Marturana I, Ferrara F, Novo S. An update on the role of markers of inflammation in atherosclerosis. *J Atheroscler Thromb* 2010; 17:1-11.

Cowling RT, Gurantz D, Peng J, Dillmann WH, Greenberg BH. Transcription factor NF-kappa B is necessary for up-regulation of type 1 angiotensin II receptor mRNA in rat cardiac fibroblasts treated with tumor necrosis factor-alpha or interleukin-1 beta. *J Biol Chem* 2002; 277:5719-24.

Davis BJ, Forbes JM, Thomas MC, Jerums G, Burns WC, Kawachi H, Allen TJ, Cooper ME. Superior renoprotective effects of combination therapy with ACE and AGE inhibition in the diabetic spontaneously hypertensive rat. *Diabetologia* 2004; 47:89-97.

de Winther MP, Kanters E, Kraal G, Hofker MH. Nuclear factor kappaB signaling in atherogenesis. *Arterioscler Thromb Vasc Biol* 2005; 25:904-14.

Degli-Esposti M. To die or not to die--the quest of the TRAIL receptors. *J Leukoc Biol* 1999; 65:535-42.

Dempsey PW, Doyle SE, He JQ, Cheng G. The signaling adaptors and pathways activated by TNF superfamily. *Cytokine Growth Factor Rev* 2003; 14:193-209.

di Mola FF, Friess H, Martignoni ME, Di Sebastiano P, Zimmermann A, Innocenti P, Graber H, Gold LI, Korc M, Büchler MW. Connective tissue growth factor is a regulator for fibrosis in human chronic pancreatitis. *Ann Surg* 1999; 230:63-71.

Donoghue M, Hsieh F, Baronas E, Godbout K, Gosselin M, Stagliano N, Donovan M, Woolf B, Robison K, Jeyaseelan R, Breitbart RE, Acton S. A novel angiotensin-converting enzyme-related carboxypeptidase (ACE2) converts angiotensin I to angiotensin 1-9. *Circ Res* 2000; 87:E1-9.

Dubois M, Kerr-Conte J, Gmyr V, Bouckenooghe T, Muharram G, D'Herbomez M, Martin-Ponthieu A, Vantyghem MC, Vandewalle B, Pattou F. Non-esterified fatty acids are deleterious for human pancreatic islet function at physiological glucose concentration. *Diabetologia* 2004; 47:463-9.

Ehses JA, Lacraz G, Giroix MH, Schmidlin F, Coulaud J, Kassis N, Irminger JC, Kergoat M, Portha B, Homo-Delarche F, Donath MY. IL-1 antagonism reduces hyperglycemia and tissue inflammation in the type 2 diabetic GK rat. *Proc Natl Acad Sci U S A* 2009; 106:13998-4003.

Emery JG, McDonnell P, Burke MB, Deen KC, Lyn S, Silverman C, Dul E, Appelbaum ER, Eichman C, DiPrinzio R, Dodds RA, James IE, Rosenberg M, Lee JC, Young PR. Osteoprotegerin is a receptor for the cytotoxic ligand TRAIL. *J Biol Chem* 1998; 273:14363-7.

Erdogan B, Aslan E, Bagis T, Gokcel A, Erkanli S, Bavbek M, Altinors N. Intima-media thickness of the carotid arteries is related to serum osteoprotegerin levels in healthy postmenopausal women. *Neurol Res* 2004; 26:658-61.

Federici M, Hribal M, Perego L, Ranalli M, Caradonna Z, Perego C, Usellini L, Nano R, Bonini P, Bertuzzi F, Marlier LN, Davalli AM, Carandente O, Pontiroli AE, Melino G, Marchetti P, Lauro R, Sesti G, Folli F. High glucose causes apoptosis in cultured human pancreatic islets of Langerhans: a potential role for regulation of specific Bcl family genes toward an apoptotic cell death program. *Diabetes* 2001; 50:1290-301.

Feige U. Osteoprotegerin. *Ann Rheum Dis* 2001; 60 Suppl 3:iii81-4.

Fiedler U, Reiss Y, Scharpfenecker M, Grunow V, Koidl S, Thurston G, Gale NW, Witzenrath M, Rosseau S, Suttorp N, Sobke A, Herrmann M, Preissner KT, Vajkoczy P, Augustin HG. Angiopoietin-2 sensitizes endothelial cells to TNF-alpha and has a crucial role in the induction of inflammation. *Nat Med* 2006; 12:235-9.

Finnberg N, El-Deiry WS. TRAIL death receptors as tumor suppressors and drug targets. *Cell Cycle* 2008; 7:1525-8.

Forbes JM, Cooper ME, Thallas V, Burns WC, Thomas MC, Brammar GC, Lee F, Grant SL, Burrell LA, Jerums G, Osicka TM. Reduction of the accumulation of advanced glycation end products by ACE inhibition in experimental diabetic nephropathy. *Diabetes* 2002; 51:3274-82.

Fujiwara K, Nagasaka A, Nagata M, Yamamoto K, Imamura S, Oda N, Sawai Y, Hayakawa N, Suzuki A, Itoh M. A stable prostacyclin analogue reduces high serum TNF-alpha levels in diabetic patients. *Exp Clin Endocrinol Diabetes* 2004; 112:390-4.

Galluzzi F, Stagi S, Salti R, Toni S, Piscitelli E, Simonini G, Falcini F, Chiarelli F. Osteoprotegerin serum levels in children with type 1 diabetes: a potential modulating role in bone status. *Eur J Endocrinol* 2005; 153:879-85.

Geusens P. Emerging treatments for postmenopausal osteoporosis - focus on denosumab. *Clin Interv Aging* 2009; 4:241-50.

Glass CK, Witztum JL. Atherosclerosis: the road ahead. *Cell* 2001; 104:503-16.

Gletsu N, Doan TN, Cole J, Sutliff RL, Bernstein KE. Angiotensin II-induced hypertension in mice caused an increase in insulin secretion. *Vascul Pharmacol* 2005; 42:83-92.

Grauslund J, Rasmussen LM, Green A, Sjølie AK. Does osteoprotegerin relate to micro- and macrovascular complications in long-term type 1 diabetes? *Scand J Clin Lab Invest* 2010; 70:188-93.

Grcević D, Katavić V, Lukić IK, Kovacić N, Lorenzo JA, Marusić A. Cellular and molecular interactions between immune system and bone. *Croat Med J* 2001; 42:384-92.

Griendling KK, Minieri CA, Ollerenshaw JD, Alexander RW. Angiotensin II stimulates NADH and NADPH oxidase activity in cultured vascular smooth muscle cells. *Circ Res* 1994; 74:1141-8.

Griffith TS, Stokes B, Kucaba TA, Earel JK Jr, VanOosten RL, Brincks EL, Norian LA. TRAIL gene therapy: from preclinical development to clinical application. *Curr Gene Ther* 2009; 9:9-19.

Gross O, Beirowski B, Koepke ML, Kuck J, Reiner M, Addicks K, Smyth N, Schulze-Lohoff E, Weber M. Preemptive ramipril therapy delays renal failure and reduces renal fibrosis in COL4A3-knockout mice with Alport syndrome. *Kidney Int* 2003; 63:438-46.

Guicciardi ME, Gores GJ. Life and death by death receptors. *FASEB J* 2009; 23:1625-37.

Hansson L, Lindholm LH, Niskanen L, Lanke J, Hedner T, Niklason A, Luomanmäki K, Dahlöf B, de Faire U, Mörlin C, Karlberg BE, Wester PO, Björck JE. Effect of angiotensin-converting-enzyme inhibition compared with conventional therapy on cardiovascular morbidity and mortality in hypertension: the Captopril Prevention Project (CAPPP) randomised trial. *Lancet* 1999; 353:611-6.

Harmon JS, Gleason CE, Tanaka Y, Poitout V, Robertson RP. Antecedent hyperglycemia, not hyperlipidemia, is associated with increased islet triacylglycerol content and decreased insulin gene mRNA level in Zucker diabetic fatty rats. *Diabetes* 2001; 50:2481-6.

Hayden MR, Sowers JR. Isletopathy in type2 diabetes mellitus: implications of islet RAS, islet fibrosis, islet amyloid, remodeling and oxidative stress. *Antioxid Redox Signal* 2007; 9:891-910.

Hehlgans T, Pfeffer K. The intriguing biology of the tumour necrosis factor/tumour necrosis factor receptor superfamily: players, rules and the games. *Immunology* 2005; 115:1-20.

Heickendorff L, Ledet T, Rasmussen LM. Glycosaminoglycans in the human aorta in diabetes mellitus: a study of tunica media from areas with and without atherosclerotic plaque. *Diabetologia* 1994; 37:286-92.

Heinonen SE, Leppänen P, Kholová I, Lumivuori H, Häkkinen SK, Bosch F, Laakso M, Ylä-Herttuala S. Increased atherosclerotic lesion calcification in a novel mouse model combining insulin resistance, hyperglycemia, and hypercholesterolemia. *Circ Res* 2007; 101:1058-67.

Hofbauer LC, Heufelder AE, Erben RG. Osteoprotegerin, RANK, and RANK ligand: the good, the bad, and the ugly in rheumatoid arthritis. *J Rheumatol* 2001; 28:685-7.

Hong YM. Atherosclerotic cardiovascular disease beginning in childhood. *Korean Circ J* 2010; 40:1-9.

Höppener JW, Ahrén B, Lips CJ. Islet amyloid and type 2 diabetes mellitus. *N Engl J Med* 2000; 343:411-9.

Jacqueminet S, Briaud I, Rouault C, Reach G, Poitout V. Inhibition of insulin gene expression by long-term exposure of pancreatic beta cells to palmitate is dependent on the presence of a stimulatory glucose concentration. *Metabolism* 2000; 49:532-6.

Janke J, Engeli S, Gorzelniak K, Luft FC, Sharma AM. Mature adipocytes inhibit in vitro differentiation of human preadipocytes via angiotensin type 1 receptors. *Diabetes* 2002; 51:1699-707.

Jawień J, Nastałek P, Korbut R. Mouse models of experimental atherosclerosis. *J Physiol Pharmacol* 2004; 55:503-17.

Johnston CI, Burrell LM, Perich R, Jandeleit K, Jackson B. The tissue renin-angiotensin system and its functional role. *Clin Exp Pharmacol Physiol Suppl* 1992; 19:1-5.

Jono S, Ikari Y, Shioi A, Mori K, Miki T, Hara K, Nishizawa Y. Serum osteoprotegerin levels are associated with the presence and severity of coronary artery disease. *Circulation* 2002; 106:1192-4.

Jono S, Otsuki S, Higashikuni Y, Shioi A, Mori K, Hara K, Hashimoto H, Ikari Y. Serum osteoprotegerin levels and long-term prognosis in subjects with stable coronary artery disease. *J Thromb Haemost* 2010; 8:1170-5.

Jørgensen GM, Vind B, Nybo M, Rasmussen LM, Højlund K. Acute hyperinsulinemia decreases plasma osteoprotegerin with diminished effect in type 2 diabetes and obesity. *Eur J Endocrinol* 2009; 161:95-101.

Josien R, Li HL, Ingulli E, Sarma S, Wong BR, Vologodskaia M, Steinman RM, Choi Y. TRANCE, a tumor necrosis factor family member, enhances the longevity and adjuvant properties of dendritic cells in vivo. *J Exp Med* 2000; 191:495-502.

Joussen AM, Poulaki V, Mitsiades N, Kirchhof B, Koizumi K, Döhmen S, Adamis AP. Nonsteroidal anti-inflammatory drugs prevent early diabetic retinopathy via TNF-alpha suppression. *FASEB J* 2002; 16:438-40.

Julius S, Kjeldsen SE, Weber M, Brunner HR, Ekman S, Hansson L, Hua T, Laragh J, McInnes GT, Mitchell L, Plat F, Schork A, Smith B, Zanchetti A; VALUE trial group. Outcomes in hypertensive patients at high cardiovascular risk treated with regimens based on valsartan or amlodipine: the VALUE randomised trial. *Lancet* 2004; 363:2022-31.

Kahn SE, Hull RL, Utzschneider KM. Mechanisms linking obesity to insulin resistance and type 2 diabetes. *Nature* 2006; 444:840-6.

Kawamori D, Kajimoto Y, Kaneto H, Umayahara Y, Fujitani Y, Miyatsuka T, Watada H, Leibiger IB, Yamasaki Y, Hori M. Oxidative stress induces nucleo-cytoplasmic translocation of pancreatic transcription factor PDX-1 through activation of c-Jun NH(2)-terminal kinase. *Diabetes* 2003; 52:2896-904.

Kearns AE, Khosla S, Kostenuik PJ. Receptor activator of nuclear factor kappaB ligand and osteoprotegerin regulation of bone remodeling in health and disease. *Endocr Rev* 2008; 29:155-92.

Kiechl S, Schett G, Wenning G, Redlich K, Oberhollenzer M, Mayr A, Santer P, Smolen J, Poewe W, Willeit J. Osteoprotegerin is a risk factor for progressive atherosclerosis and cardiovascular disease. *Circulation* 2004; 109:2175-80.

Knudsen ST, Foss CH, Poulsen PL, Andersen NH, Mogensen CE, Rasmussen LM. Increased plasma concentrations of osteoprotegerin in type 2 diabetic patients with microvascular complications. *Eur J Endocrinol* 2003; 149:39-42.

Koka V, Huang XR, Chung AC, Wang W, Truong LD, Lan HY. Angiotensin II up-regulates angiotensin I-converting enzyme (ACE), but down-regulates ACE2 via the AT1-ERK/p38 MAP kinase pathway. *Am J Pathol* 2008; 172:1174-83.

Kuno A, Yamada T, Masuda K, Ogawa K, Sogawa M, Nakamura S, Nakazawa T, Ohara H, Nomura T, Joh T, Shirai T, Itoh M. Angiotensin-converting enzyme inhibitor attenuates pancreatic inflammation and fibrosis in male Wistar Bonn/Kobori rats. *Gastroenterology* 2003; 124:1010-9.

Kwon B, Kim BS, Cho HR, Park JE, Kwon BS. Involvement of tumor necrosis factor receptor superfamily (TNFRSF) members in the pathogenesis of inflammatory diseases. *Exp Mol Med* 2003; 35:8-16.

Lamoureux F, Picarda G, Garrigue-Antar L, Baud'huin M, Trichet V, Vidal A, Miot-Noirault E, Pitard B, Heymann D, Rédini F. Glycosaminoglycans as potential regulators of osteoprotegerin therapeutic activity in osteosarcoma. *Cancer Res* 2009; 69:526-36.

Landmesser U, Hornig B, Drexler H. Endothelial function: a critical determinant in atherosclerosis? *Circulation* 2004; 109:II27-33.

Lastra G, Manrique C. The expanding role of oxidative stress, renin angiotensin system, and beta-cell dysfunction in the cardiometabolic syndrome and Type 2 diabetes mellitus. *Antioxid Redox Signal* 2007; 9:943-54.

Lau T, Carlsson PO, Leung PS. Evidence for a local angiotensin-generating system and dose-dependent inhibition of glucose-stimulated insulin release by angiotensin II in isolated pancreatic islets. *Diabetologia* 2004; 47:240-8.

Lavoie JL, Sigmund CD. Minireview: Overview of the Renin-Angiotensin System—An Endocrine and Paracrine System. *Endocrinology* 2003; 144: 2179-2183.

Lawrie A, Waterman E, Southwood M, Evans D, Suntharalingam J, Francis S, Crossman D, Croucher P, Morrell N, Newman C. Evidence of a role for osteoprotegerin in the pathogenesis of pulmonary arterial hypertension. *Am J Pathol* 2008; 172:256-64.

Lee Y, Hirose H, Ohneda M, Johnson JH, McGarry JD, Unger RH. Beta-cell lipotoxicity in the pathogenesis of non-insulin-dependent diabetes mellitus of obese rats: impairment in adipocyte-beta-cell relationships. *Proc Natl Acad Sci U S A* 1994; 91:10878-82.

Lehto S, Niskanen L, Suhonen M, Rönnemaa T, Laakso M. Medial artery calcification. A neglected harbinger of cardiovascular complications in non-insulin-dependent diabetes mellitus. *Arterioscler Thromb Vasc Biol* 1996; 16:978-83.

Leung PS, Chan HC, Wong PY. Immunohistochemical localization of angiotensin II in the mouse pancreas. *Histochem J* 1998; 30:21-5.

Leung PS, Carlsson PO. Tissue renin-angiotensin system: its expression, localization, regulation and potential role in the pancreas. *J Mol Endocrinol* 2001; 26:155-64.

Leung PS, Chappell MC. A local pancreatic renin-angiotensin system: endocrine and exocrine roles. *Int J Biochem Cell Biol* 2003; 35:838-46.

Libby P. Inflammation in atherosclerosis. *Nature* 2002; 420:868-74.

Libby P, Okamoto Y, Rocha VZ, Folco E. Inflammation in atherosclerosis: transition from theory to practice. *Circ J* 2010; 74:213-20.

Lieb W, Gona P, Larson MG, Massaro JM, Lipinska I, Keaney JF Jr, Rong J, Corey D, Hoffmann U, Fox CS, Vasan RS, Benjamin EJ, O'Donnell CJ, Kathiresan S. Biomarkers of the osteoprotegerin pathway: clinical correlates, subclinical disease, incident cardiovascular disease, and mortality. *Arterioscler Thromb Vasc Biol* 2010; 30:1849-54.

Lindholm LH, Ibsen H, Borch-Johnsen K, Olsen MH, Wachtell K, Dahlöf B, Devereux RB, Beevers G, de Faire U, Fyhrquist F, Julius S, Kjeldsen SE, Kristianson K, Lederballe-Pedersen O, Nieminen MS, Omvik P, Oparil S, Wedel H, Aurup P, Edelman JM, Snapinn S; For the LIFE study group. Risk of new-onset diabetes in the Losartan Intervention For Endpoint reduction in hypertension study. *J Hypertens* 2002; 20:1879-86.

Lindholm LH, Persson M, Alaupovic P, Carlberg B, Svensson A, Samuelsson O. Metabolic outcome during 1 year in newly detected hypertensives: results of the Antihypertensive Treatment and Lipid Profile in a North of Sweden Efficacy Evaluation (ALPINE study). *J Hypertens* 2003; 21:1563-74.

Locksley RM, Killeen N, Lenardo MJ. The TNF and TNF receptor superfamilies: integrating mammalian biology. *Cell* 2001; 104:487-501.

Lupi R, Dotta F, Marselli L, Del Guerra S, Masini M, Santangelo C, Patané G, Boggi U, Piro S, Anello M, Bergamini E, Mosca F, Di Mario U, Del Prato S, Marchetti P. Prolonged exposure to free fatty acids has cytostatic and pro-apoptotic effects on human pancreatic islets: evidence that beta-cell death is caspase mediated, partially dependent on ceramide pathway, and Bcl-2 regulated. *Diabetes* 2002; 51:1437-42.

Lupi R, Del Guerra S, Bugliani M, Boggi U, Mosca F, Torri S, Del Prato S, Marchetti P. The direct effects of the angiotensin-converting enzyme inhibitors, zofenoprilat and enalaprilat, on isolated human pancreatic islets. *Eur J Endocrinol* 2006; 154:355-61.

Lusis AJ. Atherosclerosis. *Nature* 2000; 407:233-41.

MacEwan DJ. Interactions between TNF and GnRH. *Neurochem Res* 2008; 33:678-82.

Mangan SH, Van Campenhout A, Rush C, Golledge J. Osteoprotegerin upregulates endothelial cell adhesion molecule response to tumor necrosis factor-alpha associated with induction of angiopoietin-2. *Cardiovasc Res* 2007; 76:494-505.

Marchetti P, Dotta F, Lauro D, Purrello F. An overview of pancreatic beta-cell defects in human type 2 diabetes: implications for treatment. *Regul Pept* 2008; 146:4-11.

Martin MM, Buckenberger JA, Jiang J, Malana GE, Knoell DL, Feldman DS, Elton TS. TGF-beta1 stimulates human AT1 receptor expression in lung fibroblasts by cross talk between the Smad, p38 MAPK, JNK, and PI3K signaling pathways. *Am J Physiol Lung Cell Mol Physiol* 2007; 293:L790-9.

Meier JJ, Kayed R, Lin CY, Gurlo T, Haataja L, Jayasinghe S, Langen R, Glabe CG, Butler PC. Inhibition of human IAPP fibril formation does not prevent beta-cell death: evidence for distinct actions of oligomers and fibrils of human IAPP. *Am J Physiol Endocrinol Metab* 2006; 291:E1317-24.

Meir KS, Leitersdorf E. Atherosclerosis in the apolipoprotein-E-deficient mouse: a decade of progress. *Arterioscler Thromb Vasc Biol* 2004; 24:1006-14.

Mesquita M, Demulder A, Damry N, Mélot C, Wittersheim E, Willems D, Dratwa M, Bergmann P. Plasma osteoprotegerin is an independent risk factor for mortality and an early biomarker of coronary vascular calcification in chronic kidney disease. *Clin Chem Lab Med* 2009; 47:339-46.

Mizuno A, Murakami A, Nakagawa N, Yasuda H, Tsuda E, Morinaga T, Higashio K. Structure of the mouse osteoclastogenesis inhibitory factor (OCIF) gene and its expression in embryogenesis. *Gene* 1998; 215:339-43. a

Mizuno A, Amizuka N, Irie K, Murakami A, Fujise N, Kanno T, Sato Y, Nakagawa N, Yasuda H, Mochizuki S, Gomibuchi T, Yano K, Shima N, Washida N, Tsuda E, Morinaga T, Higashio K, Ozawa H. Severe osteoporosis in mice lacking osteoclastogenesis inhibitory factor/osteoprotegerin. *Biochem Biophys Res Commun* 1998; 247:610-5. b

Monaco C, Paleolog E. Nuclear factor kappaB: a potential therapeutic target in atherosclerosis and thrombosis. *Cardiovasc Res* 2004; 61:671-82.

Moran CS, McCann M, Karan M, Norman P, Ketheesan N, Golledge J. Association of osteoprotegerin with human abdominal aortic aneurysm progression. *Circulation* 2005; 111:3119-25.

Moran CS, Cullen B, Campbell JH, Golledge J. Interaction between angiotensin II, osteoprotegerin, and peroxisome proliferator-activated receptor-gamma in abdominal aortic aneurysm. *J Vasc Res* 2009; 46:209-17.

Morena M, Terrier N, Jaussent I, Leray-Moragues H, Chalabi L, Rivory JP, Maurice F, Delcourt C, Cristol JP, Canaud B, Dupuy AM. Plasma osteoprotegerin is associated with mortality in hemodialysis patients. *J Am Soc Nephrol* 2006; 17:262-70.

Morinaga T, Nakagawa N, Yasuda H, Tsuda E, Higashio K. Cloning and characterization of the gene encoding human osteoprotegerin/osteoclastogenesis-inhibitory factor. *Eur J Biochem* 1998; 254:685-91.

Morony S, Tintut Y, Zhang Z, Cattley RC, Van G, Dwyer D, Stolina M, Kostenuik PJ, Demer LL. Osteoprotegerin inhibits vascular calcification without affecting atherosclerosis in ldlr(-/-) mice. *Circulation* 2008; 117:411-20.

Mosheimer BA, Kaneider NC, Feistritzer C, Djanani AM, Sturn DH, Patsch JR, Wiedermann CJ. Syndecan-1 is involved in osteoprotegerin-induced chemotaxis in human peripheral blood monocytes. *J Clin Endocrinol Metab* 2005; 90:2964-71.

Murphy M, Godson C, Cannon S, Kato S, Mackenzie HS, Martin F, Brady HR. Suppression subtractive hybridization identifies high glucose levels as a stimulus for expression of connective tissue growth factor and other genes in human mesangial cells. *J Biol Chem* 1999; 274:5830-4.

Nakashima Y, Plump AS, Raines EW, Breslow JL, Ross R. ApoE-deficient mice develop lesions of all phases of atherosclerosis throughout the arterial tree. *Arterioscler Thromb* 1994; 14:133-40.

Nguyen G, Delarue F, Burcklé C, Bouzhir L, Giller T, Sraer JD. Pivotal role of the renin/prorenin receptor in angiotensin II production and cellular responses to renin. *J Clin Invest* 2002; 109:1417-27.

Niskanen L, Siitonen O, Suhonen M, Uusitupa MI. Medial artery calcification predicts cardiovascular mortality in patients with NIDDM. *Diabetes Care* 1994; 17:1252-6.

Nybo M, Rasmussen LM. Osteoprotegerin released from the vascular wall by heparin mainly derives from vascular smooth muscle cells. *Atherosclerosis* 2008; 201:33-5.

Okada K, Hirano T, Ran J, Adachi M. Olmesartan medoxomil, an angiotensin II receptor blocker ameliorates insulin resistance and decreases triglyceride production in fructose-fed rats. *Hypertens Res* 2004; 27:293-9.

Olesen P, Ledet T, Rasmussen LM. Arterial osteoprotegerin: increased amounts in diabetes and modifiable synthesis from vascular smooth muscle cells by insulin and TNF-alpha. *Diabetologia* 2005; 48:561-8.

Oliveira HR, Verlengia R, Carvalho CR, Britto LR, Curi R, Carpinelli AR. Pancreatic beta-cells express phagocyte-like NAD(P)H oxidase. *Diabetes* 2003; 52:1457-63.

Onozato ML, Tojo A, Goto A, Fujita T, Wilcox CS. Oxidative stress and nitric oxide synthase in rat diabetic nephropathy: effects of ACEI and ARB. *Kidney Int* 2002; 61:186-94.

Ou D, Metzger DL, Wang X, Huang J, Pozzilli P, Tingle AJ. TNF-related apoptosis-inducing ligand death pathway-mediated human beta-cell destruction. *Diabetologia* 2002; 45:1678-88.

Ovchinnikova O, Gylfe A, Bailey L, Nordström A, Rudling M, Jung C, Bergström S, Waldenström A, Hansson GK, Nordström P. Osteoprotegerin promotes fibrous cap formation in atherosclerotic lesions of ApoE-deficient mice--brief report. *Arterioscler Thromb Vasc Biol* 2009; 29:1478-80.

Pandolfi A, Grilli A, Cilli C, Patruno A, Giaccari A, Di Silvestre, De Lutiis MA, Pellegrini G, Capani F, Consoli A, Felaco M. Phenotype modulation in cultures of vascularsmooth muscle cells from diabetic rats: association with increased nitric oxide synthase expression and superoxide anion generation. *J Cell Physiol* 2003; 196:378–385.

Paul M, Poyan Mehr A, Kreutz R. Physiology of local renin-angiotensin systems. *Physiol Rev* 2006; 86:747-803.

Paul WE. Fundamental Immunology (Book). *Lippincot Williams & Wilkins*, 2008; chapter 25: 777

Pham Y, Tu Y, Wu T, Allen TJ, Calkin AC, Watson AM, Li J, Jandeleit-Dahm KA, Toh BH, Cao Z, Cooper ME, Chai Z. Cell division autoantigen 1 plays a profibrotic role by modulating downstream signalling of TGF-beta in a murine diabetic model of atherosclerosis. *Diabetologia* 2010; 53:170-9.

Piao M, Tokunaga O. Significant expression of endoglin (CD105), TGFbeta-1 and TGFbeta R-2 in the atherosclerotic aorta: an immunohistological study. *J Atheroscler Thromb* 2006; 13:82-9.

Poitout V, Robertson RP. Minireview: Secondary beta-cell failure in type 2 diabetes--a convergence of glucotoxicity and lipotoxicity. *Endocrinology* 2002; 143:339-42.

Poitout V, Robertson RP. Glucolipotoxicity: fuel excess and beta-cell dysfunction. *Endocr Rev* 2008; 29:351-66.

Price PA, June HH, Buckley JR, Williamson MK. Osteoprotegerin inhibits artery calcification induced by warfarin and by vitamin D. *Arterioscler Thromb Vasc Biol* 2001; 21:1610-6. a

Price PA, Faus SA, Williamson MK. Bisphosphonates alendronate and ibandronate inhibit artery calcification at doses comparable to those that inhibit bone resorption. *Arterioscler Thromb Vasc Biol* 2001; 21:817-24. b

Ran J, Hirano T, Adachi M. Angiotensin II type 1 receptor blocker ameliorates overproduction and accumulation of triglyceride in the liver of Zucker fatty rats. *Am J Physiol Endocrinol Metab* 2004; 287:E227-32.

Rasmussen LM, Ledet T. Aortic collagen alterations in human diabetes mellitus. Changes in basement membrane collagen content and in the susceptibility of total collagen to cyanogen bromide solubilisation. *Diabetologia* 1993; 36:445-53.

Rasmussen LM, Tarnow L, Hansen TK, Parving HH, Flyvbjerg A. Plasma osteoprotegerin levels are associated with glycaemic status, systolic blood pressure, kidney function and cardiovascular morbidity in type 1 diabetic patients. *Eur J Endocrinol* 2006; 154:75-81.

Rauch BH, Millette E, Kenagy RD, Daum G, Fischer JW, Clowes AW. Syndecan-4 is required for thrombin-induced migration and proliferation in human vascular smooth muscle cells. *J Biol Chem* 2005; 280:17507-11.

Regoli M, Bendayan M, Fonzi L, Sernia C, Bertelli E. Angiotensinogen localization and secretion in the rat pancreas. *J Endocrinol* 2003; 179:81-9.

Reid IA, Morris BJ, Ganong WF.The renin-angiotensin system. *Annu. Rev. Physiol* 1978; 40:377-410.

Reid P, Holen I. Pathophysiological roles of osteoprotegerin (OPG). *Eur J Cell Biol* 2009; 88:1-17.

Rekhter MD. Collagen synthesis in atherosclerosis: too much and not enough. *Cardiovasc Res* 1999; 41:376-84.

Robertson RP. Chronic oxidative stress as a central mechanism for glucose toxicity in pancreatic islet beta cells in diabetes. *J Biol Chem* 2004; 279:42351-4.

Roehrich ME, Mooser V, Lenain V, Herz J, Nimpf J, Azhar S, Bideau M, Capponi A, Nicod P, Haefliger JA, Waeber G. Insulin-secreting beta-cell dysfunction induced by human lipoproteins. *J Biol Chem* 2003; 278:18368-75.

Ruiz-Ortega M, Rodríguez-Vita J, Sanchez-Lopez E, Carvajal G, Egido J. TGF-beta signaling in vascular fibrosis. *Cardiovasc Res* 2007; 74:196-206.

Rupérez M, Ruiz-Ortega M, Esteban V, Lorenzo O, Mezzano S, Plaza JJ, Egido J. Angiotensin II increases connective tissue growth factor in the kidney. *Am J Pathol* 2003; 163:1937-47.

Santos RA, Simoes e Silva AC, Maric C, Silva DM, Machado RP, de Buhr I, Heringer-Walther S, Pinheiro SV, Lopes MT, Bader M, Mendes EP, Lemos VS, Campagnole-Santos MJ, Schultheiss HP, Speth R, Walther T. Angiotensin-(1-7) is an endogenous ligand for the G protein-coupled receptor Mas. *Proc Natl Acad Sci U S A* 2003; 100:8258-63.

Santos RA, Ferreira AJ. Angiotensin-(1-7) and the renin-angiotensin system. *Curr Opin Nephrol Hypertens* 2007; 16:122-8.

Satoh M, Kashihara N, Yamasaki Y, Maruyama K, Okamoto K, Maeshima Y, Sugiyama H, Sugaya T, Murakami K, Makino H. Renal interstitial fibrosis is reduced in angiotensin II type 1a receptor-deficient mice. *J Am Soc Nephrol* 2001; 12:317-25

Schling P, Löffler G. Effects of angiotensin II on adipose conversion and expression of genes of the renin-angiotensin system in human preadipocytes. *Horm Metab Res* 2001; 33:189-95.

Schoppet M, Preissner KT, Hofbauer LC. RANK ligand and osteoprotegerin: paracrine regulators of bone metabolism and vascular function. *Arterioscler Thromb Vasc Biol* 2002; 22:549-53.

Schoppet M, Sattler AM, Schaefer JR, Herzum M, Maisch B, Hofbauer LC. Increased osteoprotegerin serum levels in men with coronary artery disease. *J Clin Endocrinol Metab* 2003; 88:1024-8.

Secchiero P, Gonelli A, Carnevale E, Milani D, Pandolfi A, Zella D, Zauli G. TRAIL promotes the survival and proliferation of primary human vascular endothelial cells by activating the Akt and ERK pathways. *Circulation* 2003; 107:2250-6.

Secchiero P, Corallini F, di Iasio MG, Gonelli A, Barbarotto E, Zauli G. TRAIL counteracts the proadhesive activity of inflammatory cytokines in endothelial cells by down-modulating CCL8 and CXCL10 chemokine expression and release. *Blood* 2005; 105:3413-9.

Secchiero P, Candido R, Corallini F, Zacchigna S, Toffoli B, Rimondi E, Fabris B, Giacca M, Zauli G. Systemic tumor necrosis factor-related apoptosis-inducing ligand delivery shows antiatherosclerotic activity in apolipoprotein E-null diabetic mice. *Circulation* 2006; 114:1522-30. b

Secchiero P, Corallini F, Pandolfi A, Consoli A, Candido R, Fabris B, Celeghini C, Capitani S, Zauli G. An increased osteoprotegerin serum release characterizes the early onset of diabetes mellitus and may contribute to endothelial cell dysfunction. *Am J Pathol* 2006; 169:2236-44. a

Seccia TM, Belloni AS, Kreutz R, Paul M, Nussdorfer GG, Pessina AC, Rossi GP. Cardiac fibrosis occurs early and involves endothelin and AT-1 receptors in hypertension due to endogenous angiotensin II. *J Am Coll Cardiol* 2003; 41:666-73.

Shao J, Iwashita N, Ikeda F, Ogihara T, Uchida T, Shimizu T, Uchino H, Hirose T, Kawamori R, Watada H. Beneficial effects of candesartan, an angiotensin II type 1 receptor blocker, on beta-cell function and morphology in db/db mice. *Biochem Biophys Res Commun* 2006; 344:1224-33.

Shargorodsky M, Boaz M, Luckish A, Matas Z, Gavish D, Mashavi M. Osteoprotegerin as an independent marker of subclinical atherosclerosis in osteoporotic postmenopausal women. *Atherosclerosis* 2009; 204:608-11.

Shin JY, Shin YG, Chung CH. Elevated serum osteoprotegerin levels are associated with vascular endothelial dysfunction in type 2 diabetes. *Diabetes Care* 2006; 29:1664-6.

Simonet WS, Lacey DL, Dunstan CR, Kelley M, Chang MS, Lüthy R, Nguyen HQ, Wooden S, Bennett L, Boone T, Shimamoto G, DeRose M, Elliott R, Colombero A, Tan HL, Trail G, Sullivan J, Davy E, Bucay N, Renshaw-Gegg L, Hughes TM, Hill D, Pattison W, Campbell P, Sander S, Van G, Tarpley J, Derby P, Lee R, Boyle WJ. Osteoprotegerin: a novel secreted protein involved in the regulation of bone density. *Cell* 1997; 89:309-19.

Sjöholm A, Nyström T. Endothelial inflammation in insulin resistance. *Lancet* 2005; 365:610-2.

Soufi M, Schoppet M, Sattler AM, Herzum M, Maisch B, Hofbauer LC, Schaefer JR. Osteoprotegerin gene polymorphisms in men with coronary artery disease. *J Clin Endocrinol Metab* 2004; 89:3764-8.

Standal T, Seidel C, Hjertner Ø, Plesner T, Sanderson RD, Waage A, Borset M, Sundan A. Osteoprotegerin is bound, internalized, and degraded by multiple myeloma cells. *Blood* 2002; 100:3002-7.

Sun Y, Zhang J, Zhang JQ, Ramires FJ. Local angiotensin II and transforming growth factor-beta1 in renal fibrosis of rats. *Hypertension* 2000; 35:1078-84.

Tahmasebi M, Puddefoot JR, Inwang ER, Vinson GP. The tissue renin-angiotensin system in human pancreas. *J Endocrinol* 1999; 161:317-22.

Tajiri Y, Möller C, Grill V. Long-term effects of aminoguanidine on insulin release and biosynthesis: evidence that the formation of advanced glycosylation end products inhibits B cell function. *Endocrinology* 1997; 138:273-80.

Takemoto M, Yokote K, Nishimura M, Shigematsu T, Hasegawa T, Kon S, Uede T, Matsumoto T, Saito Y, Mori S. Enhanced expression of osteopontin in human diabetic artery and analysis of its functional role in accelerated atherogenesis. *Arterioscler Thromb Vasc Biol* 2000; 20:624-8.

Thallas-Bonke V, Thorpe SR, Coughlan MT, Fukami K, Yap FY, Sourris KC, Penfold SA, Bach LA, Cooper ME, Forbes JM. Inhibition of NADPH oxidase prevents advanced glycation end product-mediated damage in diabetic nephropathy through a protein kinase C-alpha-dependent pathway. *Diabetes* 2008; 57:460-9.

Theoleyre S, Wittrant Y, Couillaud S, Vusio P, Berreur M, Dunstan C, Blanchard F, Rédini F, Heymann D. Cellular activity and signaling induced by osteoprotegerin in osteoclasts: involvement of receptor activator of nuclear factor kappaB ligand and MAPK. *Biochim Biophys Acta* 2004; 1644:1-7. a

Theoleyre S, Wittrant Y, Tat SK, Fortun Y, Redini F, Heymann D. The molecular triad OPG/RANK/RANKL: involvement in the orchestration of pathophysiological bone remodeling. *Cytokine Growth Factor Rev* 2004; 15:457-75. b

Thomas HE, McKenzie MD, Angstetra E, Campbell PD, Kay TW. Beta cell apoptosis in diabetes. *Apoptosis* 2009; 14:1389-404.

Tikellis C, Wookey PJ, Candido R, Andrikopoulos S, Thomas MC, Cooper ME. Improved islet morphology after blockade of the renin- angiotensin system in the ZDF rat. *Diabetes* 2004; 53:989-97.

Tikellis C, Cooper ME, Thomas MC. Role of the renin-angiotensin system in the endocrine pancreas: implications for the development of diabetes. *Int J Biochem Cell Biol* 2006; 38:737-51.

Tipnis SR, Hooper NM, Hyde R, Karran E, Christie G, Turner AJ. A human homolog of angiotensin-converting enzyme. Cloning and functional expression as a captopril-insensitive carboxypeptidase. *J Biol Chem* 2000; 275:33238-43.

Tomoyasu A, Goto M, Fujise N, Mochizuki S, Yasuda H, Morinaga T, Tsuda E, Higashio K. Characterization of monomeric and homodimeric forms of osteoclastogenesis inhibitory factor. *Biochem Biophys Res Commun* 1998; 245:382-7.

Townsend RR, DiPette DJ. Pressor doses of angiotensin II increase insulin-mediated glucose uptake in normotensive men. *Am J Physiol* 1993; 265:E362-6.

Ueland T, Jemtland R, Godang K, Kjekshus J, Hognestad A, Omland T, Squire IB, Gullestad L, Bollerslev J, Dickstein K, Aukrust P. Prognostic value of osteoprotegerin in heart failure after acute myocardial infarction. *J Am Coll Cardiol* 2004; 44:1970-6.

Ueland T, Yndestad A, Øie E, Florholmen G, Halvorsen B, Frøland SS, Simonsen S, Christensen G, Gullestad L, Aukrust P. Dysregulated osteoprotegerin/RANK ligand/RANK axis in clinical and experimental heart failure. *Circulation* 2005; 111:2461-8.

Urata H, Nishimura H, Ganten D. Mechanisms of angiotensin II formation in humans. *Eur Heart J* 1995; 16 Suppl N:79-85.

Urata H, Nishimura H, Ganten D, Arakawa K. Angiotensin-converting enzyme-independent pathways of angiotensin II formation in human tissues and cardiovascular diseases. *Blood Press Suppl* 1996; 2:22-8.

Vaccarezza M, Bortul R, Fadda R, Zweyer M. Increased OPG expression and impaired OPG/TRAIL ratio in the aorta of diabetic rats. *Med Chem* 2007; 3:387-91.

Van Campenhout A, Golledge J. Osteoprotegerin, vascular calcification and atherosclerosis. *Atherosclerosis* 2009; 204:321-9.

Venuraju SM, Yerramasu A, Corder R, Lahiri A. Osteoprotegerin as a predictor of coronary artery disease and cardiovascular mortality and morbidity. *J Am Coll Cardiol* 2010; 55:2049-61.

Vischer UM. Hyperglycemia and the pathogenesis of atherosclerosis: lessons from murine models. *Eur J Endocrinol* 1999; 140:1-3.

Vitovski S, Phillips JS, Sayers J, Croucher PI. Investigating the interaction between osteoprotegerin and receptor activator of NF-kappaB or tumor necrosis factor-related apoptosis-inducing ligand: evidence for a pivotal role for osteoprotegerin in regulating two distinct pathways. *J Biol Chem* 2007; 282:31601-9.

Wada T, Nakashima T, Hiroshi N, Penninger JM. RANKL-RANK signaling in osteoclastogenesis and bone disease. *Trends Mol Med* 2006; 12:17-25.

Wara AK, Mitsumata M, Yamane T, Kusumi Y, Yoshida Y. Gene expression in endothelial cells and intimal smooth muscle cells in atherosclerosis-prone or atherosclerosis-resistant regions of the human aorta. *J Vasc Res* 2008; 45:303-13.

Ware CF. The TNF superfamily. *Cytokine Growth Factor Rev* 2003; 14:181-4.

Westermann D, Rutschow S, Jäger S, Linderer A, Anker S, Riad A, Unger T, Schultheiss HP, Pauschinger M, Tschöpe C. Contributions of inflammation and cardiac matrix metalloproteinase activity to cardiac failure in diabetic cardiomyopathy: the role of angiotensin type 1 receptor antagonism. *Diabetes* 2007; 56:641-6.

Wong BR, Josien R, Choi Y. TRANCE is a TNF family member that regulates dendritic cell and osteoclast function. *J Leukoc Biol* 1999; 65:715-24.

Wong PF, Lee SS, Cheung WT. Immunohistochemical colocalization of type II angiotensin receptors with somatostatin in rat pancreas. *Regul Pept* 2004; 117:195-205.

Woollard KJ, Geissmann F. Monocytes in atherosclerosis: subsets and functions. *Nat Rev Cardiol* 2010; 7:77-86.

Wright HL, McCarthy HS, Middleton J, Marshall MJ. RANK, RANKL and osteoprotegerin in bone biology and disease. *Curr Rev Musculoskelet Med* 2009; 2:56-64.

Wu KK, Huan Y. Diabetic atherosclerosis mouse models. *Atherosclerosis* 2007; 191:241-9.

Xiang GD, Xu L, Zhao LS, Yue L, Hou J. The relationship between plasma osteoprotegerin and endothelium-dependent arterial dilation in type 2 diabetes. *Diabetes* 2006; 55:2126-31.

Xiang GD, Sun HL, Zhao LS. Changes of osteoprotegerin before and after insulin therapy in type 1 diabetic patients. *Diabetes Res Clin Pract* 2007; 76:199-206.

Xiang GD, Pu JH, Zhao LS, Sun HL, Hou J, Yue L. Association between plasma osteoprotegerin concentrations and urinary albumin excretion in Type 2 diabetes. *Diabet Med* 2009; 26:397-403.

Yamaguchi K, Kinosaki M, Goto M, Kobayashi F, Tsuda E, Morinaga T, Higashio K. Characterization of structural domains of human osteoclastogenesis inhibitory factor. *J Biol Chem* 1998; 273:5117-23.

Yokoyama H, Deckert T. Central role of TGF-beta in the pathogenesis of diabetic nephropathy and macrovascular complications: a hypothesis. *Diabet Med* 1996; 13:313-20.

Yongchaitrakul T, Manokawinchoke J, Pavasant P. Osteoprotegerin induces osteopontin via syndecan-1 and phosphoinositol 3-kinase/Akt in human periodontal ligament cells. *J Periodontal Res* 2009; 44:776-83.

Yoshiji H, Kuriyama S, Yoshii J, Ikenaka Y, Noguchi R, Nakatani T, Tsujinoue H, Fukui H. Angiotensin-II type 1 receptor interaction is a major regulator for liver fibrosis development in rats. *Hepatology* 2001; 34:745-50.

Yuan L, Li X, Xu GL, Qi CJ. Effects of renin-angiotensin system blockade on islet function in diabetic rats. *J Endocrinol Invest* 2010; 33:13-9.

Yusuf S, Sleight P, Pogue J, Bosch J, Davies R, Dagenais G. Effects of an angiotensin-converting-enzyme inhibitor, ramipril, on cardiovascular events in high-risk patients. The Heart Outcomes Prevention Evaluation Study Investigators. *N Engl J Med* 2000; 342:145-53.

Yusuf S, Ostergren JB, Gerstein HC, Pfeffer MA, Swedberg K, Granger CB, Olofsson B, Probstfield J, McMurray JV; Candesartan in Heart Failure-Assessment of Reduction in Mortality and Morbidity Program Investigators. Effects of candesartan on the development of a new diagnosis of diabetes mellitus in patients with heart failure. *Circulation* 2005; 112:48-53.

Zauli G, Pandolfi A, Gonelli A, Di Pietro R, Guarnieri S, Ciabattoni G, Rana R, Vitale M, Secchiero P. Tumor necrosis factor-related apoptosis-inducing ligand (TRAIL) sequentially upregulates nitric oxide and prostanoid production in primary human endothelial cells. *Circ Res* 2003; 92:732-40.

Zauli G, Corallini F, Bossi F, Fischetti F, Durigutto P, Celeghini C, Tedesco F, Secchiero P. Osteoprotegerin increases leukocyte adhesion to endothelial cells both in vitro and in vivo. *Blood* 2007; 110:536-43.

Zauli G, Melloni E, Capitani S, Secchiero P. Role of full-length osteoprotegerin in tumor cell biology. *Cell Mol Life Sci* 2009 ; 66:841-51.

Zauli G, Toffoli B, di Iasio MG, Celeghini C, Fabris B, Secchiero P. Treatment with recombinant tumor necrosis factor-related apoptosis-inducing ligand alleviates the severity of streptozotocin-induced diabetes. *Diabetes* 2010; 59:1261-5.

Zhang SH, Reddick RL, Piedrahita JA, Maeda N. Spontaneous hypercholesterolemia and arterial lesions in mice lacking apolipoprotein E. *Science* 1992; 258:468-71.

Zhang J, Fu M, Myles D, Zhu X, Du J, Cao X, Chen YE. PDGF induces osteoprotegerin expression in vascular smooth muscle cells by multiple signal pathways. *FEBS Lett* 2002; 521:180-4.